Technische Universität München

TUM School of Medicine and Health

Investigating the uptake and accumulation of Tau monomers and aggregates in human neurons

Amir Tayaranian Marvian

Vollständiger Abdruck der von der TUM School of Medicine and Health der Technischen Universität München zur Erlangung eines

Doktors der Naturwissenschaften (Dr. rer. nat.)

genehmigten Dissertation.

Vorsitz: Prof. Dr. Thomas Misgeld

Prüfende der Dissertation:

1. Prof. Dr. Stefan Lichtenthaler
2. Prof. Dr. Alessandra Moretti

Die Dissertation wurde am 07.12.2023 bei der Technischen Universität München eingereicht und durch die TUM School of Medicine and Health am 13.03.2024 angenommen.

Acknowledgment

I would like to take this opportunity to express my sincere gratitude and appreciation to the individuals who have made invaluable contributions to the completion of my doctoral thesis.

First and foremost, I would like to express my most profound appreciation to Prof. Günter Höglinger for his exceptional guidance, support, and expertise as my supervisor. His dedication, encouragement, and insightful feedback have been instrumental in shaping the direction and success of my research. I am genuinely grateful for his mentorship and the opportunities he has provided me throughout this journey.

I extend my heartfelt appreciation to Prof. Wolfgang Wurst and Prof. Stefan Lichtenthaler for their generosity in providing access to their facilities and supporting my research. Their assistance and consultation have significantly enhanced the quality and scope of my work. I am thankful for their contributions and the opportunities they have provided me.

I am also indebted to Dr. Sigrid Schwarz for her invaluable mentorship, advice, and support. Her expertise, knowledge, and insightful feedback have greatly enriched my research and helped me navigate challenges. I am truly grateful for her mentorship and its lasting impact on my academic and professional growth.

I would like to express my deepest gratitude to my parents, who have been a constant source of love, encouragement, and support throughout my academic journey. Their unwavering belief in my abilities has been a driving force behind my achievements. I am eternally grateful for their sacrifices and the opportunities they have provided me.

My heartfelt appreciation also goes to my wife, whose unconditional love, understanding, and support have been a constant source of strength and motivation. Her encouragement, patience, and belief in me have been instrumental in overcoming challenges and staying focused on my goals. I am genuinely grateful for her untiring presence and the sacrifices she has made alongside me.

Lastly, I acknowledge my colleagues and friends for their support and discussions. Their presence and collaboration have enriched my research experience and provided a stimulating academic environment.

Summary

The transmission of pathologic forms of Tau protein from one brain cell to another plays a substantial role in the progression of neurodegenerative diseases like Alzheimer's disease, progressive supranuclear palsy, and corticobasal degeneration. A crucial step in this process involves the uptake of pathogenic Tau from the surrounding extracellular environment and its accumulation within healthy neurons. Multiple studies have shown that both physiological Tau monomers and pathologic aggregates are taken up by human neurons. However, the specific similarities or differences in the accumulation mechanism of Tau monomers and aggregates in neurons remain unclear.

In order to investigate the uptake and accumulation of different forms of Tau, including monomers, oligomers, and fibrils, we generated recombinant 2N4R Tau proteins and their various aggregated species. We employed biochemical and biophysical methods to study and analyze the characteristics of each Tau species. Next, two distinct neuronal models were implemented to study the cellular and molecular mechanisms of uptake and accumulation of these Tau species in human neurons. To differentiate between the uptake processes of Tau monomers and aggregates, small molecule inhibitors that target endocytic mechanisms, as well as siRNAs that specifically target mediators involved in Tau uptake and cell sorting, were employed. These experimental approaches provided insights into the differential uptake mechanisms associated with Tau monomers versus aggregates.

The study's findings indicate that aggregated Tau is more efficiently accumulated within human neurons than monomeric Tau, primarily associated with the higher accumulation rate of intermediate aggregates, including small fibrils and oligomeric species. Interestingly, minimal competition was observed between the neuronal accumulation of monomeric and intermediate aggregates of Tau. When general endocytosis processes were inhibited, there were no discernible differences in the uptake of Tau monomers and aggregates in induced pluripotent stem cell (iPSC) neurons. However, blocking heparan sulfate proteoglycans (HSPGs) significantly reduced the uptake of Tau aggregates but not monomers. Similarly, the knockdown of genes involved in the synthesis of HSPGs, including exostosin-1 and exostosin-2, reduced the uptake and accumulation of Tau intermediate aggregates but not monomers. On the other hand, the knockdown of LDL-receptor-related protein-1 (LRP1) mainly reduced the accumulation of

Tau monomers in human neurons. Moreover, we found that this differential regulation of monomers and aggregates is not only at the level of cell internalization but also in cellular sorting since the knockdown of vacuolar protein sorting 35 (VPS35), a component of the retromer complex, differentially regulated the accumulation of Tau monomers and aggregates in both neuronal models. These findings contribute to understanding the distinct mechanisms underlying the uptake and accumulation of Tau monomers versus aggregates within neurons.

The study's findings suggest that distinct mechanisms are involved in the uptake and accumulation of Tau monomers and aggregates. This distinction opens up the possibility of developing targeted interventions that specifically address the pathological spreading of Tau aggregates without interfering with the physiological transport of Tau monomers. These results provide valuable insights into potential strategies for developing therapies to mitigate the progression of Tauopathies by specifically targeting the harmful accumulation of Tau aggregates.

Zusammenfassung

Die Übertragung pathologischer Formen des Tau-Proteins von einer Hirnzelle auf eine andere spielt eine wesentliche Rolle im Verlauf neurodegenerativer Erkrankungen wie der Alzheimer-Krankheit, der progressiven supranukleären Blickparese und der kortikobasalen Degeneration. Ein entscheidender Schritt in diesem Prozess ist die Aufnahme von pathogenem Tau aus der umgebenden extrazellulären Umgebung und seine Anhäufung innerhalb gesunder Neuronen. Mehrere Studien haben gezeigt, dass sowohl physiologische Tau-Monomere als auch pathologische Aggregate von menschlichen Neuronen aufgenommen werden. Die spezifischen Ähnlichkeiten oder Unterschiede im Mechanismus der Anhäufung von Tau-Monomeren und -Aggregaten in Neuronen bleiben jedoch unklar.

Um die Aufnahme und Anhäufung verschiedener Formen von Tau, einschließlich Monomeren, Oligomeren und Fibrillen, zu untersuchen, haben wir rekombinante 2N4R-Tau-Proteine und ihre verschiedenen aggregierten Spezies erzeugt. Wir haben mehrere biophysikalische Methoden angewendet, um die Eigenschaften jeder Tau-Spezies zu untersuchen und zu analysieren. Anschließend wurden zwei unterschiedliche neuronale Modelle implementiert, um die zellulären und molekularen Mechanismen der Aufnahme und Anhäufung dieser Tau-Spezies in menschlichen Neuronen zu untersuchen. Um zwischen den Aufnahmeprozessen von Tau-Monomeren und -Aggregaten zu unterscheiden, wurden kleine Molekülinhibitoren eingesetzt, die endozytotische Mechanismen beeinflussen, sowie siRNAs, die spezifisch auf an der Tau-Aufnahme und Zellsortierung beteiligte Mediatoren abzielen. Diese experimentellen Ansätze lieferten Einblicke in die unterschiedlichen Aufnahmemechanismen von Tau-Monomeren im Vergleich zu Aggregaten.

Die Ergebnisse der Studie deuten darauf hin, dass aggregiertes Tau effizienter in menschlichen Neuronen akkumuliert wird als monomeres Tau, hauptsächlich aufgrund der höheren Anhäufungsrate von intermediären Aggregaten, einschließlich kleiner Fibrillen und oligomerer Spezies. Interessanterweise wurde nur eine minimale Kompetition zwischen der neuronalen Anhäufung von monomeren und intermediär aggregierten Tau beobachtet. Bei der Hemmung allgemeiner Endozytoseprozesse gab es keine erkennbaren Unterschiede in der Aufnahme von Monomeren und Aggregaten in induzierten pluripotenten Stammzell-Neuronen (iPSC). Wenn jedoch Heparansulfat-Proteoglykane (HSPGs)

blockiert wurden, verringerte sich die Aufnahme von Tau-Aggregaten signifikant, nicht jedoch von Monomeren. Ähnlich reduzierte das Ausschalten von Genen, die an der Synthese von HSPGs beteiligt sind, einschließlich Exostosin-1 und Exostosin-2, die Aufnahme und Anhäufung von intermediären Tau-Aggregaten, nicht jedoch von Monomeren. Auf der anderen Seite reduzierte das Ausschalten von LDL-Rezeptor-verbundenem Protein-1 (LRP1) hauptsächlich die Anhäufung von Tau-Monomeren in menschliche Neuronen. Darüber hinaus stellten wir fest, dass diese unterschiedliche Regulation von Monomeren und Aggregaten nicht nur auf Ebene der Zellinternalisierung erfolgt, sondern auch in der zellulären Sortierung, da das Ausschalten von Vakuolärem Protein-Sorting 35 (VPS35), einem Bestandteil des Retromer-Komplexes, die Anhäufung von Tau-Monomeren und -Aggregaten in beiden neuronalen Modellen unterschiedlich regulierte.

Die Ergebnisse dieser Studie legen nahe, dass unterschiedliche Mechanismen an der Aufnahme und Anhäufung von Tau-Monomeren und -Aggregaten beteiligt sind. Diese Unterscheidung eröffnet die Möglichkeit, gezielte Interventionen zu entwickeln, die sich spezifisch mit der pathologischen Ausbreitung von Tau-Aggregaten befassen, ohne den physiologischen Transport von Tau-Monomeren zu beeinträchtigen. Diese Ergebnisse liefern wertvolle Einblicke in potenzielle Strategien zur Entwicklung von Therapien zur Minderung des Fortschreitens von Tauopathien, indem sie sich gezielt gegen die schädliche Anhäufung von Tau-Aggregaten richten.

Table of Contents

List of Figures

List of Tables

List of Abbreviations

AD	Alzheimer's disease
AFM	Atomic force microscopy
AGD	Argyrophilic grain disease
ANOVA	Analysis of variance
ARTAG	Aging-related Tau astrogliopathy
BSA	Bovine serum albumin
CBD	Corticobasal degeneration
CD	Circular dichroism
CME	Clathrin-mediated endocytosis
cof-free-fib	Co-factor-free fibrils
CTE	Chronic traumatic encephalopathy
DMSO	Dimethyl sulfoxide
eTau	Extracellular Tau
EXT1	Exostosin Glycosyltransferase 1
FL	Fluorescently labeled
F-mono	Fibrillation-derived monomeric fraction
FTLD	Frontotemporal lobar degeneration
GGT	Globular glial Tauopathies
HSPGs	Heparan sulfate proteoglycans
iPSCNs	Induced pluripotent stem cells derived neurons
L-fib	Large fibrils fraction
LRP1	Low-density lipoprotein receptor-related protein 1
LUHMES	Lund human mesencephalic
MAPT	Microtubule-associated protein TAU
MBD	Microtubule-binding domain
Mono	Monomeric fraction
NGN2	NEUROGENIN2
Oligo	Oligomeric fraction
PART/NFT-dementia	Primary age-related Tauopathies neurofibrillary tangle predominant senile dementia
PBS	Phosphate-buffered saline
PHF	Paired helical filament
PiD	Pick's disease
PSP	Progressive supranuclear palsy
SEC	Size exclusion chromatography
SEM	Standard error of the mean
S-fib	Small fibrils fraction
smNPC	Small molecule neural precursor cell
TEM	Transmission electron microscopy
ThT	Thioflavin-T
UTC	Untreated control
VPS35	Vacuolar protein sorting-associated protein 35

1. Introduction and Background

1.1 Neurodegenerative tauopathies

Neurodegeneration is a process in which neurons undergo pathological conditions, leading to neuronal dysfunction and death (Przedborski et al., 2003). The most consistent risk factor for the progression and development of neurodegenerative diseases is increasing age (Tanner, 1992). The number of individuals with neurodegenerative diseases is rising as life expectancy increases globally highlighting the particular urge to develop therapeutic strategies for neurodegenerative diseases. As an example, the worldwide number of patients with Alzheimer's disease and other dementias increased from 20.2 million in 1990 to 43.8 million in 2016 (117% increase) and to 51.62 million in 2019 (161% increase) (Collaborators, 2019; Li et al., 2022). It has been predicted that by 2050 the number of patients with dementia increase to about 152 million worldwide (Collaborators, 2022). The demographic distribution showing the dramatic increase of prevalence especially in developing countries in Asia, Africa and south America (**Figure 1.1**).

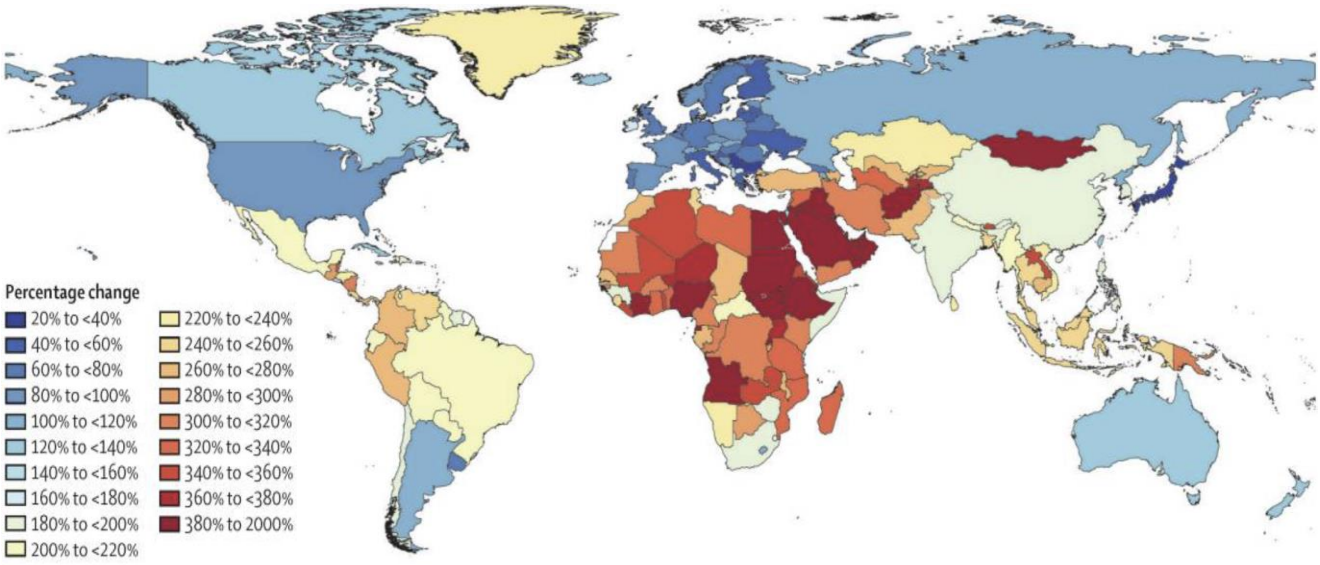

Figure 1.1 Demographic distribution of percentage change in the number of individuals with dementia between 2019 and 2050. [from (Collaborators, 2022)]

Tauopathies are a spectrum of adult-onset neurodegenerative diseases, including Alzheimer's disease (AD), Progressive supranuclear palsy (PSP), corticobasal degeneration (CBD) (Rosler et al., 2019). Their main characteristics are abnormal intracellular aggregation of the microtubule-associated protein Tau (MAPT) in various brain cells from neurofibrillary tangles (NFTs) in AD to astrocytic plaques in CBD (**Figure 1.2**). Tauopathies were categorized based on the leading cause of the disease, into primary Tauopathies, in which the Tau pathology is predominant, like PSP and CBD, and secondary Tauopathies, where other deriving forces are the triggering factor such as in AD which trigger with the pathologic invasion of amyloid-β aggregates. These forms can be distinguished based on biochemical and neuropathological features.

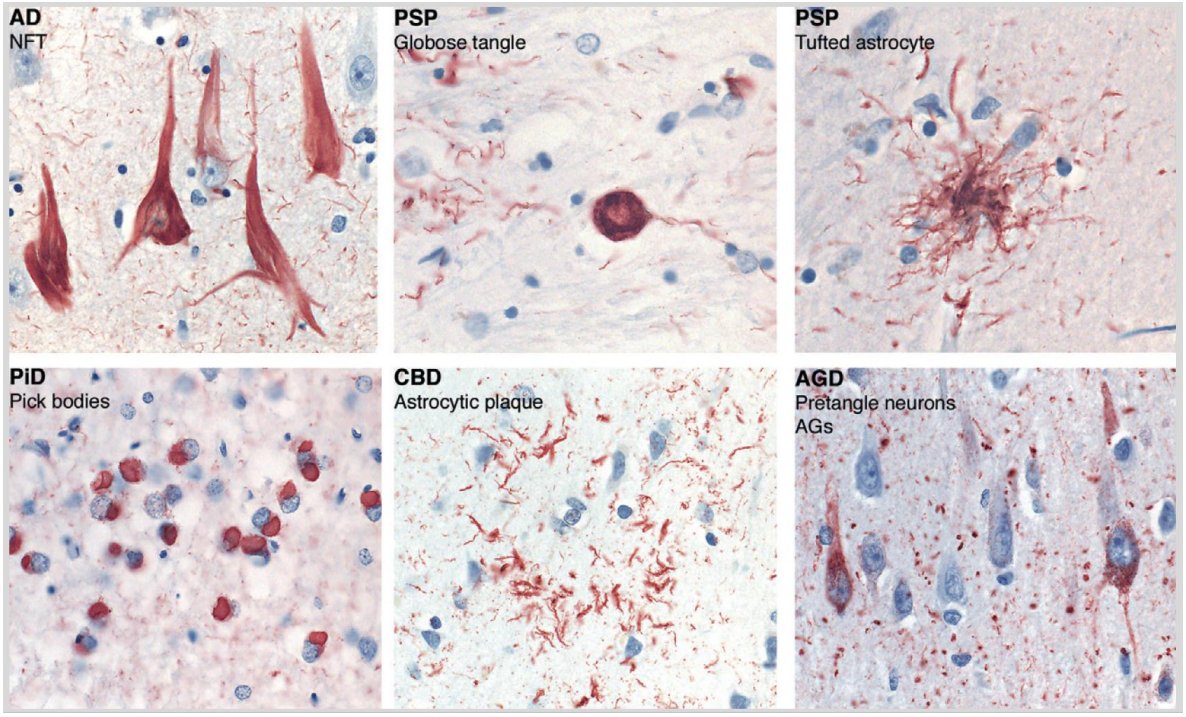

Figure 1.2 Different classes of tauopathies. Pathologic Tau inclusion in various Tauopathies by using AT8 anti-phosphorylated Tau antibody [from (Clavaguera et al., 2020)]. PiD: Picks disease, AD: Alzheimer's disease, PSP: progressive supranuclear palsy, CBD: corticobasal degeneration, AGD: argyrophilic grain disease. NFT: Neurofibrillary tangles.

1.2 Tau protein

Tau protein is a member of the microtubule-associated protein (MAP) family stabilizing microtubule filaments (Cleveland et al., 1977). They are primarily expressed in neurons and predominantly present in axons, also barely detectable in astrocytes and oligodendrocytes (Binder et al., 1985; LoPresti et al., 1995). *MAPT* (microtubule-associated protein Tau) is the encoding gene for Tau proteins located on chromosome 17q21. The alternative splicing of exons (E)2, E3, and E10 of the total 16 exons on human *MAPT* led to the formation of six isoforms ranging from 352 to 441 amino acids in length (**Figure 1.3A**), each of which possesses different propensity toward interaction with microtubules (Andreadis et al., 1992; Butner & Kirschner, 1991; Goedert & Jakes, 1990; Goedert et al., 1989). Structurally, Tau is a hydrophilic protein with an acidic N-terminal and roughly neutral C-terminal, categorized as the projection and microtubule assembly domains, respectively (Wang & Mandelkow, 2016). Despite the β–sheet folding of Tau in pathological conditions, physiologically, Tau is a natively unfolded or intrinsically disordered protein with little tendency for aggregation (Mukrasch et al., 2009).

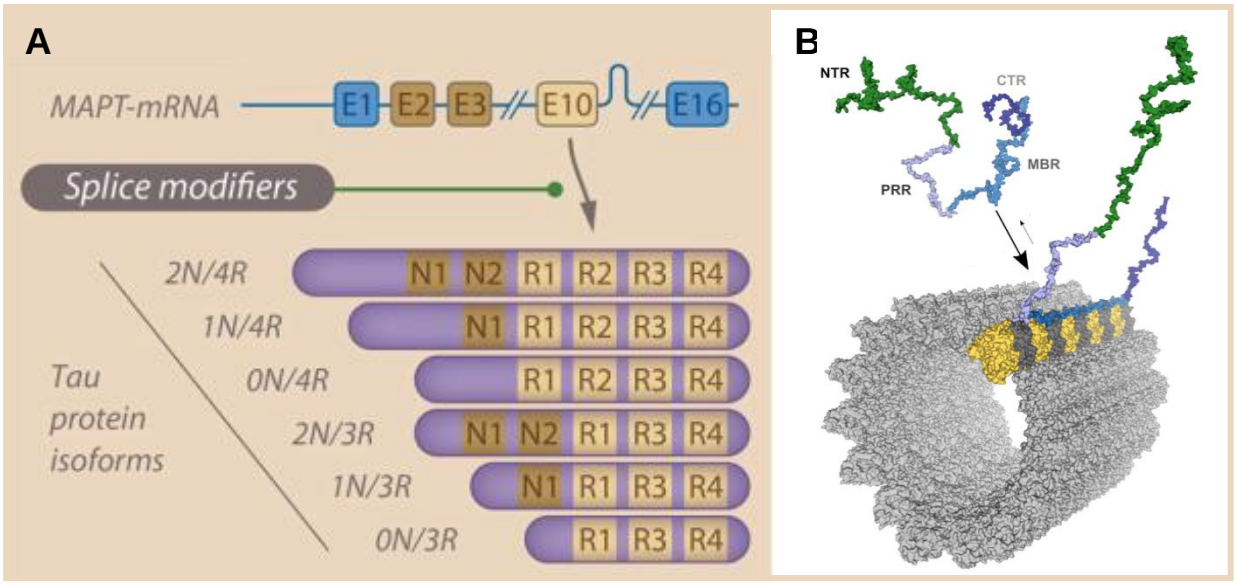

Figure 1.3 Tau isoforms and microtubule interaction. A) Alternative splicing of exon 2, 3, and 10 of Tau mRNA form 6 different isoforms of Tau protein [from (Rosler et al., 2019)]. B) A schematic representation of the full-length Tau isoform interaction with microtubule. NTR: N-terminal region, PRR: Proline-rich region, MBR: Microtubule-binding region, CTR: C-terminal region [from (Brandt et al., 2020)].

Tau is mainly sorted in axonal regions, where it stabilizes microtubules via the interaction of microtubule-binding domain (MBD) with tubulins which regulate the dynamics of microtubule formation and dissociation (Mandelkow & Mandelkow, 2012). The MBD comprises three repeats in 3R isoforms and four repeats in 4R isoforms. The latter shows a higher propensity for microtubule binding (**Figure 1.3B**). Likewise, several lines of evidence suggest that this protein is vital for axonal elongation, maturation, and neuronal migration (Caceres & Kosik, 1990; Takei et al., 2000). Tau regulates the distance between adjacent microtubules in axons by cross-bridging and plays a critical role in microtubule-associated transport (Chen et al., 1992).

Tau regulates the axonal transport via competing with motor proteins and cargoes, leading to a reduction in both anterograde and retrograde transport rates (Dixit et al., 2008; Kanaan et al., 2011; Utton et al., 2005; Vershinin et al., 2007). The physiological functions of Tau are tightly regulated by modifications such as phosphorylation, acetylation, methylation, ubiquitination, and truncation. Phosphorylation, as a well-known modification in Tau, occurs in various sites of the protein through which destabilizes microtubules with distinct mechanisms, including a reduction in Tau binding affinity toward microtubules or Tau detachment from microtubules (Hanger et al., 2009; Lu et al., 1999). Under the influence of kinases such as glycogen synthase kinase 3β or microtubule affinity-regulating kinase, the affinity of Tau to microtubules can be reduced, which is necessary for microtubule plasticity (Biernat et al., 2002; Sang et al., 2001). Besides microtubule-associated functions, other cellular processes have been associated with Tau, making it a hub protein **(Figure 1.4)** (Brandt et al., 2020). Moreover, *in vivo* studies revealed that Tau knockout mice develop glucose intolerance, pancreatic disorders, anxiety-related behavior, and memory impairment suggesting a wide range of undiscovered functions of Tau (Zhang et al., 2022).

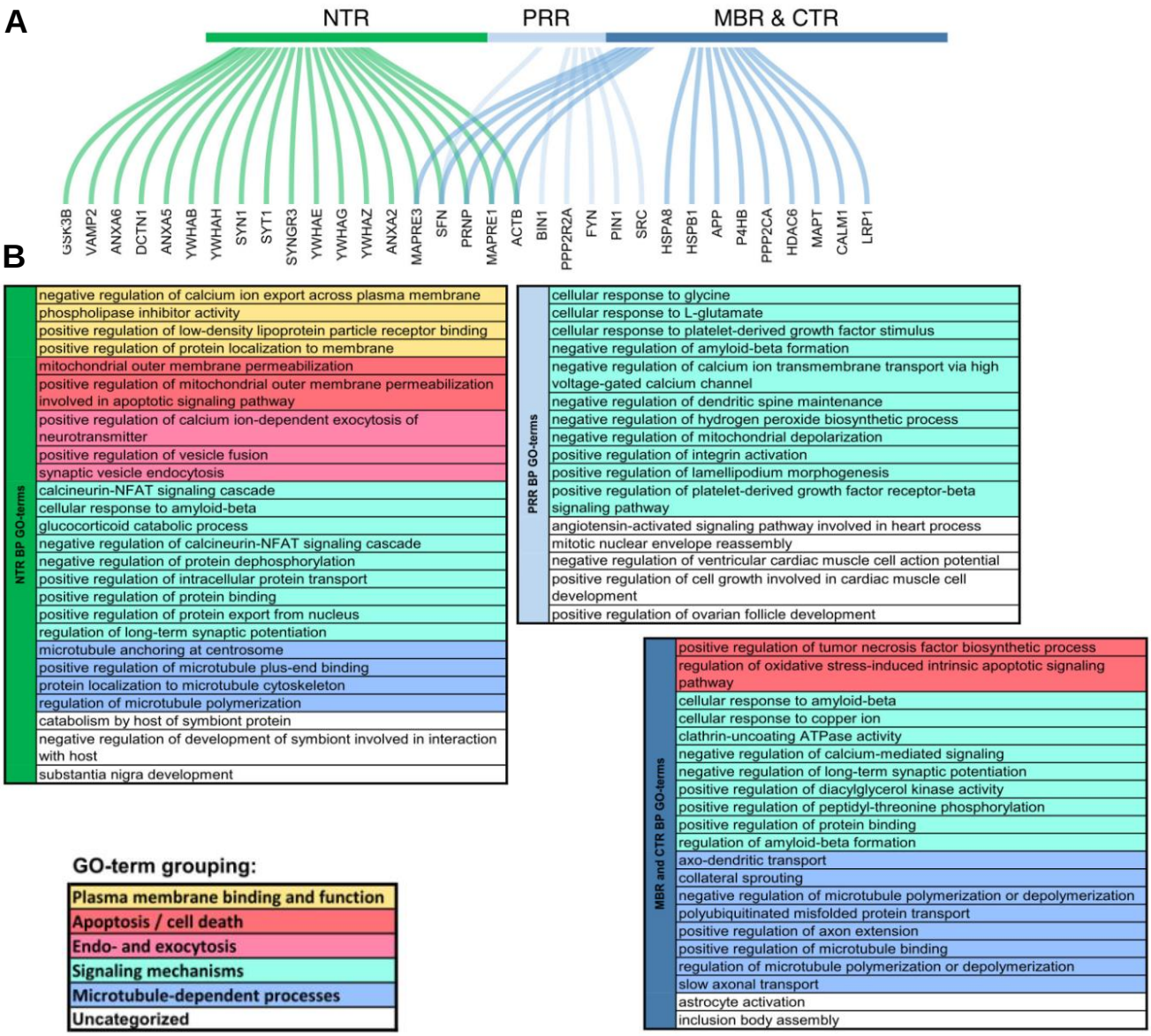

Figure 1.4 Various interacting partners and physiological functions of Tau protein. The genes responsible for the interaction partners of specific regions of Tau are depicted. Colored curved lines indicate the mapping of the interaction partner to the respective Tau region, with green representing NTR (1–171), light blue representing PRR (172–243), and blue representing MBR and CTR combined (244–441). B) A summarized representation of the Gene Ontology (GO) terms associated with the interaction partners mapped to different regions of Tau is shown. The GO terms were grouped and color-coded according to the provided legend. NTR: N-terminal region, PRR: Proline-rich region, MBR: Microtubule-binding region, CTR: C-terminal region [from (Brandt et al., 2020)].

1.3 Tau pathology

As mentioned before, the pathology of Tau is associated with the presence of Tau inclusions in the patient's brain, which are made of fibrillar structures and highly phosphorylated Tau (**Figure 1.5**). The β-sheet reach structures formed from the self-assembly of Tau monomers are called amyloid fibrils (Nizynski et al., 2017). These structures made by the interaction of two hexapeptide motifs in the MBD of 4R Tau, ^{275}VQIINK^{280,} and ^{306}VQIVYK^{311}, which show a high propensity for participating in β-sheet conformation and promote the generation of early aggregates in the pathological condition (Ganguly et al., 2015; von Bergen et al., 2001; von Bergen et al., 2000) (**Figure 1.6)**. The 3R Tau can also form a β-sheet reach fibrillar structure without the first hexapeptide motif, however, with lower efficiency (Zhong et al., 2012). The presence of the second motif ^{306}VQIVYK^{311} is necessary and sufficient for the self-assembly of Tau protein (Li & Lee, 2006).

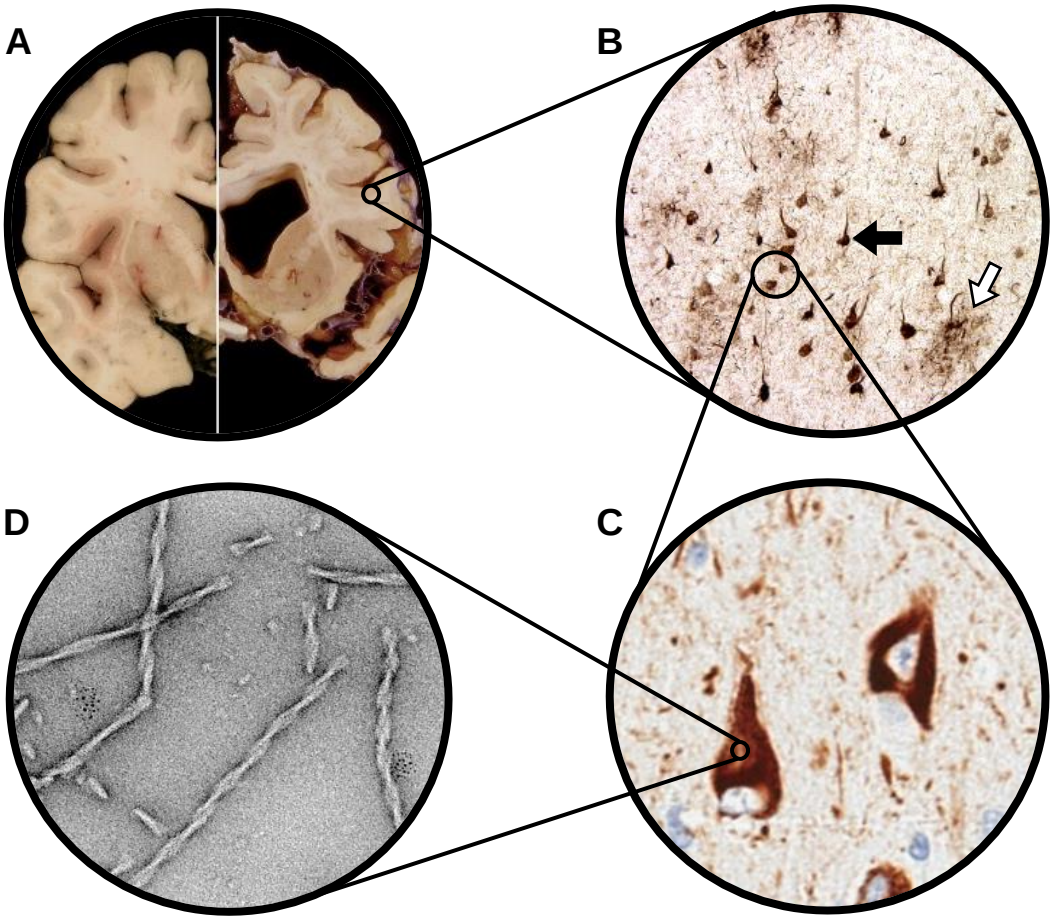

Figure 1.5 Tau pathology at different dimensions. A) Brain sections of healthy (left) and Alzheimer's disease (right) patients (https://www.alzheimers-brace.org/alzheimers-disease-ad/. Retrieved 2023/10/24.). B) Amyloid inclusions of Tau (black arrow) and Amyloid-β (white arrow) [from (Binder et al., 2005)]. C) Tau pathology in the form of neurofibrillary tangles [from (Moloney et al., 2021)]. D) Tau fibrils extracted from human brain samples [from (Mandelkow et al., 2007)]. The association between pictures is illustrative.

Tau fibrillization does not occur spontaneously at physiological conditions, in contrast to some other amyloid-forming proteins (Kuret et al., 2005), perhaps due to the electrostatic repulsion of cationic amino acids as well as a rate-limiting conformational barrier (Chirita et al., 2005). Generally, the interaction of C- and N-terminal regions with the MBD stabilizes Tau monomers and prevents fibrillization (Horowitz et al., 2006). Cleavage of these regions, however, increases the aggregation propensity of Tau (Berry et al., 2003). Diminishing the positive charge of Tau through extensive phosphorylation (Alonso et al., 1996) or interactions with anionic compounds induce Tau fibrillization (Chirita et al., 2003; Goedert et al., 1996; Holmes et al., 2013; Kampers et al., 1996; Sibille et al., 2006; Wilson & Binder, 1997).

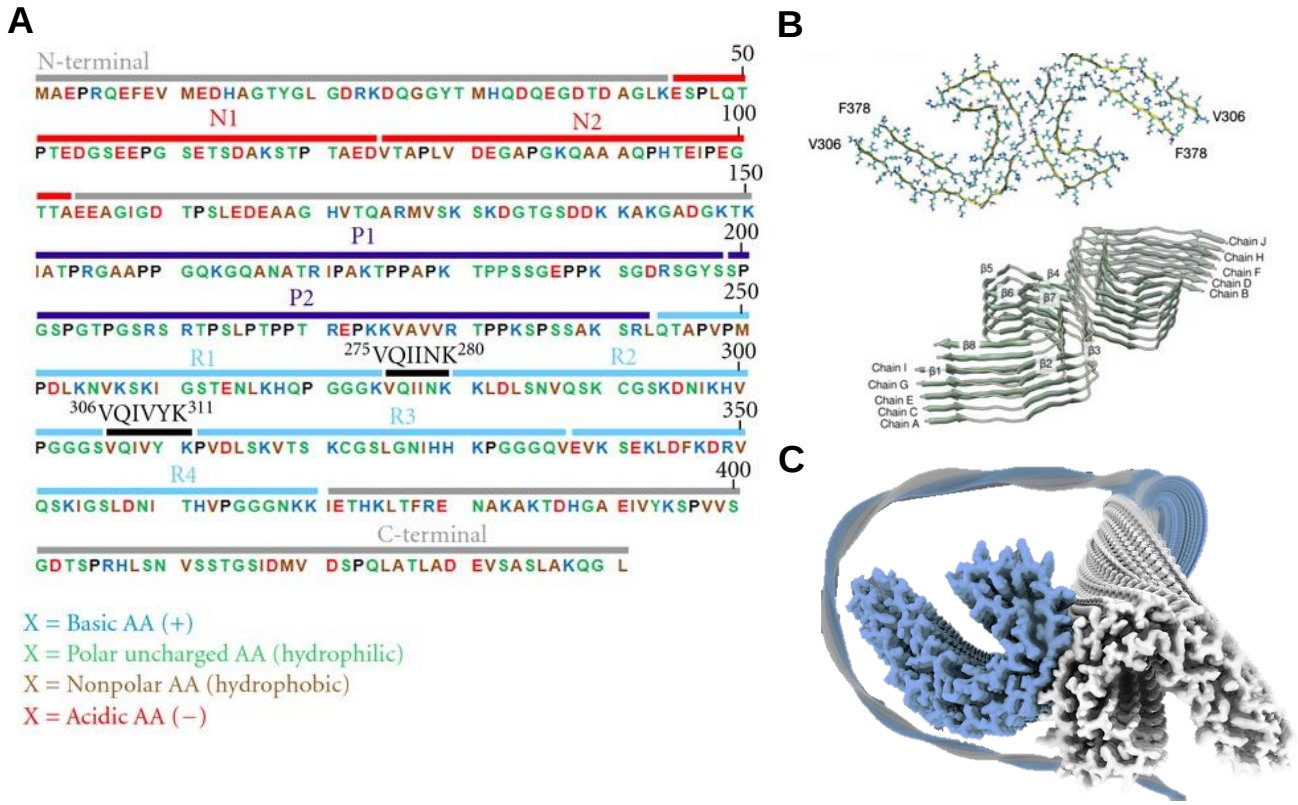

Figure 1.6 Tau protein sequence and the structure of β-sheet containing-core of Tau aggregates. The amino acid sequence of Tau protein is composed of N-terminal regions (N1 & N2) with mainly acidic residues, a Proline-reach domain with basic nature (P1 & P2), a microtubule-binding domain with four repeat-domains in the longest isoform which is mainly basic (R1 - R4), and a C-terminal region with a neutral collective charge at pH 7.0 [from (Kolarova et al., 2012)]. B) Cryo-electron microscope-based core structure of paired helical filaments composed of 10 monomeric chains (residues 306 - 378) with eight β-sheet domains [from (Leonard et al., 2021)]. C) Graphical simulation of Tau fibrils' core based on the cryo-electron microscope imaging (https://www2.mrc-lmb.cam.ac.uk/groups/scheres/index.html. Retrieved 2023/10/24).

Tau fibrillation follows a nucleation-dependent polymerization that forms a sigmoidal kinetics pattern composed of three steps: nucleation, elongation, and plateau (**Figure 1.7A**) (Lee et al., 2007). The rate-limiting step of this process is the nucleation phase which is kinetically referred to as a lag phase. The primary misfolded intermediates and oligomers that trigger pathologic aggregation are formed during the nucleation phase (Kaniyappan et al., 2017). Detecting and characterizing early-stage and intermediate assemblies are challenging due to the variability of aggregated species and the highly dynamic molecular transition in this phase (Ren & Sahara, 2013). Tau oligomers with granular structure have been identified *in vitro* upon fibrillation of recombinant Tau and in different stages of AD (Maeda et al., 2007; Patterson et al., 2011).

Similarly, the presence of Tau oligomers in the brain of tauopathy patients has been reported in various studies (Gerson et al., 2014; Lasagna-Reeves, Castillo-Carranza, Sengupta, Sarmiento, et al., 2012; Ward et al., 2013). Based on the sigmoidal model of amyloid fibrillation, the conversion of oligomers into small primary fibrils triggers the exponential elongation phase in which early fibrils grow via the recruitment of monomers to form mature fibrillar structures (Margittai & Langen, 2004). Ultimately, the process would be in the plateau phase when the fibril formation and dissociation rates reach an equilibrium. Moreover, adding intermediate structures, such as oligomers, at the beginning of the fibrillation process can accelerate the process by circumventing the nucleation phase, a process called seeded aggregation (**Figure 1.7B**) (Jackson et al., 2022). The final product of a fibrillation process is an aggregated mixture which is a heterogenous population composed of various species of Tau from

monomeric to oligomeric, small fibrils, and long fibrils (Maeda et al., 2007). These various species can be separated using biophysical techniques (**Figure 1.8**).

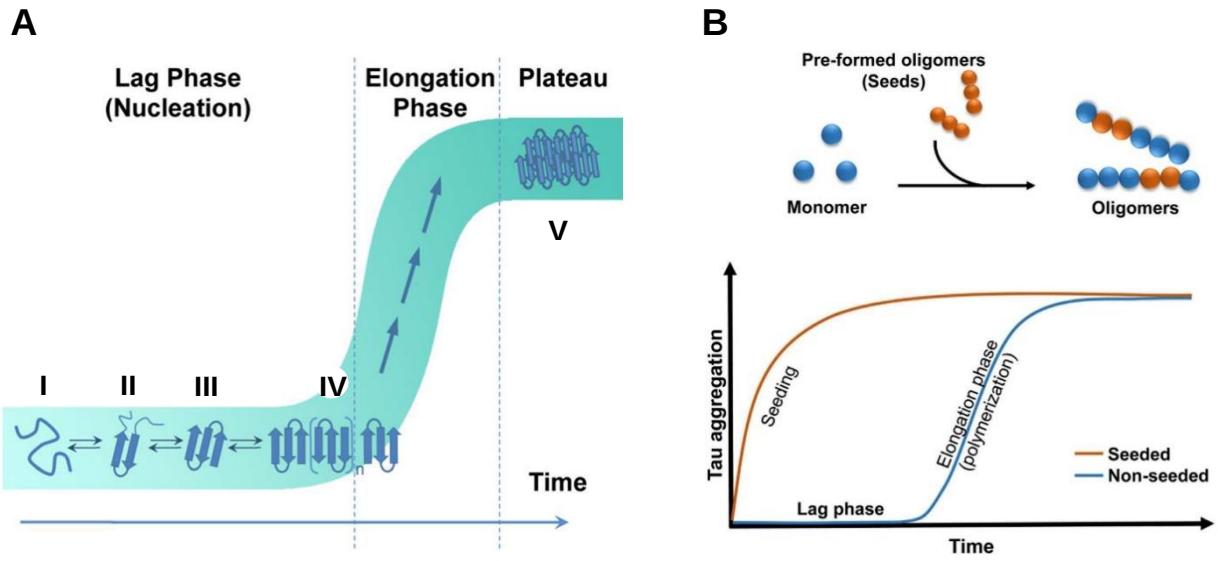

Figure 1.7 Amyloid fibrillation process. A) The process begins with a slow nucleation phase in which soluble, monomeric, or natively unfolded proteins (I) undergo a structural transition to form β-structures (II). These β-structures then aggregate, forming the initial nucleus (III) and protofibrils (IV). Following this, a fast elongation phase occurs, where monomers and higher-order oligomers extend the nucleates, forming mature fibrils at the plateau (V) [From (Savelieff et al., 2013)]. B) The addition of preformed-oligomers reduces the lag phase and accelerates the fibrillation process [from (Jackson et al., 2022)].

At least three sets of hypotheses can explain the pathogenic mechanism of Tau fibrillation (Wang & Mandelkow, 2016). First, Tau aggregates can gain toxic function and disrupt cellular processes such as synaptic and mitochondrial functions. Second, Tau aggregation causes loss of the physiological functions of Tau, leading to dysfunctions such as microtubule disassembly and axonal transport deficit. Third, Tau pathology can mislocalize Tau protein in cells, such as an increase in the postsynaptic load of Tau, leading to synaptic dysfunctions. Moreover, Tau pathology has been associated with neuroinflammation, which can lead to the development or progression of neurodegenerative diseases (Samudra et al., 2023).

Mutations can accelerate and induce the pathology of Tau, such as loss of functions or toxic gain of function mutations, which has been recognized in different types of Tauopathies (Wolfe, 2009). Many mutations are related to the microtubule-binding role of Tau and reduce its binding affinity toward microtubules, increasing the chance for aggregation (well reviewed in (Strang et al., 2019)). As an example, P301S mutation reduces the tendency of Tau to bind to microtubules and, on the other hand, increases the propensity of Tau to form pathologic aggregates (Bugiani et al., 1999; Sperfeld et al., 1999). Thus this mutation has been used in various experimental models to simulate the pathology of Tau *in vitro* and *in vivo*.

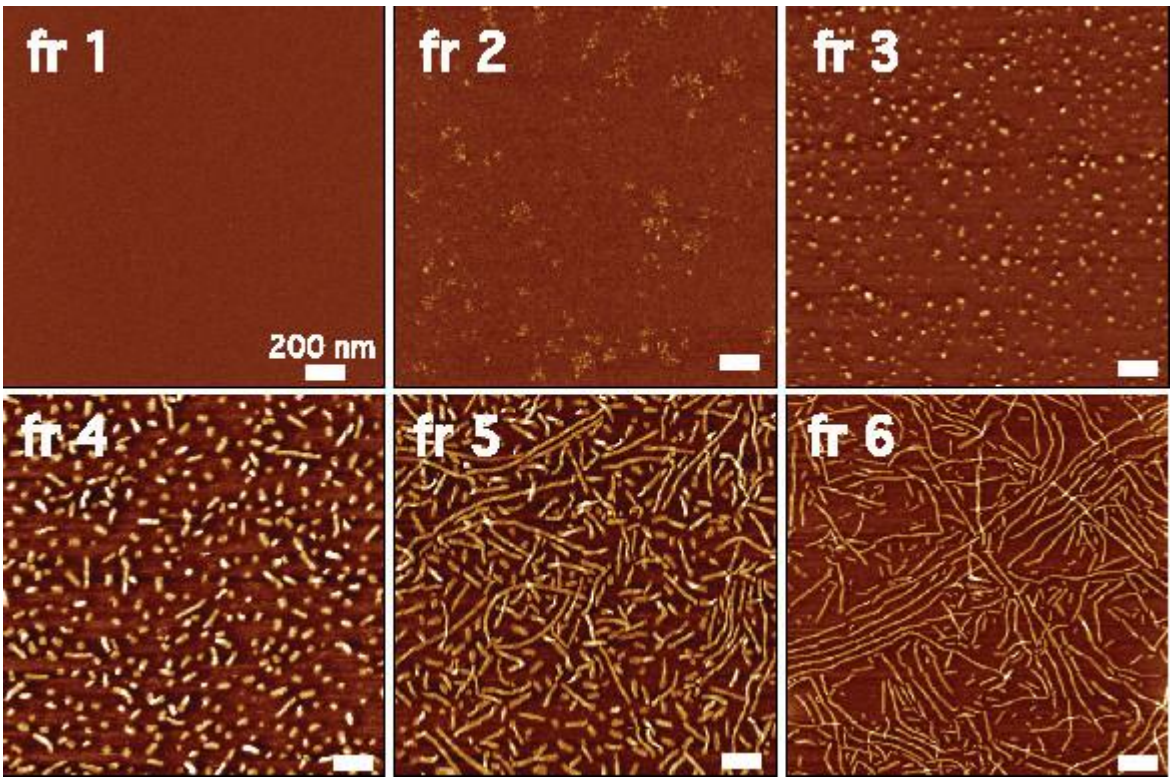

Figure 1.8 Various species of Tau aggregated mixture. A mixture of recombinant Tau aggregates was fractionated using sucrose gradient into six fractions [from (Maeda et al., 2007)].

1.4 Tau pathology spreading

Tau pathology spreading has been associated with disease progression in various Tauopathies based on Braak staging (Braak & Braak, 1991; Braak et al., 2011). A similar staging system has been conceptualized for various 4-repeat Tauopathies, specifically for progressive supranuclear palsy (PSP), where Tau pathology has a primary role (Kovacs et al., 2020). A growing body of evidence suggests that Tau pathology propagation is a prion-like process that occurs via cell-to-cell transfer of abnormal Tau seeds that nucleate the abnormal accumulation of Tau in healthy cells (Mudher et al., 2017). The process by which Tau pathology is transmitted from one cell to another is called intercellular Tau spreading (**Figure 1.9**). The prion-like hypothesis of Tau spreading suggests an unidentified pathological form of Tau that transports from diseased cells to naïve cells and triggers the aggregation of Tau (Goedert & Spillantini, 2017). This process involves three main steps: 1) the release of spreading Tau species from diseased cells, 2) the uptake of extracellular Tau by healthy cells, and 3) the formation of new aggregates within recipient cells through the recruitment of normal endogenous Tau (seeding).

The cell-to-cell transmission of Tau was reported for the first time in 2009, *in vitro* (Frost et al., 2009) and *in vivo* (Clavaguera et al., 2009). The mechanism of intercellular Tau spreading is considered a prion-like process (Holmes & Diamond, 2014). However, unlike prion diseases, Tauopathies are not regarded as infectious (Josephs, 2017). This hypothesis highlights the importance of targeting extracellular pathogenic Tau seeds and their transport system into healthy neurons to block disease progression (Holmes & Diamond, 2014). Thus, discovering the internalization mechanism of Tau seeds and the molecular mediators of Tau uptake is of great importance.

Many studies have tried to find the main Tau species culprit for seeding and propagation. However, since the process is prolonged and models are not entirely representative, the answer to this question is still elusive (Rosler et al., 2019). In the upcoming sections, we will review the various species of Tau found in the extracellular environment, examine the mechanisms of Tau release and uptake, and discuss the different Tau species and their potential as seeds in the propagation of Tau pathology.

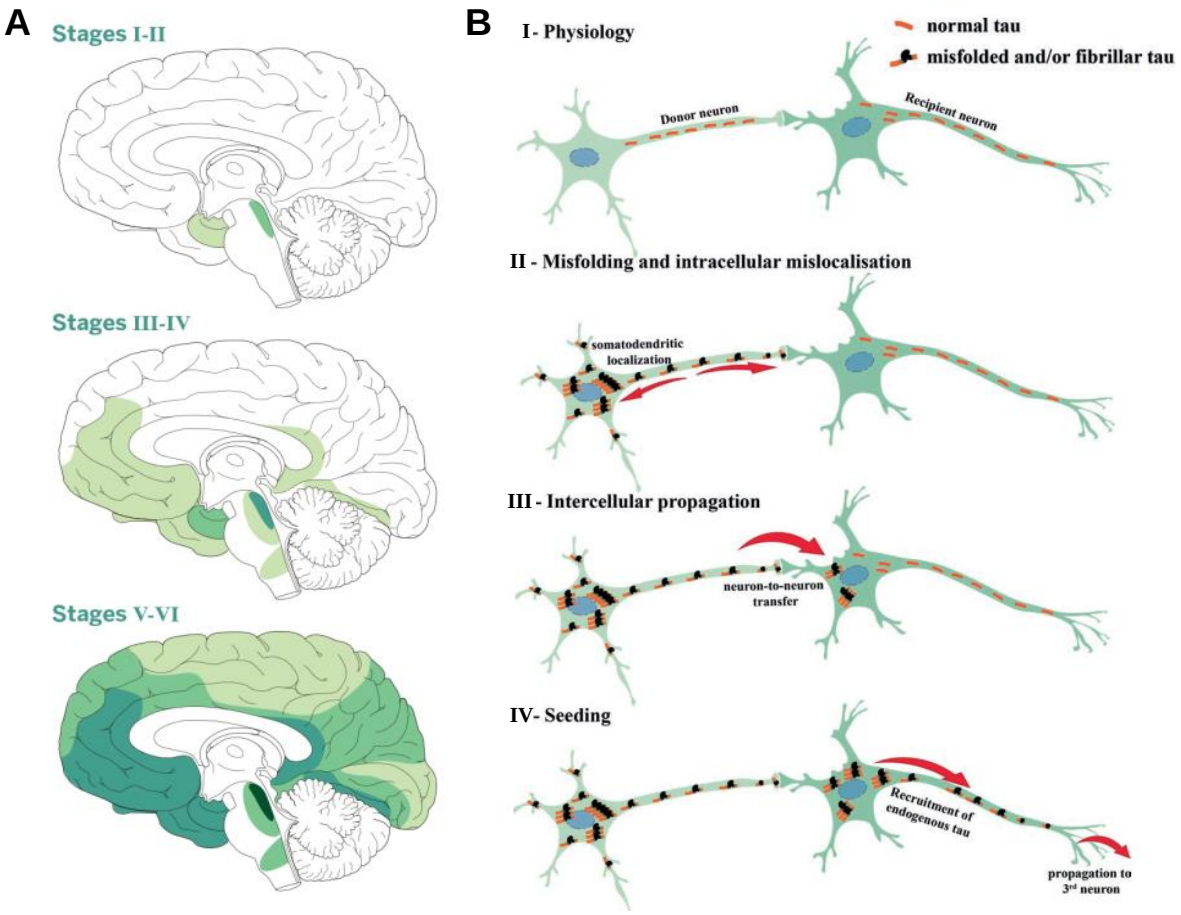

Figure 1.9 Tau pathology spreading. A) Braak stages of Tau pathology progression in AD brain [from (Goedert, 2015)]. B) A proposed mechanism of cell-to-cell transport of Tau pathology. Normal Tau proteins (orange) are distributed within neurons while primarily concentrated in the axonal region (I). Initiation of Tau propagation occurs through early misfolding, accumulating misfolded Tau in both the somatodendritic area and synaptic terminals of neurons (II). Transfer of misfolded Tau proteins between neurons transpires through synapses (III). Within the recipient neuron, the misfolded Tau proteins recruit endogenous Tau, triggering a seeding mechanism that transmits their misfolding properties and begins a new round of pathology spreading (IV) [from (Dujardin & Hyman, 2019)].

1.5 Extracellular Tau

Despite its primary role as an intracellular microtubule-associated protein, various forms of Tau have been detected in the extracellular environment, referred to as extracellular Tau (eTau) (Fig. 5). eTau has been observed in the culture medium of neuroblastoma cells, normal primary neurons (Karch et al., 2012), and iPSC-derived neurons (Bright et al., 2015). It has also been found in the interstitial fluid (ISF) and cerebrospinal fluid (CSF) of mice (Yamada et al., 2011) and in the human brain (Magnoni et al., 2012). In body fluids, Tau exists in both a vesicle-free form and within extracellular vesicles (Dujardin et al., 2014). eTau associated with extracellular vesicles has been identified in the culture medium of Tau-overexpressing neuroblastoma cells (Saman et al., 2012), mouse brain (Polanco et al., 2016), and human plasma (Stern et al., 2016). However, the proportion of Tau in the vesicle-associated form is relatively low, accounting for only 1% in the conditioned medium of Tau-overexpressing HEK293 cells, 3% in rat cortical neurons, and 10% in rat primary embryonic cortical neurons (Dujardin et al., 2014; Wang et al., 2017; Yan et al., 2016). Recent studies using conditioned medium from iPSC-derived neurons and human CSF have confirmed that less than 1% of Tau is associated with exosomes (Guix et al., 2018).

C-terminal cleaved eTau has been detected in the CSF of mice (Barten et al., 2011). In the CSF of healthy individuals and patients with PSP, eTau predominantly consists of truncated forms, comprising mid-region residues and lacking the MBD (Barthelemy et al., 2016). Phosphorylated forms of eTau have also been identified in the CSF of PSP and CBD patients as well as in healthy individuals (Noguchi et al., 2005). Notably, a recent study demonstrated a direct correlation between reduced levels of phosphorylated Tau (specifically at threonine 181) in the CSF and the severity and high rate of disease progression in PSP (Rojas et al., 2018).

The presence of phosphorylated Tau (pTau) aggregates in the extracellular space of healthy neurons is rare (Kanmert et al., 2015), and such aggregates are also not typically found in the CSF of healthy individuals (Sengupta et al., 2017). However, in the brains of patients with PSP, tangles located outside of cells, known as ghost tangles, have been observed as remnants of deceased neurons (Arima et al., 1999; Zwang et al., 2023). Additionally, eTau aggregates, including oligomers and seed-competent

species with high molecular weight, have been reported in the CSF of patients with Tauopathies (Sengupta et al., 2017; Takeda et al., 2016).

eTau has been implicated in pathological processes through two distinct mechanisms. Firstly, eTau can directly induce toxicity and neuronal dysfunction. Studies have shown that treating hippocampal neurons with Tau can lead to cell death by disrupting calcium homeostasis. This toxic effect is observed with both soluble monomeric and oligomeric forms of eTau, as well as with phosphorylated or insoluble paired helical filaments (PHFs) (Gomez-Ramos et al., 2006). Additionally, it has been discovered that muscarinic receptors M1 and M3 are involved in eTau-driven neurotoxicity, with residues 391 to 407 of Tau interacting with these receptors with higher affinity than acetylcholine (Gomez-Ramos et al., 2009; Gomez-Ramos et al., 2008). These findings suggest a dual role of eTau, with potential physiological functions as well as detrimental effects. Furthermore, treatments with recombinant truncated and oligomeric Tau have been shown to induce synaptic dysfunction. Also, exposure to the secretome of iPSC-derived neurons containing synaptotoxic forms of Tau inhibited long-term potentiation (Fa et al., 2016; Florenzano et al., 2017; Hu et al., 2018; Kaniyappan et al., 2017). Injection of Tau oligomers, but not monomers and fibrils, into subcortical regions, impaired memory and induced synaptic dysfunction (Lasagna-Reeves et al., 2011). Notably, clearance of extracellular Tau oligomers using specific antibodies protected against locomotor and memory deficits in a mouse model of 4R-Tauopathy (Castillo-Carranza et al., 2014).

The second pathological mechanism that involves eTau is related to the intercellular propagation of Tau pathology. In this case, eTau is not considered to be directly toxic for the cells but it is involved in the spreading of pathology. In various tauopathies, specific Tau antibodies have revealed the stereotypical stages of Tau pathology, where it sequentially affects anatomically connected brain areas in a hierarchical pattern known as Braak stages (Braak & Braak, 1991; Braak et al., 2011; Kovacs et al., 2020; Stamelou et al., 2021). This concept provides a basis for understanding the cell-to-cell propagation of Tau pathology during disease progression in AD patients, which will be discussed in more detail in the next chapters.

1.6 Tau secretion

Secretion of pathogenic Tau is the first step in the chain of events for the cell-to-cell spreading of Tau pathology. According to previous studies, Tau secretion is regulated by different mechanisms depending on the cellular conditions (**Figure 1.10**). Under normal physiological conditions, vesicle-associated Tau is primarily secreted through ectosomes, while exosomal secretion becomes more prevalent as cellular Tau accumulation increases (Dujardin et al., 2014). Aside from vesicle-associated pathways, an alternative non-canonical exocytic mechanism has been proposed for Tau release (Fontaine et al., 2016). This process involves the chaperone Hsc70 in conjunction with its co-chaperone, DnaJ. Moreover, Tau can directly translocate through the plasma membrane (Katsinelos et al., 2018). This unique secretion process is mediated by Tau's interaction with phosphatidylinositol 4,5-bisphosphate and sulfated proteoglycans. Notably, this unconventional secretion process preferentially targets hyperphosphorylated Tau, which is more abundant in the cytoplasm when detached from microtubules. An ATP-independent direct translocation mechanism for Tau secretion through the plasma membrane has also been identified (Merezhko et al., 2018). This non-vesicular process is facilitated by heparan sulfate proteoglycans (HSPGs) and predominantly targets phosphorylated oligomeric Tau species concentrated in plasma membrane microdomains.

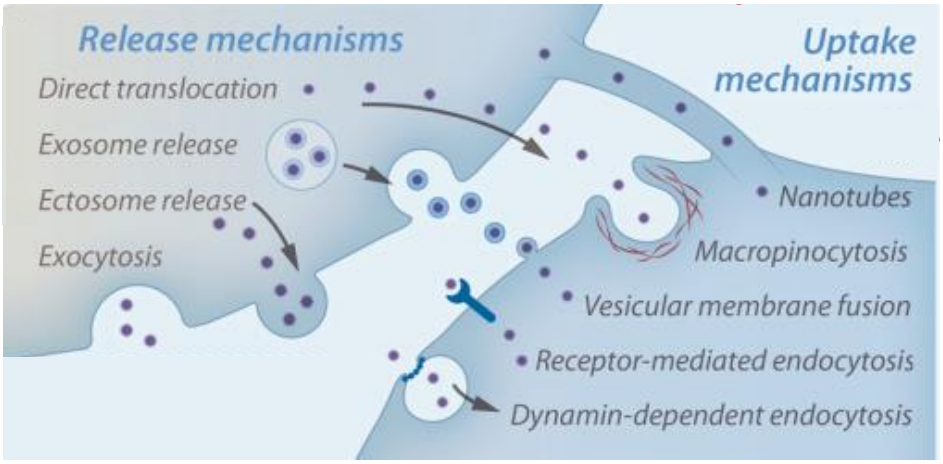

Figure 1.10 Schematic view of intercellular spreading mechanisms of Tau pathology. Primarily pathological Tau seeds are released from disease cells and are taken up by naïve

cells, which leads to a new round of aggregation and pathology in the healthy cells. Various identified Tau release and uptake mechanisms were shown (Rosler et al., 2019).

1.7 Tau seeds

The prion-like theory of pathology spreading suggests that specific Tau species capable of seeding Tau aggregation in healthy cells are promising targets for therapeutic interventions to halt disease progression. However, the identification of these Tau seeds has proven challenging. Previous efforts to pinpoint the exact seeding species have yet to be successful.

To shed light on the properties of Tau seeds, a study was conducted in nontransgenic mice injected with enriched pathological Tau derived from patients with AD, PSP, and CBD (Narasimhan et al., 2017). The findings revealed distinct differences in the potency of Tau strains to propagate and exhibited cell-type specificity. Notably, PSP-Tau showed a faster aggregation rate compared to AD-Tau in the brains of the injected mice. Furthermore, glial Tau pathology was observed exclusively in mice injected with PSP- and CBD-Tau. These results indicate that the specific strain of Tau responsible for seeding aggregation plays a critical role in disease propagation, emphasizing the importance of identifying the seeding Tau species to develop effective therapeutic strategies. The discovery and characterization of these seeding Tau species hold great promise in advancing the development of targeted therapies to disrupt the spread of Tau pathology and potentially halt the progression of Tauopathies.

Tau seeds are hypothesized to possess two key characteristics. Firstly, they must be able to transfer from diseased cells to healthy cells, which depends on factors such as solubility, molecular weight, and accessibility to cellular release and uptake processes. Tau species with high solubility, low molecular weight, and efficient mobility are more likely to exhibit transmissibility. Secondly, Tau seeds should have the capacity to induce aggregation in the host cell, necessitating the presence of the MBD and specific structural features that make them potent seeds. **Figure 1.11** illustrates various extracellular Tau species with various potential to play the role of seed in the process of Tau pathology spreading.

Figure 1.11 Schematic view of extracellular Tau species that may play the role of Tau seeds. Various forms of Tau species are present in the extracellular media, including monomers, oligomers, post-translationally modified, fragmented, digested fibrils, and fragmented monomers [from (Rosler et al., 2019)].

Previous studies exploring transcellular spreading mechanisms of Tau have primarily focused on the assumption that Tau seeds need to be transported via the extracellular environment, such as the ISF or CSF. However, the predominant species of Tau found in the CSF is mid-region truncated Tau, which lacks the MBD (Barthelemy et al., 2016). Despite its high solubility and small size, the absence of the MBD suggests that this particular Tau species may not possess the ability to induce aggregation. It should be noted that the composition of CSF does not fully reflect the content of ISF surrounding neurons in the brain parenchyma. Studies have shown that the concentration of Tau in the ISF is approximately ten times higher than in the CSF (Yamada et al., 2011), suggesting that CSF Tau may not accurately represent the Tau species present within the central nervous system (CNS).

Therefore, to gain a comprehensive understanding of the seeding Tau species involved in disease propagation, it is crucial to investigate the Tau content in the ISF and perform detailed analyses and profiling of Tau fragments, modified monomers, and aggregates in the CSF and ISF of individuals with Tauopathies. These investigations can provide valuable insights into the specific Tau species present under pathological conditions and their potential role in the propagation of Tau pathology. However, the current technology of using microdialysis to study ISF protein contents has a limitation related to dialysis membrane pore size, which omits the higher molecular weight species like aggregates from the analysis.

Phosphorylation is an extensively studied modification shown to increase Tau's propensity to aggregate (Despres et al., 2017) and enhance its secretion (Plouffe et al., 2012). However, no study has provided

evidence that adding monomeric phosphorylated Tau (pTau) to a pool of physiological Tau monomers can seed aggregation in cell-free or cell-based assays.

The most extensively investigated species of Tau as transmissible seeds are fibrillar structures, which have demonstrated a high capacity to induce aggregation (Goedert & Spillantini, 2017). Nevertheless, the large size, high molecular weight, and insolubility of Tau fibrils may limit their ability to be transported over long distances. Moreover, structural studies have revealed that Tau fibrils possess a highly interactive and adhesive fuzzy-coated surface that further limits their transport (Wegmann et al., 2013) (**Figure 1.12**). Studies on Tau propagation have suggested that cell-to-cell transport primarily occurs through synapses (Ahmed et al., 2014), indicating that Tau seeds must traverse fine neurites to reach synapses and be released into the synaptic cleft for uptake by neighboring neurons. Tau seeds must be small (compared to large fibrillar forms), highly mobile, or transported by microtubule-associated motor proteins for efficient long-distance transport. Thus, larger fibrils are improbable seed candidates.

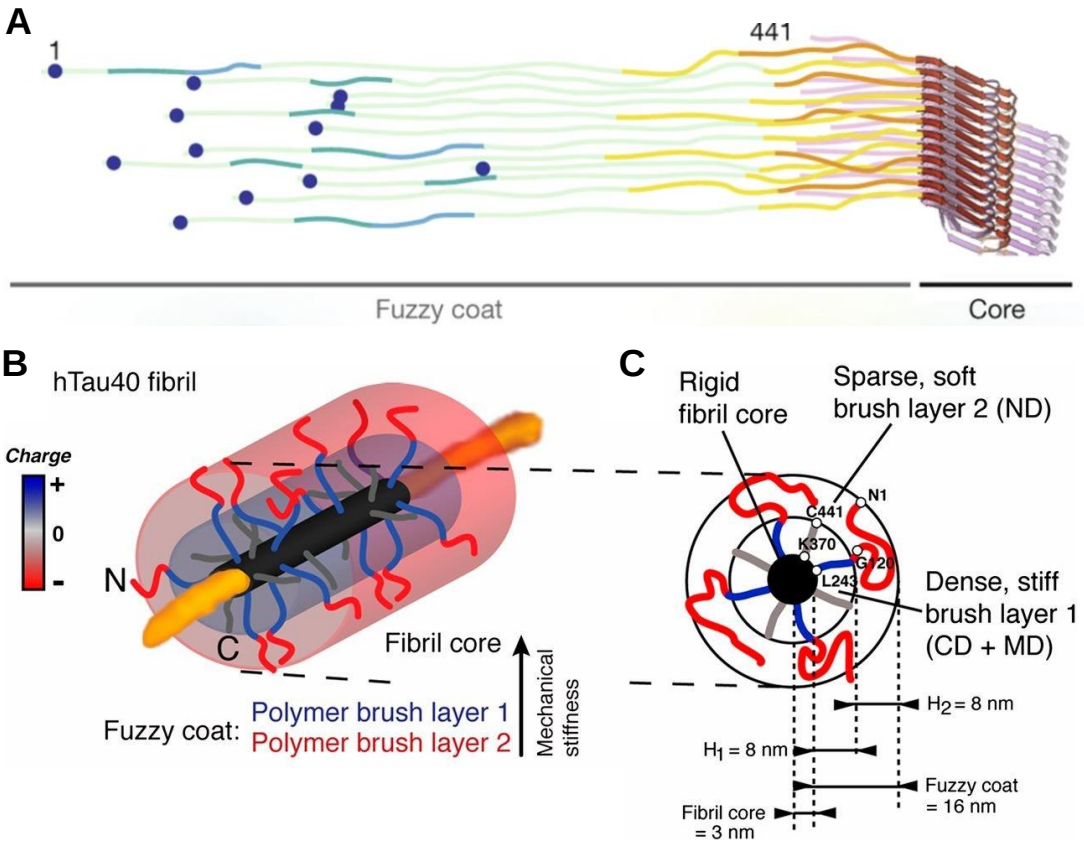

Figure 1.12 The fuzzy coat of Tau fibrils. A) Flanking regions in the N- and C- terminal side of the microtubule-binding domain do not participate in the β-sheet structure of the fibril core and form the fuzzy coat [from (Fitzpatrick et al., 2017)]. B) The fuzzy coat around Tau fibrils is composed of two polymer brush layers with different charges. C) Section through Tau fibril with four Tau molecules involved in the structure illustrating the rigid fibril core, stiff brush layer, and soft brush layer [from (Wegmann et al., 2013)].

Protease activity within cells, particularly in cells with proteinaceous inclusions and an active autophagy-lysosomal system, can lead to the digestion of fibrils primarily in the flanking regions of Tau's C- and N-terminus, while the core of the fibrils remains resistant to protease digestion (von Bergen et al., 2006). These "digested fibrils" lacking the flanking regions retain their high capability to induce aggregation, albeit with reduced size and adhesion, making them potential candidates for transmissible seeds. Factors such as physical pressure, specific protease activity, or self-disaggregation of fibrils can also cause breaks in the fibril core, forming short fibril fragments (Kundel et al., 2018). These "fragmented fibrils" with smaller size and aggregation-inducing potential can be considered potent Tau seed species (Jackson et al., 2016).

Sonicated fibrils derived from the MBD of Tau are short fibrils lacking the fuzzy that have been utilized as seeds to simulate the effects of "fragmented digested fibrils" (Guo & Lee, 2011; Michel et al., 2014; Strang et al., 2018). These sonicated fibrils have the seeding potential of normal fibrils but are smaller and less interactive thus more transmissible. They serve as a model for studying the propagation of Tau and its potential role as a transmissible seed.

In addition to fibrillar structures and fragmented/digested fibrils, intermediate aggregates with varying molecular weights and sizes can also be considered potential candidates for Tau seeds. Among these, small soluble oligomers of Tau that possess aggregation-inducing capacity have been identified in the brains of patients with various tauopathies (Gerson et al., 2014; Lasagna-Reeves, Castillo-Carranza, Sengupta, Sarmiento, et al., 2012; Ward et al., 2013). Given their presence in diseased brains, the soluble oligomers represent reasonable candidates for Tau spreading with both seeding and transmissibility features.

Traditionally, Tau monomers have not been considered pathology-inducing seeds. However, a study has challenged this notion by demonstrating that monomeric Tau obtained from an aggregation mixture is capable of inducing aggregation (Mirbaha et al., 2018). This study proposes that under physiological conditions, the aggregation-prone domain VQIINK/VQIVYK is not accessible in Tau monomers. However, this region becomes exposed in the seed-competent monomers, allowing for aggregation. Due to their high solubility, small size, and aggregation-inducing capacity, these monomeric Tau species could be potent candidates for seeding Tau pathology, however, further research is needed.

Although evidence supports Tau propagation in tauopathies, essential questions remain unanswered. It is unclear which form of Tau is the pathological spreading species and whether different strains contribute to distinct Tauopathies. The mechanisms of release and uptake of Tau seeds, and whether they propagate as vesicle-free or vesicle-associated entities, have yet to be fully understood. Furthermore, the extent of Tau spreading through diffusion in the ISF versus local transmission via synaptic connections is still debated. Despite these uncertainties, targeting eTau holds promise for therapeutic interventions in Tauopathies.

1.8 Tau uptake

1.8.1 Endocytic mechanisms

Previous studies suggested that under the physiological condition, Tau is present in the CSF as well as the extracellular medium of iPSC-derived neurons (Barthelemy et al., 2016; Sato et al., 2018), which is an unexpected observation considering the intracellular function of Tau. Prior studies also showed that Tau monomers and aggregates are efficiently internalized into neurons, suggesting that Tau entry into neurons is not a disease-specific phenomenon but a constitutive biological process (Evans et al., 2018). Nevertheless, the similarities and distinctions in cellular and molecular mechanisms of Tau monomers' and aggregates' uptake are still elusive.

Our understanding of the Tau species taken up by recipient cells is limited. Some studies suggest that small monomeric or oligomeric Tau species are preferentially internalized (Evans et al., 2018; Frost et al., 2009; Rauch et al., 2018; Usenovic et al., 2015; Wu et al., 2013), while others propose that only

high-molecular weight oligomeric and fibrillated Tau are internalized (Mirbaha et al., 2015; Takeda et al., 2015). Recent research has also shown that the isoform composition of extracellular Tau oligomers influences intracellular accumulation (Swanson et al., 2017). The specific cellular mechanisms involved in Tau uptake and intracellular accumulation are still under debate; however, various mechanisms have been proposed (**Figure 1.10**).

The process of macropinocytosis, a subtype of bulk endocytosis specialized in internalizing fluids and macromolecular structures, has been implicated in the cellular uptake of Tau fibrils (Holmes et al., 2013). It has been observed that eTau fibrils induce dynamic rearrangement of the plasma membrane, leading to the formation of macropinosomes.

Different uptake mechanisms with distinct kinetics have been proposed for monomeric and fibrillar Tau species. Monomeric Tau is suggested to enter neurons through a slow macropinocytosis mechanism dependent on actin polymerization, while monomeric and aggregated Tau species are proposed to enter neurons via dynamin-dependent endocytosis (Evans et al., 2018). Notably, the entry of aggregated Tau into neurons does not depend on actin, suggesting that it may not utilize macropinocytosis, as observed in non-neuronal cells (Holmes et al., 2013). Moreover, Tau uptake may occur through receptor-mediated endocytosis (Gomez-Ramos et al., 2009; Lasagna-Reeves, Castillo-Carranza, Sengupta, Guerrero-Munoz, et al., 2012; Wu et al., 2013).

Other mechanisms proposed for cell-to-cell Tau propagation include the formation of tunneling nanotubes between cells and the involvement of extracellular vesicles as shuttles (Clavaguera et al., 2015; DeLeo & Ikezu, 2018; Guix et al., 2018; Tardivel et al., 2016; Wang & Han, 2018). However, the specific uptake mechanisms through these routes still need to be better understood.

1.8.2 Molecular mediators

Despite many small-scale studies, few Tau uptake regulators are still known (**Figure 1.13**). Activation of M1/M3 muscarinic receptors by Tau increases intracellular calcium, which can trigger endocytosis of extracellular Tau (Gomez-Ramos et al., 2008). The extracellular domain of amyloid precursor protein has also been implicated in incorporating Tau fibrils into cells (Takahashi et al., 2015). Bridging

integrator 1 (BIN1) was also shown to be involved in the clathrin-mediated endocytosis of Tau (Calafate et al., 2016).

HSPGs have been known to play an essential role in the uptake of proteopathic Tau seeds (Holmes et al., 2013). A specific chain length and sulfation pattern of HSPGs are necessary to uptake Tau aggregates (Stopschinski et al., 2018). Macropinocytosis-mediated uptake of Tau is dependent on cell HSPGs, with 6-O-sulfation playing a critical role in the interaction between Tau and heparan sulfates (Holmes et al., 2013; Mirbaha et al., 2015; Stopschinski et al., 2018; Zhao et al., 2017). Inhibitors of HSPGs, such as soluble heparin, have been shown to decrease Tau uptake *in vitro* and *in vivo* (Holmes et al., 2013).

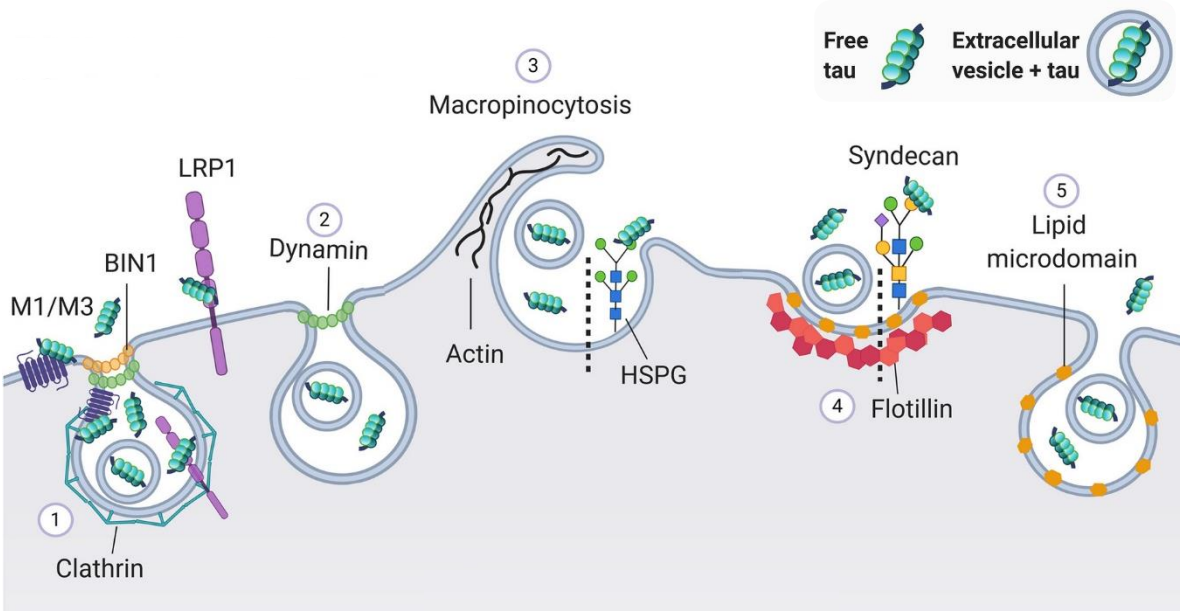

Figure 1.13 Molecular mediators of Tau uptake. 1) Muscarinic acetylcholine receptor subtype M1 and M3, and bridging integrator 1 (BIN1) are suggested to be involved in Tau uptake mediated by clathrin-coated pits. LDL-receptor-related protein-1 (LRP1) is also known as a receptor for clathrin-mediated endocytosis of Tau. 2) Dynamin is involved in clathrin-mediated and some sort of clathrin-independent endocytosis of Tau. 3) Actine polymerization and heparan sulfate proteoglycans (HSPGs) are involved in Tau macropinocytosis. 4) Lipid microdomains that exhibit a high cholesterol concentration and sphingolipids facilitate Tau entry through a process that relies on flotillins and Syndecan, a

member of the HSPG family. 5) Tau uptake via lipid microdomains can also be independent of flotillins [from (De La-Rocque et al., 2021)].

A recent study suggests that besides HSPGs, LDL-receptor-related protein-1 (LRP1) is a crucial mediator of Tau uptake (J. N. Rauch et al., 2020). In the study of Rauch et al., while the knockout of the LRP1 gene in iPSC-derived neurons completely blocked the uptake of monomeric Tau, the uptake of Tau fibrils was reduced only by 50%, suggesting the presence of unknown alternative uptake machinery for pathologic aggregates, which is independent of LRP1. Moreover, a study on the regulators of monomeric and fibrillar Tau uptake by using a whole-genome CRISPR knockout screen on iPSC neurons identified LRP1 as one of the two top-ranked genes required for monomeric Tau uptake. However, it was outside the 500 top-ranked genes needed for Tau aggregates' uptake (Evans et al., 2020). A more recent study also confirmed that LRP1 is not the only receptor of Tau (Cooper et al., 2021).

Some studies indicate the role of clathrin-independent endocytosis as a Tau internalization mechanism, which involves lipid microdomains enriched in cholesterol and sphingolipids on the plasma membrane, flotillin as alternative vesicle coating proteins, and syndecans as members of HSPG family (Hudak et al., 2019). Further research would be crucial for understanding the role of various molecular mediators on the uptake and spreading of Tau pathology.

2. Objective

In this project, we first aimed to study the neuronal uptake and accumulation of extracellular Tau monomers and aggregates to find similarities and distinctions between the physiological and pathological transport of Tau. For this purpose, we expressed and purified recombinant Tau protein and generated a Tau aggregated mixture. Next, to increase the accuracy of the study, we fractionated the Tau aggregated mixture and characterized various features of different Tau species by biophysical and biochemical techniques. Then we aimed to find the most promising candidate of Tau species to play the role of seed in pathology spreading by using various biological models including uptake assay, endosomal escape assay, and seeded aggregation assay. After finding the most reliable Tau seeding species, we aimed to compare the neuronal uptake and accumulation of pathogenic Tau seed and physiologic Tau monomers at cellular and molecular levels to address their similarities and distinctions.

3. Material and methods

3.1 Production of recombinant protein and aggregates

3.1.1 Generation and characterization of recombinant Tau protein

The Tau protein was obtained through expression and purification methods described by Goedert and Jakes with some modifications (Goedert & Jakes, 1990). Initially, Escherichia coli BL21 (Rosetta 2 (DE3), Merck) cells were transformed with the 2N4R Tau plasmid (pRK172) and cultivated in terrific broth supplemented with ampicillin at 37 °C. Tau expression was induced when the culture reached an optical density (OD) of 1-1.5 by adding 1 mM IPTG. After a 6-hour incubation at 37 °C and 180 rpm, the cells were harvested through centrifugation at 4000 g for 10 minutes at 4 °C. The resulting pellet was then resuspended in buffer A (20 mM MES pH 6.8, 50 mM NaCl, 1 mM MgSO4, 1 mM EGTA, 1 mM DTT, 1 mM PMSF) and frozen at -20 °C overnight. Subsequently, a freeze-thaw cycle was performed, followed by sonication of the suspension for 1 min/ml with 50% amplitude (UP200St, Hielscher). Streptomycin sulfate (MP Biomedicals) was added to a final concentration of 1%, and the lysate was clarified by centrifugation at 10,000 g for 10 minutes at 4 °C. The supernatant was collected, and NaCl was added to elevate the concentration from 50 mM to 200 mM. The resulting extract was boiled at 95 °C for 15 minutes, followed by incubation on ice for 10 minutes. The sediments were removed through centrifugation at 20,000 g for 10 minutes at 4 °C. The supernatant was collected and dialyzed overnight with two changes of buffer A. The semi-purified protein was loaded onto an SP HP HiTrap column (GE Healthcare) and eluted using a gradient of buffer B (20 mM MES pH 6.8, 500 mM NaCl, 1 mM MgSO4, 1 mM EGTA, 1 mM DTT, 1 mM PMSF) on an ÄKTA™ pure system (GE Life Sciences). The fractions obtained were analyzed using Bis-Tris SDS-PAGE (12%) and stained with Imperial protein stain (Thermo Fisher Scientific). The pooled fractions were concentrated using a 10 kDa Vivaspin 15R concentrator (Sartorius) and purified further using a Superdex 200 Increase 10/300 GL column (GE Healthcare) pre-equilibrated with PBS. Elution from the column was performed at a flow rate of 0.3 ml/min, and the fractions were analyzed by measuring absorbance at 215 nm. The concentration of the pooled fractions was determined using the Bicinchoninic acid (BCA) assay kit (Thermo Fisher

Scientific). Finally, the recombinant protein was diluted to 6 mg/ml concentration, aliquoted, and stored at -80 ^{o}C following a snap-freezing step in liquid nitrogen.

3.1.2 Biochemical labeling of Tau monomers and aggregates with fluorescent tags

Tau monomers, at a concentration of 3 mg/ml (~65 μM), were labeled using ATTO488-NHS ester or ATTO633-NHS ester fluorescent dyes (ATTO-TEC, Siegen, Germany) following the manufacturer's instructions. The protein solution was adjusted to pH 8.3 using a 0.2 M sodium bicarbonate solution (Sigma-Aldrich) and incubated with 200 μM dye at room temperature for 1 hour in the dark. Unbound dye molecules were removed using Bio-Spin 6 size exclusion spin columns (Bio-Rad Laboratories).

Two approaches were employed for labeling Tau aggregates:

A) In the "pre-aggregation labeling" approach, 10% of pre-labeled monomers (~1 label per monomer) were mixed with 90% of unlabeled monomers before incubation in the fibrillation conditions.

B) In the "post-aggregation labeling" approach, the aggregated mixture obtained after the fibrillation process was incubated with 200 μM ATTO dye, following a similar protocol to the monomer labeling. Excess unbound labels were removed through washing steps during the fractionation process.

The success of labeling was verified by running the protein on SDS-PAGE followed by fluorescence imaging. The degree of labeling (DOL) was calculated using **Equation 3.1**:

$$\mathrm{DOL} = \frac{A_{max} \times \mathrm{MW}}{[\mathrm{Protein}] \times \varepsilon_{dye}} \qquad \text{(Eqn. 3.1)}$$

where A_{max} represents the absorbance of ATTO488 at 500 nm, MW is the molecular weight of 2N4R Tau (21.8 kDa), [Protein] is the concentration of Tau protein, and ε_{dye} is the extinction coefficient of the dye at its maximum absorbance (ATTO488 = 90,000). The protein concentration of Tau was determined using the BCA assay.

3.1.3 Induction of amyloid fibrillation in recombinant Tau protein

A mixture containing 3 mg/ml of 2N4R Tau (~65 μM) and 130 μM Heparin (~3000 kDa, MP Biomedicals) was prepared in PBS buffer at pH 7.4, supplemented with 1 mM DTT to induce Tau

fibrillation in a 2 ml microtube at 37 °C. Roughly 100-200 µl of the mixture was subjected to shaking at 1400 rpm with a 3 mm glass bead using a Thermomixer (Eppendorf Thermomixer) to accelerate the process.

The kinetics of fibrillation were monitored over time by periodically sampling the mixture and measuring thioflavin T (ThT) fluorescence. For ThT analysis, 2 µl of the aggregation sample was mixed with 98 µl of 10 µM ThT in 10 mM Tris at pH 8.0. Fluorescence measurements were performed in a black 96-well plate using a CLARIOStar microplate reader (BMG Labtech, Offenburg, Germany) at the excitation wavelength (Ex) 488 nm and emission wavelength (Em) 520 nm. The obtained ThT fibrillation data were fitted after normalization using the Finke-Watzky equation (Morris et al., 2008) (**Equation 3.2**):

$$F(t) = \frac{1}{1+e^{-\nu\,(t-t_{1/2})}} \qquad \text{(Eqn. 3.2)}$$

where $t_{1/2}$ is the time required to produce half the total product, and ν is the growth rate.

3.1.4 Induction of amyloid fibrillation in bovine serum albumin (BSA)

BSA was dissolved in 20 mM Tris buffer at pH 7.4 to 5 mg/ml. Then 100-200 µl volume of this mixture was incubated in a 2 ml microtube with a 3 mm glass bead using a Thermomixer (Eppendorf Thermomixer) set at 70 °C with 1000 rpm shaking.

4% BSA-CF488A (Biotium) was added to 96% unlabeled BSA prior to incubation under the fibrillation conditions to generate fluorescent BSA aggregates. This mixture was then subjected to the same incubation conditions mentioned above. The formation of amyloid fibrils was confirmed using the PROTEOSTAT® Protein aggregation assay (ENZ-51023, Enzo).

3.1.5 Isolating different Tau aggregated species via physical fractionation

The aggregates obtained from the fibrillation process of labeled or unlabeled Tau were separated into four fractions: large fibrils (L-fib), small fibrils (S-fib), soluble oligomers (Oligo), and fibrillation-derived monomers (F-mono), using the following stepwise procedure:

I) The fibrillation mixture was transferred to 1.5 ml microtubes in 100-150 µl portions and centrifuged at 16,000 g for 1 hour at 4 °C. The resulting pellet was dispersed and washed twice with 100 µl of PBS using the same centrifugation setting. This pellet was dispersed in PBS, resulting in a large fibrils (L-fib) fraction.

II) The supernatant obtained from step one was collected and transferred to 1.5 ml Eppendorf ultracentrifuge tubes in portions of 100 µl. It was then subjected to ultracentrifugation at 100,000 g for 30 minutes at 4 °C. The resulting pellet was dispersed and washed with 100 µl of PBS using the same centrifugation setting. The final pellet was dispersed in PBS, forming the small fibrils (S-fib) fraction.

III) The supernatant obtained from the second step was collected and filtered through a 100 kDa ultrafilter (Amicon Ultra 0.5 ml, Millipore) in 100-500 µl portions for 10 minutes at 4 °C. The retained phase was washed twice with 500 µl of PBS, concentrated, and referred to as soluble oligomers (Oligo).

IV) The pass-through of step three was concentrated and washed twice with 500 µl of PBS using a 10 kDa ultrafilter (Amicon Ultra 0.5 ml, Millipore). The final concentration results in a fibrillation-derived monomers (F-mono) fraction.

The labeling efficiency and protein concentration were determined, as mentioned in section 3.2. However, the aggregates were first treated with 3 M Guanidine hydrochloride to unfold the fractions content before analysis.

3.2 Characterization of aggregates

3.2.1 Dot-blot immunoassay for detection of conformationally changed Tau

Samples were collected at various stages of the fibrillation process or after fractionation, diluted 1:15 in PBS, and then applied to a 0.2 µm nitrocellulose membrane (Bio-Rad Laboratories) using a dot blot chamber (11055, Life technologies). After loading, the membranes were washed three times with PBS, released from the chamber, and blocked for 1 hour at room temperature using 30% Roti-Block solution (Carl Roth, Karlsruhe, Germany). Following the blocking step, the membranes were incubated overnight at 4 °C with primary antibodies while continuously agitated. After three washes with Tris-buffered saline supplemented with 0.05% Tween-20 (TBST) from Sigma-Aldrich, HRP-coupled secondary antibodies

were added and incubated at room temperature for 1 hour. Subsequently, the membranes underwent another round of washing steps in TBST. The membranes were incubated for visualization in Clarity Western ECL Substrate (Bio-Rad Laboratories), and imaging was performed using the Odyssey Fc imaging system (LI-COR Biotechnology).

In this study, the primary antibodies used were as follows: Tau-5 (1:1000; MAB361, Merck Millipore, Billerica, MA) as a general monoclonal anti-Tau antibody; TNT-1 (1:1000; MABN471, Merck Millipore, Billerica, MA), which specifically identified the phosphatase-activating domain in the N-terminal region of Tau, exposed only in a pathological conformation (Kanaan et al., 2011); TOMA-1 (1:500; MABN819, Merck Millipore, Billerica, MA) an anti-Tau oligomer-specific conformational antibody (Castillo-Carranza et al., 2014); MC1 (1:500; a gift from Dr. Peter Davis), which indicated a pathological conformation by binding to two discontinuous Alzheimer's disease-specific epitopes in the N-terminal and microtubule-binding domain (Jicha et al., 1997). The secondary antibody for all was an HRP-linked anti-mouse IgG (1:2000; Vector Laboratories, Burlingame, CA).

3.2.2 Size exclusion chromatography

Superdex 200 Increase 10/300 GL columns (GE Healthcare) were pre-equilibrated with two column volumes of elution buffer (PBS) for size exclusion chromatography. Samples at a concentration of 0.1 mg/ml were loaded onto the columns using an ÄKTA™ pure system (GE Life Sciences), and the chromatography was run at a flow rate of 0.5 ml/minute. The elution profile was monitored at wavelengths of 214 nm and 280 nm. Fractions were collected from the chromatography and subjected to further analysis using dot-blot assay and DLS.

3.2.3 Dynamic light scattering (DLS)

DLS measurements were performed using a Malvern Zetasizer-Nano instrument. The measurements were conducted on a water suspension of the samples at a concentration of 0.03 mg/ml, and the device utilized a 4 mW He-Ne laser (633 nm).

3.2.4 Atomic force microscopy (AFM)

AFM imaging was conducted using the NanoWizard® 4 system (JPK, Berlin, Germany), coupled with SPM software and an integrated Axiovert 200 inverted microscope (Zeiss, Jena, Germany). qp-BioAC-CB1 cantilevers (NanoWorld, Neuenburg, Switzerland) with a resonance frequency of 90 kHz and a spring constant of 0.3 N/m were utilized. The cantilevers were calibrated using the contact-free method. AFM imaging was performed in air at ambient temperature after diluting the samples in distilled water. The diluted samples were dried on freshly prepared surfaces of the highest grade V1 AFM Mica Discs (Ted Pella) and washed thrice with distilled water. The imaging parameters included setpoint values of 0.4-0.6 nN, z-lengths ranging from 86 to 126 nm, and pixel times of 2.2-5.5 ms. The acquired images were processed, optimized, and zoomed in using the data processing software version 6.0.50 (JPK, Berlin, Germany). The processing steps involved subtracting a polynomial fit from each scan line independently, replacing outlier pixels with the median value of neighboring pixels, and applying a low-pass filter (2-dimensional Savitzky–Golay smoothing; smoothing width: 5, order: 4).

3.2.5 Transmission electron microscopy (TEM)

TEM of Tau aggregates followed a previously described protocol (Mohammad-Beigi et al., 2020). Briefly, 3 µl of Tau aggregates were loaded onto glow-discharged 400 mesh Formvar/carbon grids (EM resolutions) and allowed to adhere for 20 seconds. The grids were blot-dried and stained three times with uranyl formate (3 µl, 15 seconds for each time). TEM imaging was performed using a Tecnai G2 Spirit BioTWIN microscope (FEI) operating at 120 kV acceleration. Images were captured with a TemCam-F416(R) CMOS camera (TVIPS).

3.2.6 UV-circular dichroism (UV-CD)

UV-CD spectroscopy of different fractions of Tau aggregates was carried out using a Chirascan V100 CD spectrometer (Applied Photophysics). Protein samples of 2-6 µg were loaded into a 1-mm path-length cuvette, and UV-CD spectra were recorded between 180 and 280 nm with a step size of 1 nm and a scanning speed of 10 nm/min. The measurements were performed at room temperature.

3.3 Cell culture and analysis

3.3.1 Culturing and differentiation of induced pluripotent stem cells derived neurons (iPSCNs)

Small molecule neuroprogenitor cells (smNPCs) were generated from induced pluripotent stem cells to facilitate lentiviral transduction and enable easy identification. This was achieved through embryoid body formation and stable integration of an inducible NGN2 vector, as previously described (Dhingra et al., 2020; Strauss et al., 2021). The NGN2_smNPCs were cultured in N2B27 medium supplemented with specific components: 48.425% DMEM/F12 Medium, 48% Neurobasal Medium, 0.5% N2-supplement, 1% B27 supplement without Vitamin A (Life Technologies, Carlsbad, CA, United States), 0.025% Insulin (Sigma-Aldrich, St. Louis, MO, United States), 0.5% Non-essential amino acids, 0.5% GlutaMax, 1% Penicillin/Streptavidin (Life Technologies, Carlsbad, CA, United States), and 0.05% β-Mercaptoethanol. The medium was supplemented with 0.5 µM Purmorphamine, 3 µM CHIR99021, and 64 µg/ml ascorbic acid (Th. Geyer, Renningen, Germany). The cells were maintained at 37 °C with 5% CO2 throughout expansion and differentiation in a tissue culture incubator.

For neuronal differentiation, plates were coated with 100 µg/ml Poly-L-ornithine diluted in 0.1 M borate buffer (pH 8.4) and were incubated overnight at 4 °C. Subsequently, the plates were incubated with 10 µg/ml Laminin at 37 °C. NGN2_smNPCs were directly seeded onto the coated plates in an induction medium composed of N2B27 medium supplemented with 2.5 µg/ml doxycycline and 2 µM DAPT. At day 3, the entire medium was replaced with N2B27 medium supplemented with 2.5 µg/ml doxycycline, 10 µM DAPT, 10 ng/ml BDNF, 10 ng/ml GDNF, 10 ng/ml NT3 (PeproTech, Princeton, NJ, United States), and 0.5 µg/ml laminin. From day 6 onwards, the medium was changed by 50% every 3 days with fresh differentiation medium excluding doxycycline and DAPT.

3.3.2 Culturing and differentiation of Lund human mesencephalic (LUHMES) cells

LUHMES cells were cultured in EasYFlasks (Nunclon DELTA, VWR, Darmstadt, Germany) coated with 50 µg/ml poly-L-ornithine, as previously described (Lotharius et al., 2005). The expanding medium

used for culture consisted of DMEM-F12 supplemented with 1% N2 supplement and 0.04 µg/ml basic fibroblast growth factor (bFGF; PeproTech, Rocky Hill, CT).

For differentiation, plates were prepared by coating them with 50 µg/ml poly-L-ornithine first and then with 5 µg/ml bovine fibronectin (Sigma-Aldrich). The cells were directly seeded onto these coated plates in the differentiation medium, which consisted of DMEM/F12 with 1% N2 supplement, 1 µg/ml tetracycline, 0.5 µg/ml dibutyryl cyclic-AMP (Sigma-Aldrich), and 2 ng/ml glial cell-derived neurotrophic factor (GDNF; R&D Systems, Minneapolis, MN).

Throughout both the expansion and differentiation stages, the cells were maintained at 37°C with 5% CO2 in a tissue culture incubator.

3.3.3 Isolation and culturing of mouse primary cortical neurons

Cortices were collected from embryonic mice at the developmental stage of E16-E17. These tissues were subjected to incubation in a digestion medium composed of DMEM containing 200 U of papain and 1 mg/mL L-cysteine, with a pH of 7.4. The incubation was carried out at a temperature of 37°C for a duration of 20 minutes. Subsequently, the digested tissues underwent mechanical dissociation in a plating medium consisting of DMEM containing 10% FBS and 1% penicillin/streptomycin. The dissociated cells were then plated onto transparent-bottom black 96-well plates coated with 25 µg/mL of poly-D-lysine. The plating density was set at 100,000 cells per well. Four hours after plating, the medium was replaced with Neurobasal medium supplemented with 2% B27, 1% penicillin/streptomycin, 0.5 mM GlutaMAX, and 1 µM AraC. The neurons were maintained in a cell culture incubator with a temperature of 37°C and a CO2 concentration of 5% until they were treated with Tau and analyzed.

3.3.4 Cell viability assay

smNPCs were differentiated in transparent bottom black 96-well plates (PerkinElmer) to investigate the toxicity of Tau species. On days 13-15 of differentiation, the cells were treated with 250 nM of Tau species (equivalent to monomer concentration) for 24 hours. After removing the media, cell viability was assessed using the cell viability indicator of the neural outgrowth staining kit according to the manufacturer's instructions (A15001, Life Technologies).

Fluorescence measurements were performed using a CLARIOStar microplate reader (BMG Labtech, Offenburg, Germany) with a bottom matrix of 15 × 15. The fluorescence signals were recorded at an excitation wavelength of 480 nm and an emission wavelength of 520-535 nm.

3.3.5 Biosensor assay for Tau endogenous aggregation

The endogenous aggregation was induced in HEK293T cells overexpressing mutant P301S 0N4R Tau, C-terminally tagged with Venus protein, via the following procedure as previously described (McEwan et al., 2017). HEK293T cells were cultured in complete DMEM (C-DMEM) supplemented with 10% (vol/vol) FCS, 100 U/ml penicillin, and 100 μg/ml streptomycin at 37 °C in a 5% CO2 atmosphere.

Transparent bottom black 96-well plates (PERK6055302, PerkinElmer) coated with poly-L-lysine (Sigma, P4707) were used for the Tau seeding assay. The cells were seeded in C-DMEM on day 2. The wells were washed twice with PBS, and Tau seeding was induced by adding OptiMEM (Gibco™, 51985026) containing 1% (vol/vol) Lipofectamine 2000 (Life Technologies) and 400 nM (equivalent monomer concentration) of Tau species for 1 hour. After seeding, the seeding medium was removed, and C-DMEM was added. On day 4, the media were changed to FluoroBrite DMEM (Gibco™, A1896701) containing 1X BackDrop background suppressor (Thermo Fisher Scientific, B10512). The cells were then imaged using a fluorescence microscope and plate reader.

3.3.6 Neuronal entry assay

First, 0N4R P301S-Tau-HiBiT were fibrillated to form Tau aggregates and fractionated to generate four different fractions of L-fib, S-fib, Oligo, and F-mono using the abovementioned method. Next, the neuronal entry assays were conducted following the methodology described in a previous study (Tuck et al., 2022). Primary neurons were prepared from postnatal mouse pups at day 0/1 C57BL/6. At 2 days *in vitro* (DIV), the neurons were infected with AAV1/2 hSyn::-eGFP-P2A-LgBiT-nls particles at a multiplicity of 50,000 genome copies per cell. On DIV 7, Tau-HiBiT treatments were prepared in maintenance media at 2 μg/ml concentration.

For the *in vitro* reconstitution assay, 50% of the media was used, and the total signal in the maintenance media (RLU in media) was quantified by adding excess recombinant LgBiT for 30 minutes. The remaining media was used for the neuronal entry assays. Neurons were subjected to 100% media change

and incubated with Tau-HiBiT preparations for a specific duration as indicated. The cytosolic entry of Tau was quantified (RLU in cells) and followed by incubation for 42 minutes with PrestoBlue cell viability reagent according to the manufacturer's instructions (Thermo Fisher Scientific). Fluorescence intensity was measured using a CLARIOstar microplate reader (BMG Labtech) with excitation at 540-570 nm and emission at 580-610 nm. The total viable cells per well were calculated using a standard curve of viable cells per well and adjusted for background fluorescence. The percentage of cytosolic entry normalized to cells was determined by dividing the RLU in cells by RLU in media and normalizing it to the total viable cells per well.

3.3.7 Uptake and accumulation assay

To initiate differentiation, smNPCs or LUHMES cells were seeded in a black clear-bottom 96-well tissue culture plate (PerkinElmer, PERK6055302). These cells were then treated with fluorescently labeled (FL) Tau monomers, aggregates, or fractions. The specific concentrations and incubation times varied across different experiments and were detailed in the results section.

Following the treatment, the FL-Tau media was removed from each well. Subsequently, 100 µl of FluoroBrite DMEM (Gibco™, A1896701) supplemented with 1X BackDrop background suppressor (Thermo Fisher Scientific, B10512) was added to facilitate fluorescence measurements. The fluorescence of the ATTO488 label was measured using a CLARIOStar microplate reader (BMG Labtech, Offenburg, Germany). The excitation wavelength was set at 490 nm, and emission was detected within 510 - 530 nm. A matrix of 15 × 15 was scanned from the bottom of the wells to capture fluorescence intensities. The values obtained from each well were adjusted by subtracting the background fluorescence of untreated cells, which served as a blank, to normalize the fluorescence readings. Representative fluorescence images were also captured using live imaging through a Leica DMI6000 B microscope (Leica Microsystems, Germany).

In order to ensure the comparability of cellular uptake and accumulation among different treatments and conditions, the viability of the cells was assessed using the calcein viability assay, as previously mentioned. The treatment conditions were carefully adjusted to remain within the non-toxic range, allowing for accurate evaluation of the cellular responses.

Comparing the uptake of Tau monomers and aggregated mixtures: recombinant 2N4R Tau monomers were first labeled with ATTO488. The labeled monomers were then mixed with unlabeled monomers in a ratio of 1:9. This mixture was divided into two parts: part A, which was kept at 4 °C as monomers, and part B, which was subjected to incubation under fibrillation conditions as aggregates (referred to as "pre-aggregation labeling" in section 3.2). Next, iPSCNs at day 13-18 of differentiation were treated with parts A (Mono) and B (Agg) at various concentrations and different incubation times at 37 °C to examine the kinetics and titration of Tau uptake.

Comparing the uptake of Tau fractions: The Tau fractions were labeled using the "post-aggregation labeling" strategy described in section 3.2 to compare the uptake of Tau fractions. Both iPSCNs at day 13-18 of differentiation and LUHMES at day 6-8 of differentiation were treated with labeled fractions at different concentrations and incubation times to study the kinetics and titration.

Tau uptake competition assay: cells were treated with either 50 or 100 nM (Monomer equivalent) of ATTO488 labeled Tau monomers or small fibrils. Simultaneously, they were treated with 4- or 5-times higher concentrations of unlabeled monomers or small fibrils for a duration of 16-20 hours. Due to the lower uptake of monomers compared to small fibrils, a 10-fold higher degree of labeling (labeling efficiency: ~2) was used for FL-Mono, compared to the FL-aggregates (labeling efficiency: ~0.1-0.2).

Pre-treatment experiments: LUHMES cells on day six were treated with 100 µM Heparin, 250 nM monomers, or 150 nM small fibrils (Monomer equivalent) for two hours. Subsequently, the media was removed, and the cells were washed once with PBS before being treated with fluorescently labeled Tau monomers or small fibrils.

Small molecules treatment: iPSCNs at days 13-18 and LUHMES neurons at days 6-8 of differentiation were treated with the small molecules listed in **Table 3.1A**, with a specified concentration for 30 minutes. After a washing step with 100 µl of PBS, the cells were incubated with 250 nM Tau for 3 hours. In the case of the small molecules in **Table 3.1B**, cells were co-treated with the small molecules at a specified concentration and Tau at 25-50 nM for 18-20 hours.

Table 3.1 List of small molecules.

Name	Company	Catalog
A		
Chlorpromazine	Santa Cruz	sc-357313
Cytochalasin D	MP Biomedicals	0215077101
5-(N-Ethyl-N-isopropyl) -Amiloride (EIPA)	Santa Cruz	sc-202458
Dyngo-4a	selleckchem	S7163
Genistein	Santa Cruz	sc-3515
Nystatin	Sigma	N6261
B		
bafilomycin A1	Santa Cruz	sc-201550A
Chloroquine diphosphate salt	Sigma	C6628
MG132	Tocris Bioscience	1748
Atropine Sulfate	Sigma	PHR1379
Pirenzepine Dihydrochloride	Sigma	15378983
Heparin sodium salt ~3000 kDa	MP Biomedicals	19411480

Dyngo-4a impact on LUHMES neurons: Cells were treated with increasing concentrations of Dyngo-4a (ranging from 1 to 5 µM) for 30 minutes. After one washing step, neurons were treated with 100 µM Dextran-fluorescein isothiocyanate (Dextran-FITC) or 5 µM low-density lipoprotein-BODIPY (LDL-BODIPY) for 3 hours. Parallel cells were treated with a standard medium for 3 hours and then incubated with 0.1 µM calcein green for 30 minutes to assess viability.

Gene-knockdown experiments: cells were treated with 10 nM siRNAs targeting LRP1, EXT1, EXT2 (siPOOLs from siTOOLs), and VPS35 (Silencer Select siRNAs from Thermo Fisher Scientific). The treatment was performed in the presence of 0.075 µl/well of RNAiMax lipofectamine (Thermo Fisher Scientific, 13778075) in a 1:1 mixture of differentiation medium and OptiMEM for 24 hours. The siRNA treatments were conducted on day 2 post-seeding, and the media was changed the following day. Neurons at day 6-8 of differentiation were then treated with 25-50 nM (Monomer equivalent) of Tau monomers and small fibrils for 18-20 hours. The knockdown was confirmed by immunocytochemistry.

3.3.8 Confocal imaging

For the experiments, smNPCs and LUHMES were seeded on 8-well ibidi µ-slides (ibidi, Gräfelfing, Germany) and incubated in the differentiation medium for 15 and 7 days, respectively. After differentiation, neurons were treated with ATTO633-labeled Tau Mono and ATTO488-labeled Tau S-fib for 3 hours. Imaging was conducted either immediately after the treatment or 21 hours later. In the latter case, cells were washed and then incubated in the differentiation medium until imaging. Prior to imaging, the cells were stained with 1 µM Cell TraceTM Calcein Red-Orange (Thermo Fisher Scientific) for 30 minutes. Subsequently, the media were replaced with FluoroBrite DMEM containing 1X BackdropTM background suppressor (Thermo Fisher Scientific). Live Z-stack images were captured using a Zeiss LSM 880 microscope (Carl Zeiss, Oberkochen, Germany) equipped with a 63x oil immersion objective and 2X digital zoom.

3.4 Statistical analysis

Statistical analysis was conducted using GraphPad Prism 8.0.2 (GraphPad Software, La Jolla, CA, USA) or the Excel data analysis package. The data in the figures are expressed as mean ± standard error of the mean (SEM). For data analysis, one-way ANOVA followed by Dunnett's post hoc test was employed, except for the siRNA experiment, in which two-way ANOVA followed by the Sidak test was utilized. Statistical significance was defined as p-values less than 0.05.

4. Results

4.1 Production and analysis of recombinant Tau aggregates induced by heparin

To examine the uptake and accumulation of extracellular Tau (eTau), we produced a monomeric form of recombinant 2N4R Tau protein and induced the formation of amyloid aggregates using heparin-induced *in vitro* fibrillation. The confirmation of aggregate formation was achieved by utilizing thioflavin-T (ThT) as a marker for β-sheet conformation (**Figure 4.1A**). We validated the pathological relevance of these aggregates through dot-blot immunoassay, employing conformation-specific Tau antibodies such as MC1 (indicative of pathological Tau conformation), TNT-1 (recognizing pathological misfolded Tau), and TOMA (targeting oligomeric Tau). Throughout different stages of fibrillation, the heparin-induced Tau aggregates were detected by all the conformation-specific Tau antibodies (**Figure 4.1B**).

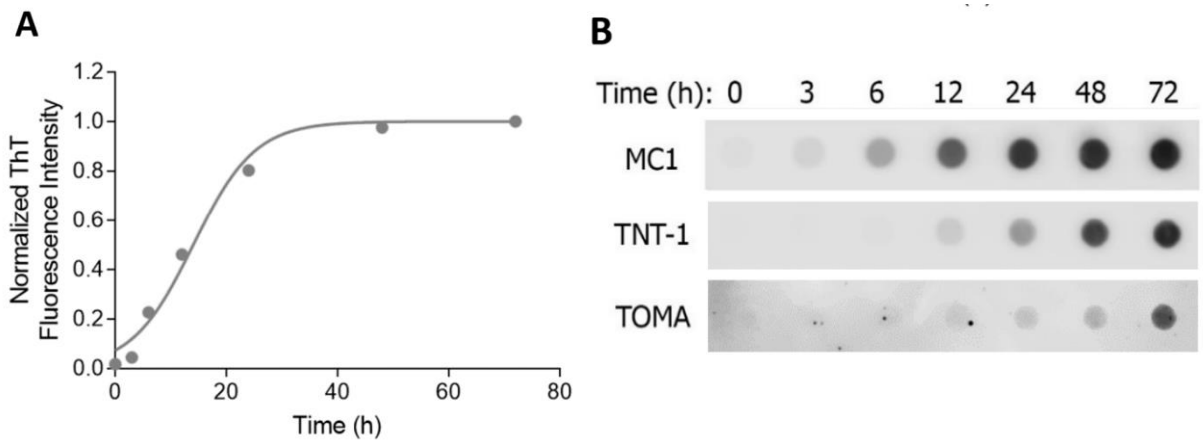

Figure 4.1 Characterization of recombinant Tau protein fibrillation process. A) The fibrillation kinetics of recombinant human 2N4R Tau, monitored using Thioflavin T (ThT) fluorescence. The data is fitted with the Finke-Watzky model, which describes a two-step nucleation-autocatalysis process. B) Dot-blot analysis of Tau aggregates at various time points during the fibrillation process depicted in Panel A. The analysis utilizes three conformation-sensitive Tau antibodies (MC1, TNT-1, and TOMA) to detect the aggregates.

After 72 hours of fibrillation, atomic force microscopy (AFM) examination revealed the presence of various aggregated structures, including long and short fibrils as well as oligomers in the fibrillation mixture (**Figure 4.2A**). By employing size exclusion chromatography (SEC) combined with immunoassay on the soluble fraction of the aggregation mixture, we identified a peak of high molecular weight species that reacted with both the total Tau antibody (Tau5) and MC1, indicating the existence of soluble oligomeric species (**Figure 4.2B and C**). Dynamic light scattering measurements on SEC fractions of monomeric and oligomeric Tau demonstrated that the average hydrodynamic sizes of monomers and oligomers were 7.86 ± 1.54 nm and 36.92 ± 11.07 nm, respectively (**Figure 4.2D**).

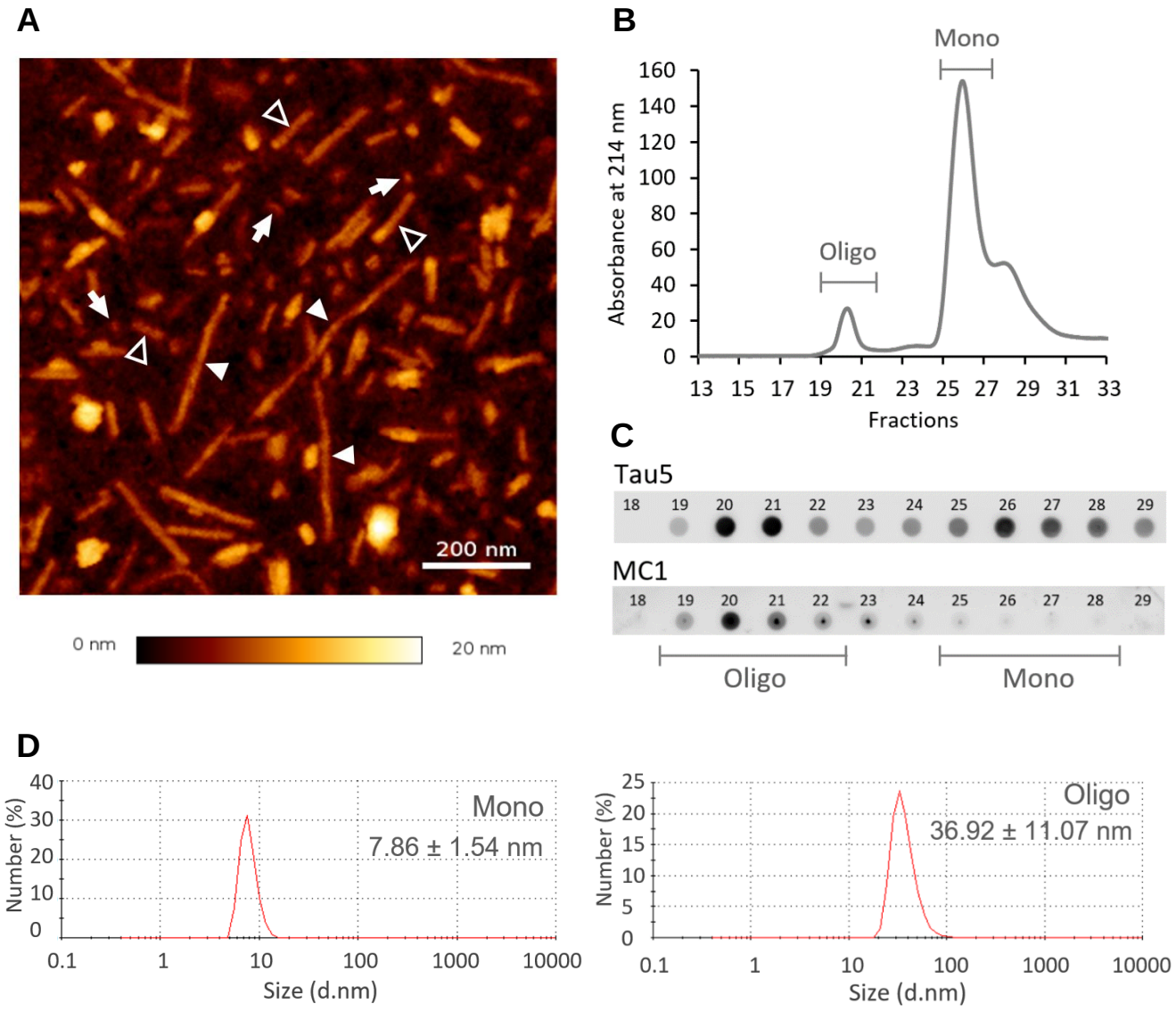

Figure 4.2 Characterization of recombinant Tau aggregates. A) Atomic-force microscopic image of a mixture of aggregates obtained after 72 hours of fibrillation. Filled arrowheads indicate large fibrils, small fibrils are indicated by open arrowheads, and oligomers are indicated by arrows. The scale bar represents 200 nanometers. B) Size-exclusion chromatography (SEC) analysis of the soluble fraction of the aggregates. Insoluble fibrils have been removed through ultracentrifugation. The graph depicts the absorbance at 214 nanometers in the eluting fractions, which include Tau oligomers (Oligo) and monomers (Mono). C) Dot-blot analysis of the SEC fractions from Panel B using the antibodies Tau5 and MC1. D) Dynamic-light scattering measurements performed on the Mono and Oligo Tau species obtained from SEC. The graph illustrates the hydrodynamic size distribution of the soluble Tau species, with the diameter represented in nanometers (d.nm).

4.2 Examining the cellular accumulation of Tau monomers and aggregates in induced pluripotent stem cell-derived neurons (iPSCNs)

To monitor Tau uptake and intracellular accumulation in neurons, we developed an assay using recombinant monomeric and aggregated Tau in iPSCNs. **Figure 4.3A** illustrates that cultured cortical neurons were incubated with fluorescently labeled Tau (Tau-ATTO488 NHS-ester). Before measurement, the differentiation media were replaced with a low-fluorescence medium containing a non-permeable fluorescence quencher to eliminate background fluorescence caused by fluorescent eTau sticking to cell surfaces, which could interfere with intracellular fluorescence measurement. A quencher's presence is critical because the fuzzy coat of Tau aggregates is composed of a highly interactive, sticky surface that is challenging to remove (Wegmann et al., 2013). Live fluorescence imaging and quantification using a fluorescence plate reader demonstrated that the quencher significantly reduced the background fluorescence of Tau-treated iPSCNs, particularly for Tau aggregates (**Figure 4.3B and C**). Additionally, fluorescence imaging confirmed the presence of fluorescent Tau protein only in association with cell bodies or neurites, proving the validity of the assay (**Figure 4.3D**).

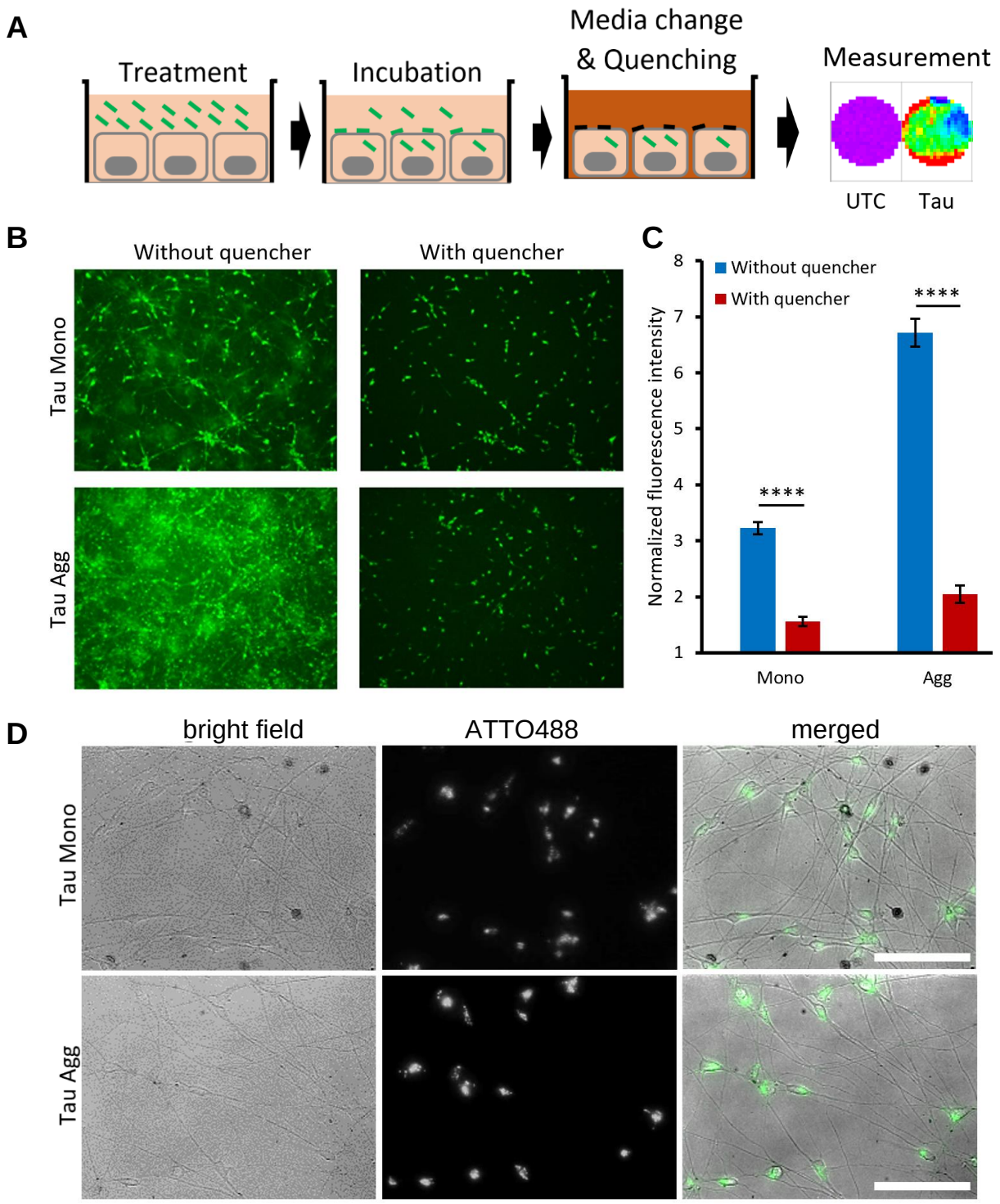

Figure 4.3 Tau uptake and accumulation assay in iPSC-derived neurons. A) A schematic representation of the uptake and accumulation assay is shown. Cells are initially treated with Tau labeled with the fluorescent dye ATTO488. After a specific incubation

period, the culture medium is replaced with a quenching medium, eliminating the extracellular fluorescence while preserving the intracellular fluorescence. The fluorescence emitted from the cells is then quantified using a fluorescence plate reader, with the cells being cultured in a 96-well plate with a transparent bottom. B) iPSC-derived neurons were treated with either 100 nM Tau monomers (Mono) or aggregates (Agg) for 48 hours. The images capture the fluorescence signal emitted by the cells in the presence and absence of a quencher. C) The measurements of the same experiment were obtained using a plate reader, and the fluorescence values are presented in the presence and absence of the quencher. Error bars represented SD; n=4 per experimental condition. One-way ANOVA followed by a post-hoc test; ****$p<0.0001$. The fluorescence values were normalized to the background signal. D) Live images of iPSCNs (DIV 15) are presented. The cells were treated with either ATTO488-labeled Tau monomers or aggregates, both at a concentration of 100 nM, for a duration of 24 hours in the presence of the quencher. The scale bar in the image represents 100 µm.

Previous studies have suggested that monomeric and aggregated Tau species utilize distinct but overlapping mechanisms for cellular uptake (Evans et al., 2018). However, the efficiency of intracellular accumulation after prolonged incubation periods of one day or more has not been reported. In our experimental setup, iPSCNs were treated with native Tau monomers or heparin-induced aggregates. After adding the quencher, fluorescence was measured to indicate the quantity of internalized protein. Examining the time course of extracellular Tau species' interaction with cells revealed a higher rate of intracellular accumulation for aggregates compared to monomers (**Figure 4.4A**). Similarly, incubating iPSCNs with increasing concentrations of Tau for 24 hours demonstrated distinct saturation levels for both monomers and aggregates in terms of intracellular accumulation.

Interestingly, the saturation level was much higher for aggregates than monomers (**Figure 4.4B**), despite an equal labeling efficiency for both monomers and aggregates. As described in the methods section, aggregates were formed from the same pool of labeled monomers during the labeling process, thus having the same labeling efficiency. The equal labeling rate ensures the comparability of the results, indicating that more Tau protein aggregates accumulated in neurons over time compared to monomers. The comparison of intracellular fluorescence intensity reflects the protein mass rather than the moles of internalized fibrils since one fibril molecule comprises ten to thousands of monomers. Our findings

suggest that Tau protein accumulates more rapidly in iPSCNs when it is in pathologic aggregated form compared to when it is in the physiological native monomeric form.

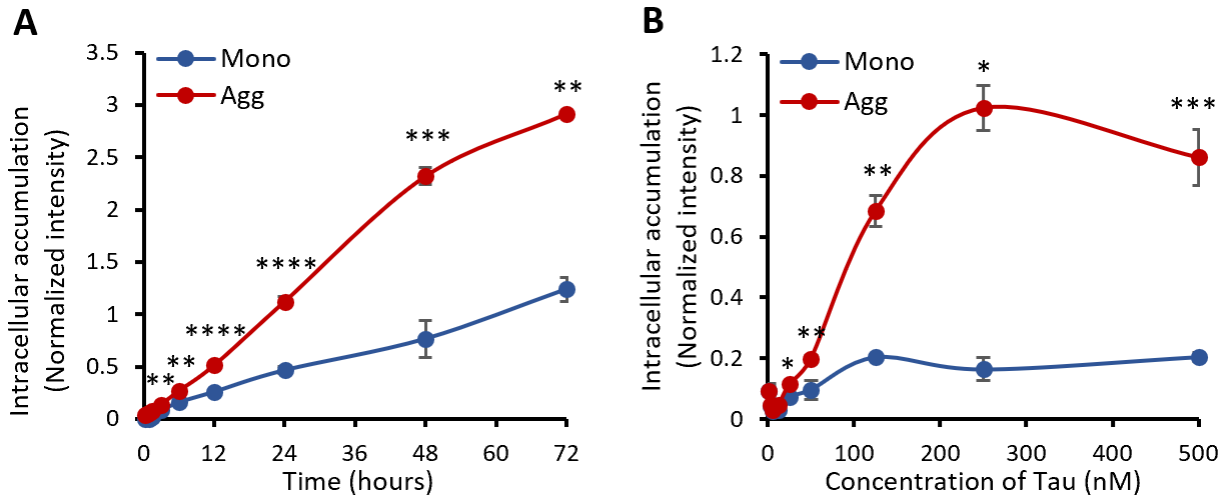

Figure 4.4 The uptake and accumulation of Tau monomers and aggregates in iPSC-derived neurons. A) The uptake of 100 nM ATTO488-labeled Tau monomers (Mono) and aggregates (Agg) was assessed over time using a fluorescence plate reader in the presence of the quencher. B) The concentration-dependent uptake of ATTO488-labeled Tau monomers and aggregates was measured after 24 hours on a fluorescence plate reader in the presence of the quencher. The fluorescence values obtained were normalized to the background. Error bars show SD; n=3 per experimental condition. One-way ANOVA followed by a post-hoc test; *p<0.05, **p<0.01, ***p<0.001, ****p<0.0001 vs. Mono.

To determine whether the uptake and accumulation of Tau is a specific process or a general endocytic event for bulky protein aggregates, we used bovine serum albumin (BSA) as an amyloidogenic protein and generated fluorescently labeled BSA aggregates. The formation of aggregates of fluorescently labeled BSA (BSA-CF488A) was confirmed using the PROTEOSTAT® Protein aggregation kit (**Figure 4.5A**). iPSCNs were treated with labeled BSA monomers and aggregates to investigate the neuronal uptake of BSA-CF488A, and fluorescence signals were analyzed after 24 hours. Before adding the quencher, the fluorescence signal from the labeled protein assemblies was visible. However, in the presence of the quencher, almost all fluorescence signal was eliminated (**Figure 4.5B**). Despite the interaction of BSA assemblies with the cell membrane, the absence of uptake and intracellular

accumulation suggests that internalizing and accumulating Tau monomers and aggregates in neurons is not a passive and unspecific process.

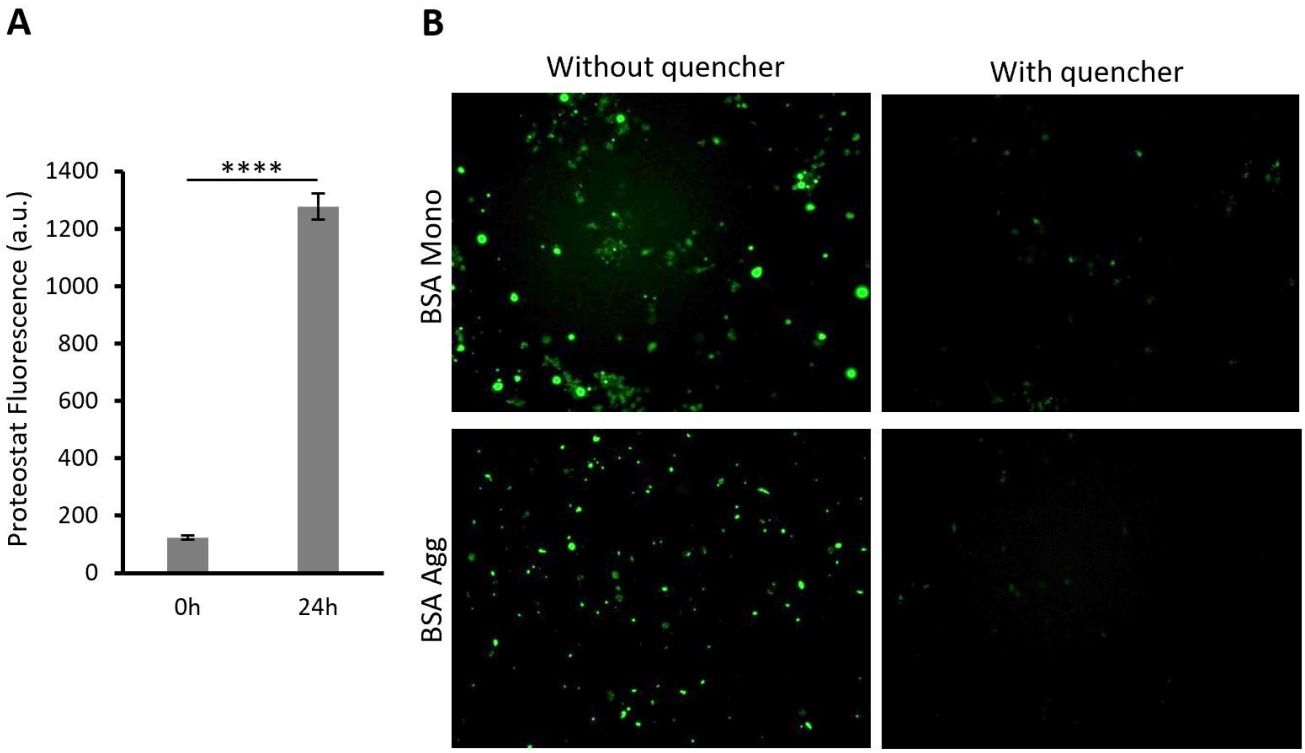

Figure 4.5 Bovine serum albumin (BSA) uptake and accumulation in iPSC-derived neurons. A) The aggregation of 4% BSA-CF488A was measured using a PROTEOSTAT® Protein aggregation kit before and after 24 hours of fibrillation. B) Fluorescence images were taken of cells treated with 100 nM 4% BSA-CF488A monomers (Mono) and aggregates (Agg) after 24 hours, both in the absence and presence of the quencher. Error bars show SD; n=4 per experimental condition. One-way ANOVA followed by a post-hoc test; ****$p<0.0001$.

4.3 Isolation of various Tau species from the Tau aggregated mixture

Patient-derived samples have revealed the existence of various structures of Tau aggregates (Iqbal et al., 2016). Similarly, AFM imaging showed that our heparin-induced Tau aggregate mixture consisted of different Tau structures (**Figure 4.2A**). To further investigate which species are responsible for the higher rate of cellular accumulation observed in Tau aggregates compared to native monomers, we

isolated and characterized each species. A multi-step procedure involving centrifugation, ultracentrifugation, and ultrafiltration was employed to separate different Tau species based on their biophysical properties, including molecular weight and size **(Figure 4.6)**.

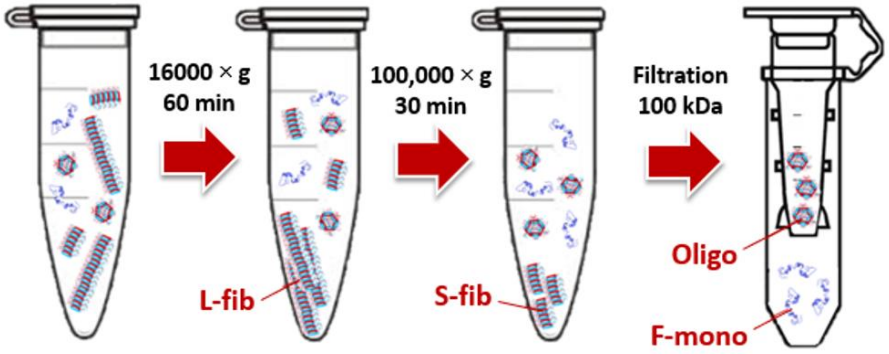

Figure 4.6 Schematic illustration of fractionation method. The protocol involves two rounds of centrifugation at different speeds (16,000 ×g and 100,000 ×g) to separate large insoluble fibrils (L-fib) and small fibrils (S-fib). Following this, a 100 kDa filtration step is performed, which separates the soluble oligomers (Oligo) that remain on the filter from the fibrillation-derived monomers (F-mono) that pass through the filter.

The formation of different Tau aggregate species during the fibrillation process was examined through fractionation and dot-blot analysis using conformational Tau antibody (MC1) (**Figure 4.7**). The fibrillation-derived monomeric fraction (F-mono) did not show reactivity toward MC1, while a dot appeared for the soluble oligomeric fraction (Oligo) after 6 hours of fibrillation, for the small fibrils fraction (S-fib) after 12 hours, and mainly for the large fibrils fraction (L-fib) after 24 hours. This result indicates a gradual formation of higher-ordered Tau structures over time under the fibrillation conditions.

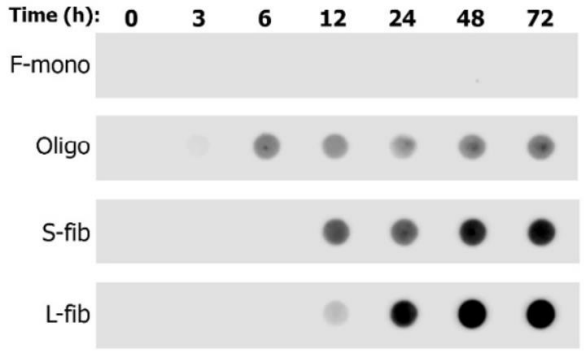

Figure 4.7 Monitoring the formation of Tau fraction by native immunoassay. Dot-blot analysis was performed in native conditions to analyze the content of each fraction, including large fibrils (L-fib), small fibrils (S-fib), oligomers (Oligo), and fibrillation-derived monomers (F-mono) during the fibrillation process without disturbing the conformational status using the Tau5 and MC1 antibodies.

Circular dichroism (CD) analysis was performed to study the conformational differences, confirming that F-mono exhibited a random coil structure with a minimum at around 200 nm, while the other fractions showed a red shift in the minimum peak, indicating the presence of β-sheet structures (**Figure 4.8A**). The Oligo fraction had a minimum of 203 nm, positioned between F-mono and S- or L-fib fractions, suggesting an intermediate structure with less β-sheet content than fibrils. The viability of cells treated with different fractions was assessed, and it was found that the Oligo fraction at a concentration of 250 nM exhibited significant toxicity after 24 hours, while the other fractions and native Tau monomers had no impact on cell viability at this concentration and incubation time (**Figure 4.8B**). No toxicity was observed at lower concentrations or shorter incubation times for any of these species (data not shown). Lastly, AFM and transmission electron microscopy (TEM) were used to investigate further the structural differences between fibrils and oligomers, revealing distinct morphologies (**Figure 4.8C and D**). The S-fib fraction displayed elongated fibrillar structures, while the Oligo fraction mainly consisted of short aggregates with a spherical appearance in AFM but appearing as short rod-shaped structures at higher TEM resolution.

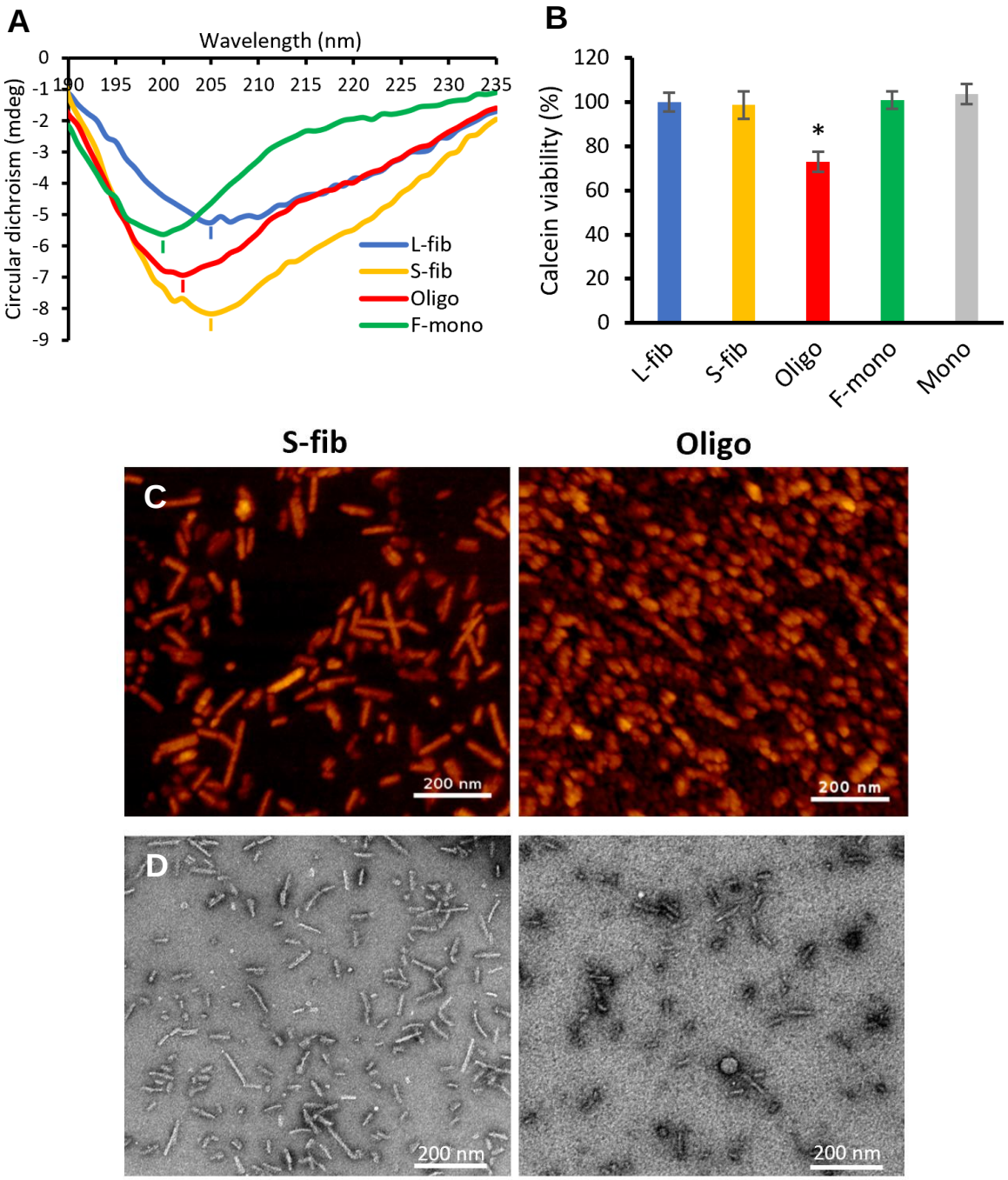

Figure 4.8 Characterization of Tau fractions. A) The circular dichroism spectrum was used to display the conformational status of Tau in each fraction, including large fibrils (L-fib), small fibrils (S-fib), oligomers (Oligo), and fibrillation-derived monomers (F-mono). The millidegrees (mdeg) values indicate the degree of conformational changes in the protein. B) To assess the impact on cell viability, iPSC-derived neurons were treated for 24 hours with 250 nM of either the mentioned Tau fractions or recombinant Tau monomers (Mono).

Error bars represent SD; n=3 per experimental condition. One-way ANOVA followed by a post-hoc test; *p<0.05. C) Atomic force microscopy images, and D) transmission electron microscopy images of small fibrils and soluble aggregates (oligomers).

4.4 Studying the neuronal internalization of various Tau species

Tau aggregates were labeled with fluorescent tags following fibrillization and then fractionated into four different species, as described earlier, to determine which Tau species are responsible for the higher intracellular accumulation of aggregates compared to monomers (**Figure 4.4**). The degree of labeling was determined to ensure comparability among the fractions based on fluorescence intensity (**Table 4.1**). Before the cellular experiments, any change in the aggregates' conformations must be addressed since the fluorescence labeling was a post-aggregation process. Analysis of the labeled and unlabeled fractions using circular dichroism (CD) showed similar negative peaks, indicating that labeling did not affect the conformation of the Tau species (**Figure 4.9**).

Table 4.1 Efficiency of labeling for various Tau fractions.

No.	Fractions	The average degree of labeling (dye-to-protein molar ratio)
1	Large fibrils	0.417
2	Small fibrils	0.466
3	Oligomers	0.428
4	Fibrillation-derived monomers	0.421

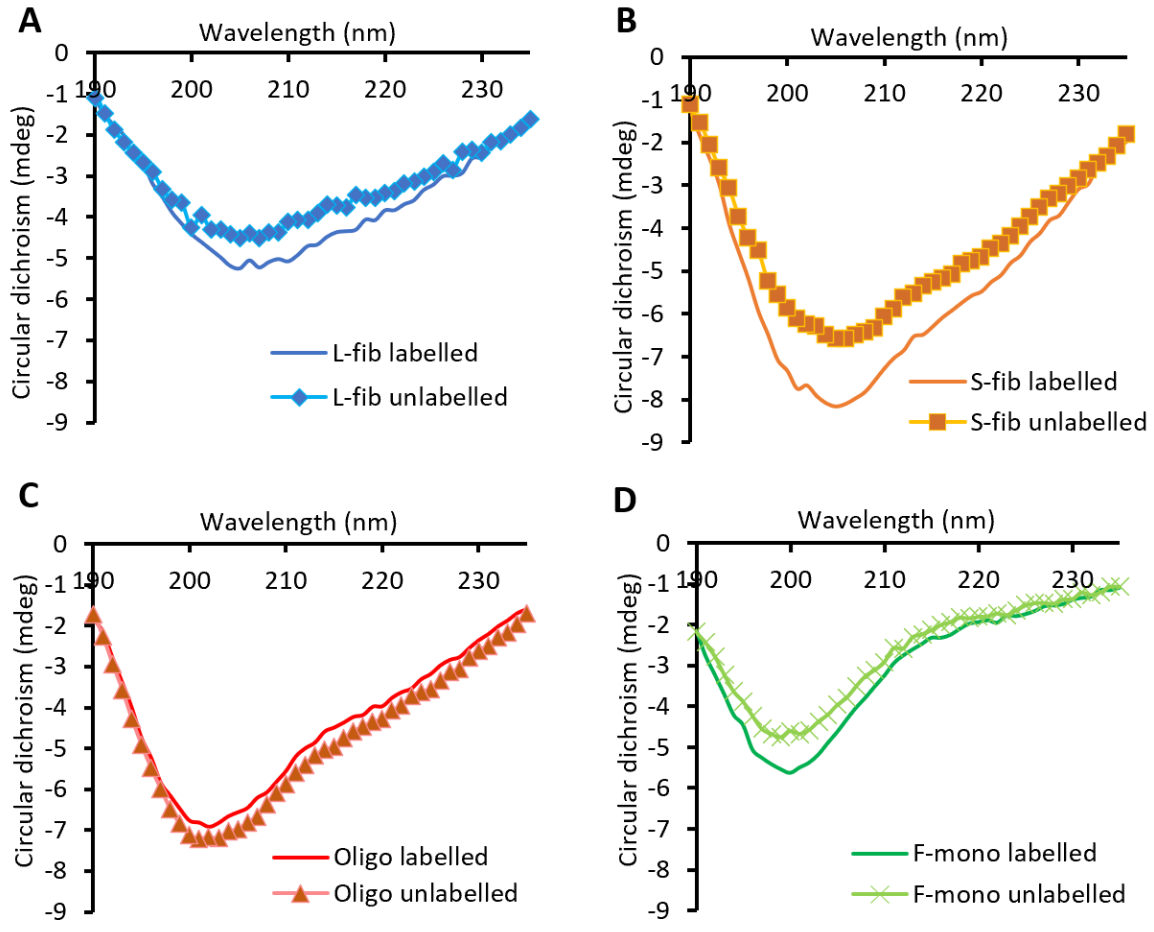

Figure 4.9 Circular dichroism of Tau fraction in the absence and presence of the fluorescent tag. The circular dichroism graphs show the conformational differences between labeled (ATTO488-labeled) and unlabeled Tau monomers and aggregates in various fractions: A) Large fibrils (L-fib), B) Small fibrils (S-fib), C) Oligomers (Oligo), and D) Fibrillation-derived monomers (F-mono). mdeg: millidegrees.

Kinetic and titration analysis demonstrated that S-fib and Oligo had a higher accumulation rate in iPSCNs compared to large L-fib and F-mono in iPSCNs (**Figure 4.10**). This suggests that cells internalize small and intermediate aggregates more efficiently than monomers or large aggregates. Furthermore, when studying the fluorescence intensity before adding the fluorescence quencher, it was observed that L-fib, similar to S-fib and oligomers, exhibited high fluorescence, while monomer-treated cells showed low fluorescence even without the quencher (**Figure 4.11A**), suggesting a similar cell and surface interaction rate of L-fib with other aggregated species. Examining the fluorescence in the

extracellular medium after 12 hours revealed that most of the fluorescence signal from insoluble fractions (L-fib and S-fib) was eliminated, while for soluble monomers, the majority of the fluorescence signal was present in the extracellular medium **(Figure 4.11B)**. Soluble oligomers were found both on the cell surface and in the extracellular medium, likely due to their mixed properties of solubility and interactive character. Notably, the presence or absence of cells in each well did not significantly affect the fluorescence of each fraction in the extracellular medium, indicating that the interaction of Tau aggregates with the coated surface of culture dishes is independent of cell presence. These findings suggest that aggregates, unlike monomers, have a strong affinity for cells and surfaces, but their cellular internalization depends on properties such as size.

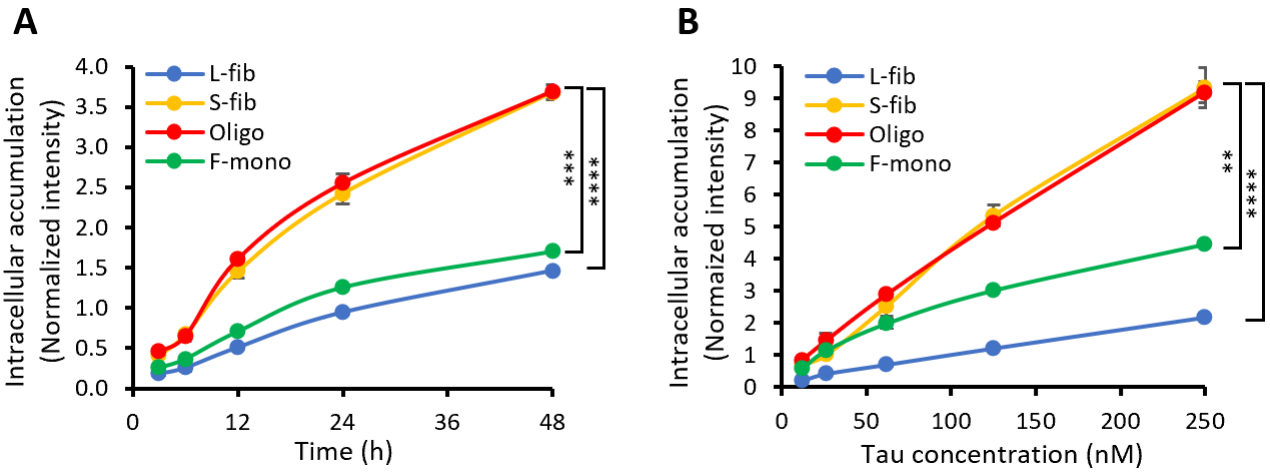

Figure 4.10 Uptake and intracellular accumulation of Tau fractions in iPSC-derived neurons. A) The graph represents the kinetics of intracellular accumulation of different Tau species over 48 hours. The Tau species include large fibrils (L-fib), small fibrils (S-fib), oligomers (Oligo), fibrillation-derived monomers (F-mono), and recombinant monomers (Mono) were tested. The accumulation of these Tau species was measured within cells, and the graph shows how their levels change over time. B) The titration curve illustrates the intracellular accumulation of different Tau species after 20 hours of incubation. The Tau species are likely varied concentrations of the same species, and the curve shows how the intracellular accumulation increases with increasing concentrations of Tau. Error bars represent SD; n=3 per experimental condition. One-way ANOVA followed by a post-hoc test; **p<0.01, ***p<0.001, ****p<0.0001.

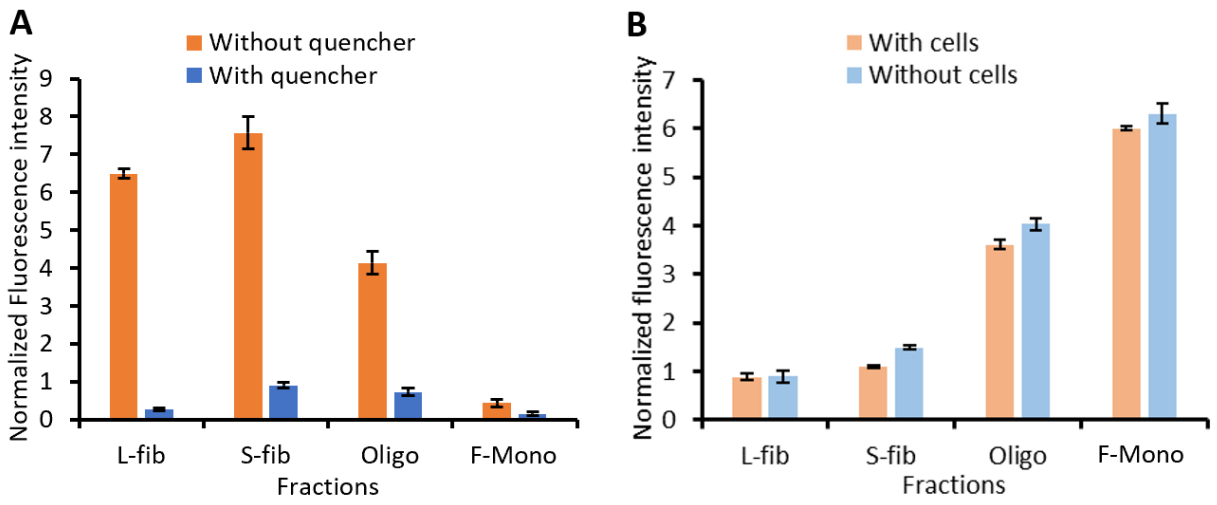

Figure 4.11 Studying the cell and surface interaction of Tau fractions. A) The fluorescence measurement of cells treated with 50 nM Tau fractions for 12 hours, including large fibrils (L-fib), small fibrils (S-fib), oligomers (Oligo), and fibrillation-derived monomers (F-mono) before and after the addition of the quencher. B) The fluorescence intensity in the extracellular medium after 12 hours of exposure to wells without cells or wells containing iPSC-derived neurons for various Tau species. Error bars represent SD; n=3 per experimental condition.

To account for potential differences between human cell models, the uptake and accumulation of Tau species were also investigated in Lund human mesencephalic (LUHMES) neurons (Lotharius et al., 2005). Like iPSCNs, the kinetics and titration analysis demonstrated that in LUHMES neurons, fluorescently labeled S-fib and Oligo accumulated more than L-fib and F-mono (**Figure 4.12A and B**). However, the accumulation rate of F-mono in LUHMES neurons was considerably lower compared to L-fib.

Comparing the intracellular accumulation of Tau in the two neuronal models revealed that native monomers accumulated much more in iPSCNs than in LUHMES neurons (**Figure 4.12C**). In contrast, S-fib accumulation in both cell models was similar (**Figure 4.12D**). Additionally, while the accumulation pattern in iPSCNs tended to reach a plateau after approximately 24 hours, no apparent plateau was observed for S-fib accumulation in LUHMES neurons until 48 hours.

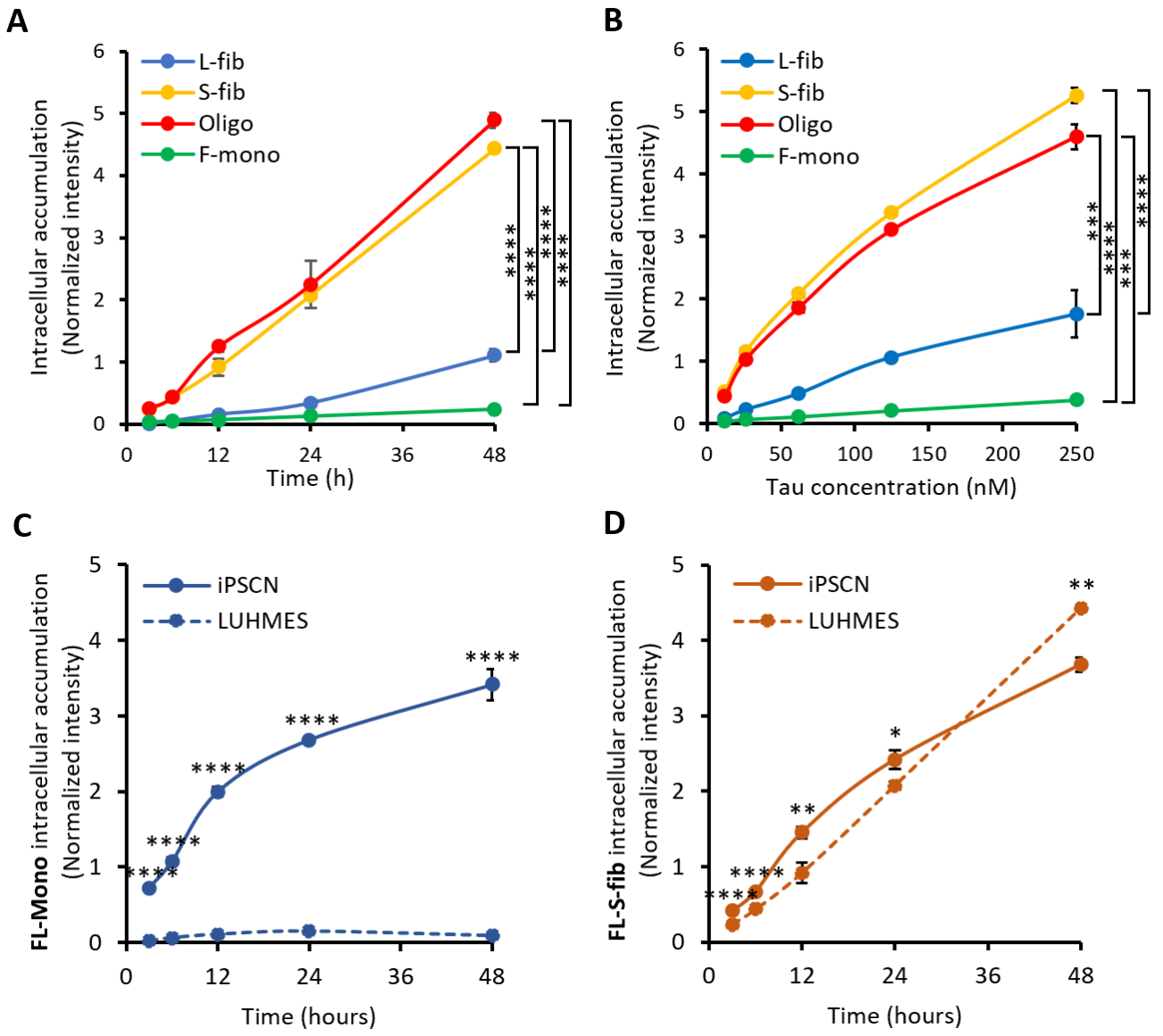

Figure 4.12 Uptake and intracellular accumulation of Tau species in LUHMES neurons. A) The kinetics of intracellular Tau accumulation in LUHMES neurons over 48 hours. The neurons were exposed to different Tau fractions, including large fibrils (L-fib), small fibrils (S-fib), oligomers (Oligo), and fibrillation-derived monomers (F-mono). B) The titration curve of intracellular Tau accumulation in LUHMES neurons after 20 hours of exposure to various concentrations of Tau fractions (ranging from 12.5 to 250 nM). C) The kinetics of intracellular accumulation in iPSCNs and LUHMES neurons when exposed to 100 nM fluorescently labeled monomers (FL-Mono). D) The kinetics of intracellular accumulation in iPSCNs and LUHMES neurons when exposed to 100 nM fluorescently labeled small fibrils (FL-S-fib). For C and D, significance was calculated for iPSCNs versus

LUHMES neurons at each time point. Error bars represent SD; n=3 per experimental condition. One-way ANOVA followed by post-hoc test; *p<0.05, **p<0.01, ***p<0.001 and ****p<0.0001.

4.5 Studying the endosomal escape, and seeded aggregation of various Tau species

A neuronal entry assay was conducted to assess the ability of different Tau species to enter the cytosol using primary mouse neurons expressing a large 18 kDa subunit (LgBiT) of split luciferase called NanoLuc (Nluc), while a small 11 amino acid peptide HiBiT-tagged Tau fractions were added exogenously to the extracellular medium (Dixon et al., 2016; Tuck et al., 2022). Intracellular luminescence indicating cytosolic entry occurs when the extracellular Tau-HiBiT interacts with the endogenous LgBiT in the cytosol and reconstitutes the complete Nluc (**Figure 4.13A**). 0N4R P301S-Tau-HiBiT was fibrillated and fractionated in this study to investigate their neuronal entry. The results (**Figure 4.13B**) showed a significantly higher neuronal entry for Tau aggregates compared to F-mono or native monomers. This data suggests that the differences observed in the overall neuronal accumulation of S-fib and Oligo are present at the level of cytosolic entry. However, no differences were observed between S-fib and Oligo in this assay compared to L-fib.

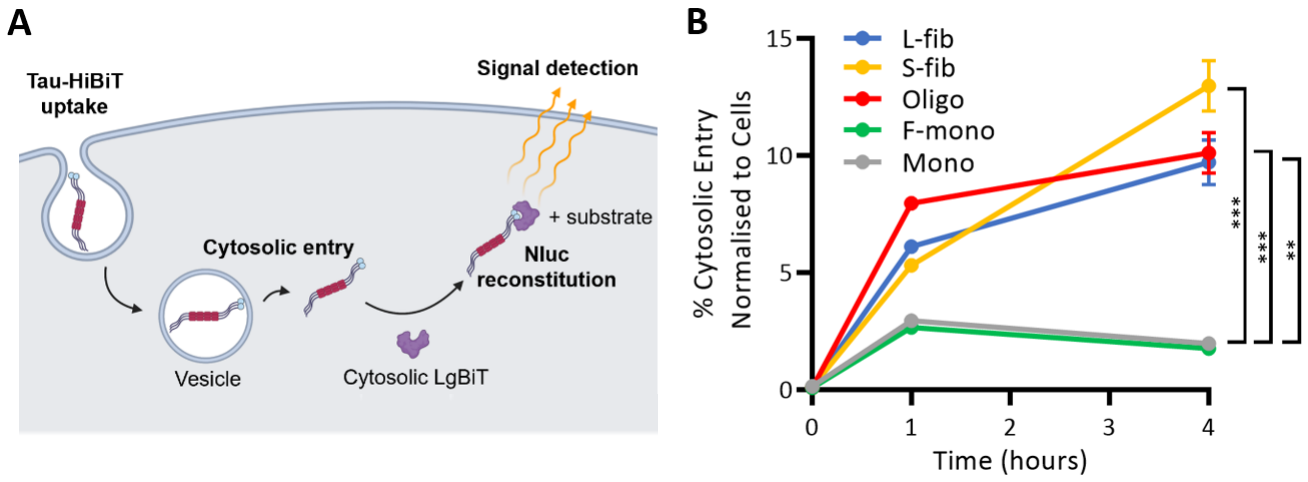

Figure 4.13 Cytosolic entry of Tau fractions in primary mouse neurons. A) The schematic diagram illustrates the Tau entry assay. In this assay, 0N4R P301S-Tau-HiBiT

assemblies are added to cells that express cytosolic LgBiT. The uptake of Tau assemblies by the cells can lead to their entry into the cytosol. Once inside the cytosol, Tau-HiBiT mediates the reconstitution of Nluc activity by binding with LgBiT. Adding a cell-permeable substrate triggers the production of photons by Nluc, which can be quantified to measure the luminescent signal. The luminescent signal indicates the amount of Tau-HiBiT that has entered the cytosol. B) The graph shows the percentage of Tau-HiBiT that enters the cytosol of GPLN neurons after exposure to different species of Tau, including Tau-HiBiT large fibrils (L-fib), small fibrils (S-fib), oligomers (Oligo), fibrillation-derived monomers (F-mono), and native monomers (Mono). Error bars represent SD; n=3 per experimental condition. Two-way ANOVA with Dunnett's multiple comparisons tests; ***$p<0.001$ and **$p<0.01$.

According to the prion-like spreading hypothesis, potent propagating seeds are necessary to induce the endogenous aggregation of native monomeric Tau in naive cells (Clavaguera et al., 2015). A HEK293 cell line with stable overexpression of 0N4R Tau containing the P301S mutation and C-terminally tagged with Venus fluorescence protein was used to examine whether the Tau fractions in the assay can induce endogenous aggregation and are relevant to disease propagation (McEwan et al., 2017). Under normal conditions, these biosensor cells exhibit the distribution of Tau associated with microtubules. However, transfection of these cells with Tau seeds leads to the formation of bright fluorescent puncta, representing Tau inclusions (**Figure 4.14A**). The amount of puncta formation was estimated by comparing the total fluorescence intensity, which provides an evaluation of the entire cell population. The fluorescence measurement with a plate reader revealed significantly higher fluorescence intensity in cells treated with L-fib, S-fib, and Oligo compared to those treated with F-mono and Mono alone (**Figure 4.14B**). In this assay, lipofectamine was used for transferring seeds into the cells, mainly to facilitate endosomal escape. Thus the results only reflect the potency of seeding endogenous Tau protein but not the uptake efficiency of different species.

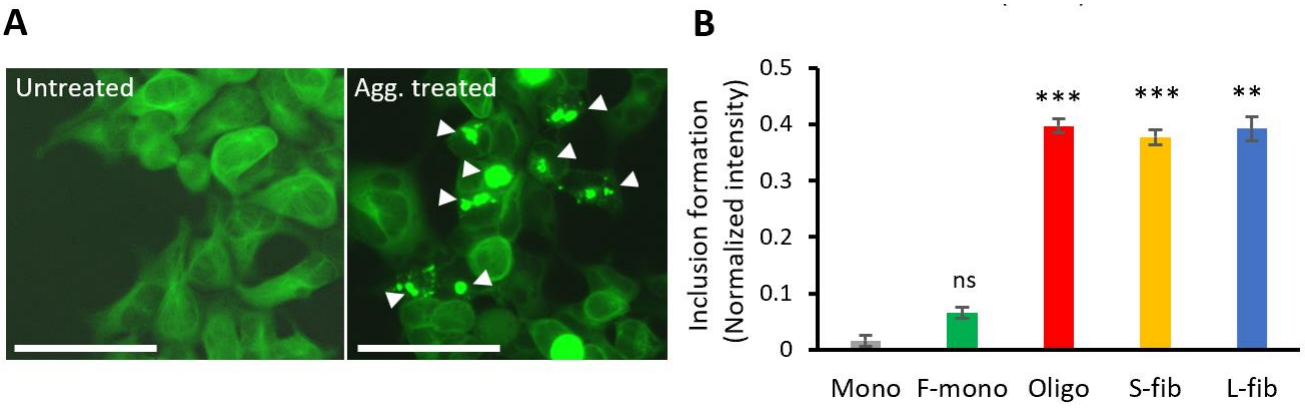

Figure 4.14 Studying the induction of endogenous aggregation by Tau fractions. A) The fluorescence microscopic images show HEK293-biosensor cells expressing P301S Tau-venus. The images compare untreated cells with cells treated with 200 nM unlabeled Tau aggregates (Agg) and lipofectamine. The arrows indicate the presence of inclusions of endogenous P301S Tau-venus. Scale bar 61.7 nm. B) A fluorescence plate reader performs fluorescence analysis on cells treated with 200 nM Tau fractions, including Tau-HiBiT large fibrils (L-fib), small fibrils (S-fib), oligomers (Oligo), fibrillation-derived monomers (F-mono), and native monomers (Mono). Error bars represent SEM; n=3 per experimental condition. One-way ANOVA followed by a post-hoc test; ns: none significant, **p<0.01, and ***p<0.001.

4.6 Studying uptake competition between Tau monomers and aggregates

We aimed to investigate the competition between native monomeric Tau and aggregated Tau in neuronal internalization and intracellular accumulation, examining whether they share similar or distinct entry pathways (Evans et al., 2018). In our study, we treated iPSCNs with a constant concentration of fluorescently labeled Tau monomers (FL-Mono) or small fibrils (FL-S-fib), along with increasing concentrations of unlabeled Tau monomers or small fibrils. After approximately 20 hours of incubation, we measured the intracellular fluorescence intensity. Our findings demonstrated that increasing the concentration of unlabeled monomers or small fibrils reduced the intracellular accumulation of FL-Mono (**Figure 4.15A**). However, the impact of unlabeled monomers was significantly greater than that of small fibrils, except at a low concentration of 10 nM. This suggests that native monomeric Tau competes more with Tau monomers in neuronal uptake and accumulation compared to small fibrils.

Conversely, the accumulation of FL-S-fib in iPSCNs significantly decreased in the presence of both unlabeled monomers and small fibrils (**Figure 4.15B**). However, the impact of small fibrils was notably greater than that of monomers at all concentrations, indicating a higher competition between unlabeled small fibrils and FL-S-fib.

Similarly, fluorescently labeledOligo (FL-Oligo) accumulation in iPSCNs was significantly reduced when exposed to five-fold concentrations of both unlabeled monomers and oligomers (**Figure 4.16A**). However the effect of oligomers was significantly higher than that of monomers, indicating stronger competition between similar Tau species rather than different species. Overall, these findings suggest that, in iPSCNs, Tau monomers and aggregates only mildly compete with each other in uptake and accumulation, indicating the distinct but overlapping entry pathways.

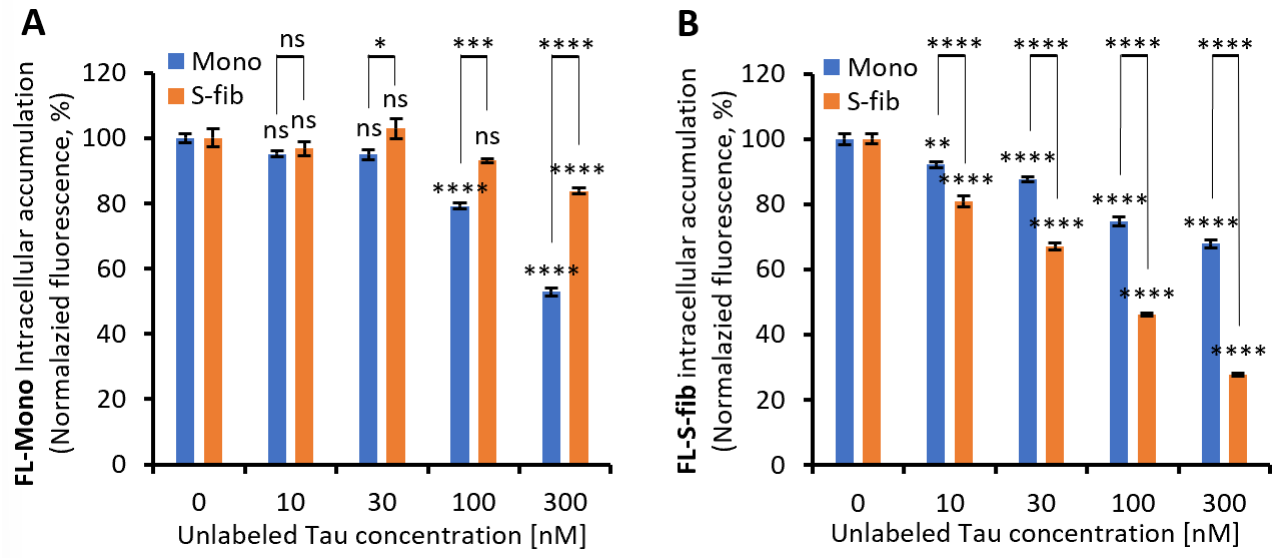

Figure 4.15 Uptake competition between Tau monomers and small fibrils in iPSC-derived neurons. A) The uptake and accumulation of 50 nM fluorescently labeled Tau monomers (FL-Mono) were measured in iPSCNs in the presence of increasing concentrations of unlabeled Tau monomers and small fibrils. B) The uptake and accumulation of 50 nM fluorescently labeled Tau small fibrils (FL-S-fib) were measured in iPSCNs in the presence of increasing concentrations of unlabeled Tau monomers and small fibrils. The cells were exposed to these Tau species for 20 hours. Significance was calculated by comparing Mono and S-fib at each concentration versus "0" and versus each other. Error bars represent SEM; n≥3 independent experiments per experimental condition. Two-way

ANOVA followed by Tukey post-hoc test; ns: none significant, *p<0.05, **p<0.01, ***p<0.001, ****p<0.0001.

To investigate the potential role of heparin, a known inhibitor of Tau uptake (Holmes et al., 2013) in the result of competition, a novel type of recombinant Tau aggregates that were generated without any co-factor like heparin was tested (Chakraborty et al., 2021). We found that unlabeled monomers significantly reduced the uptake of labeled monomers in iPSCNs, whereas treatment with unlabeled co-factor-free fibrils (Cof-free-fib) did not affect the accumulation of labeled monomers (**Figure 4.16B**). Similarly, the neuronal accumulation of fluorescently labeled Cof-free-fib (FL-Cof-free-fib) was significantly reduced in the presence of unlabeled cofactor-free fibrils but not monomers (**Figure 4.16C**). These results confirm that the uptake competition between Tau fibrils is unrelated to the presence of heparin. Additionally, we observed no significant interspecies impact on uptake and accumulation using cof-free-fib, indicating the absence of competition between monomers and cof-free-fib. This finding suggests a greater distinction between Tau monomers' uptake and accumulation pathways with cof-free-fib compared to heparin-induced S-fib.

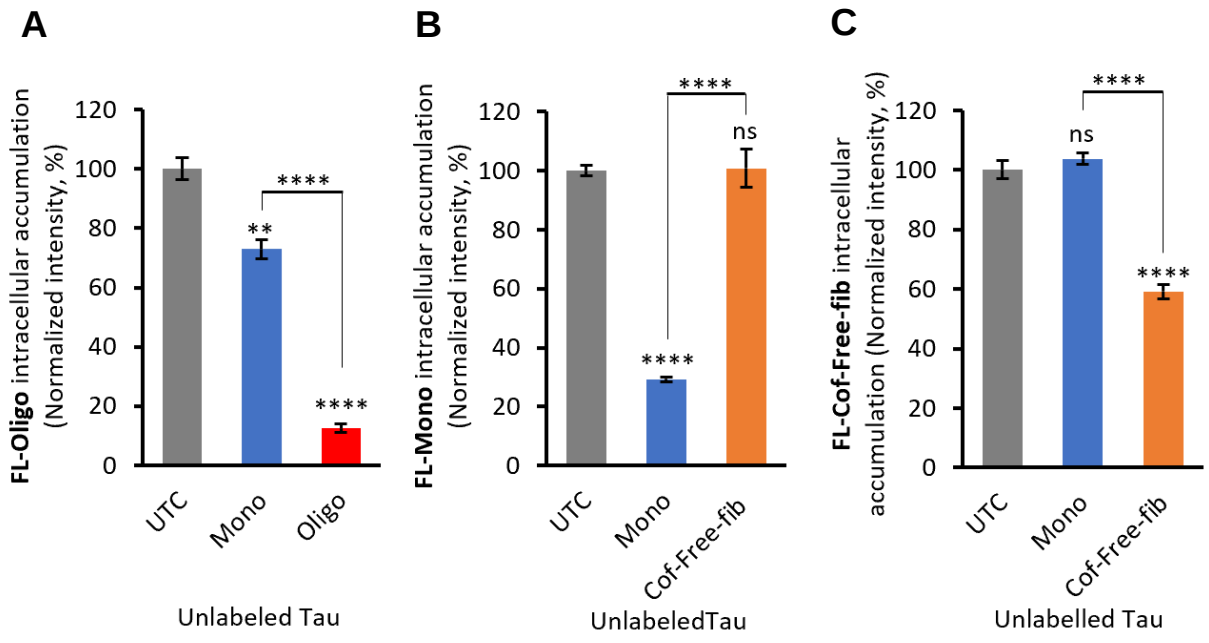

Figure 4.16 Uptake competition of Tau monomers, oligomers, and cofactor-free-fibrils in iPSC-derived neurons. A) The neuronal accumulation of 50 nM fluorescently labeled Tau oligomers (FL-Oligo) in iPSCNs was examined after 20 hours of incubation. Some cells

were left as untreated control (UTC), and others were exposed to a 5-fold higher concentration (250 nM) of unlabeled Tau monomers (Mono) or oligomers (Oligo). B) The uptake and accumulation of FL-Mono in the presence of a 4-fold higher concentration of unlabeled Tau Mono and cofactor-free fibrils (Cof-free-fib) after 20 hours of incubation. C) The uptake and accumulation of fluorescently labeled Cof-free-fib (FL-Cof-free-fib) in the presence of a 4-fold higher concentration of unlabeled Tau Mono and Cof-free-fib after 20 hours of incubation. Significance was calculated by comparing Mono and S-fib at each concentration versus "0" and versus each other. Error bars represent SEM; n≥3 independent experiments per experimental condition. Two-way ANOVA followed by Tukey post-hoc test; ns: none significant, *p<0.05, **p<0.01, ***p<0.001, ****p<0.0001.

To determine if the specific pattern of Tau uptake competition is exclusive to iPSCNs or applicable to other neuronal types, we conducted the assay in LUHMES neurons as a different neuronal model. The results confirmed a competitive effect between monomers at concentrations of 100 nM and higher. However, we observed no significant cross-species competition for FL-Mono accumulation, even at the highest concentration of 300 nM of unlabeled S-fib (**Figure 4.17A**). On the other hand, the intracellular accumulation of FL-S-fib was only reduced when cells were co-treated with 30 nM unlabeled S-fib or higher concentrations, while co-treatment with monomers had no effect (**Figure 4.17B**). These findings corroborate the previous data obtained from iPSCNs, in the separation between the uptake of Tau monomers and aggregates. More interestingly, our data suggest that there is no significant cross-competition between the uptake and accumulation of Tau monomers and aggregates in LUHMES neurons, indicating completely distinct pathways.

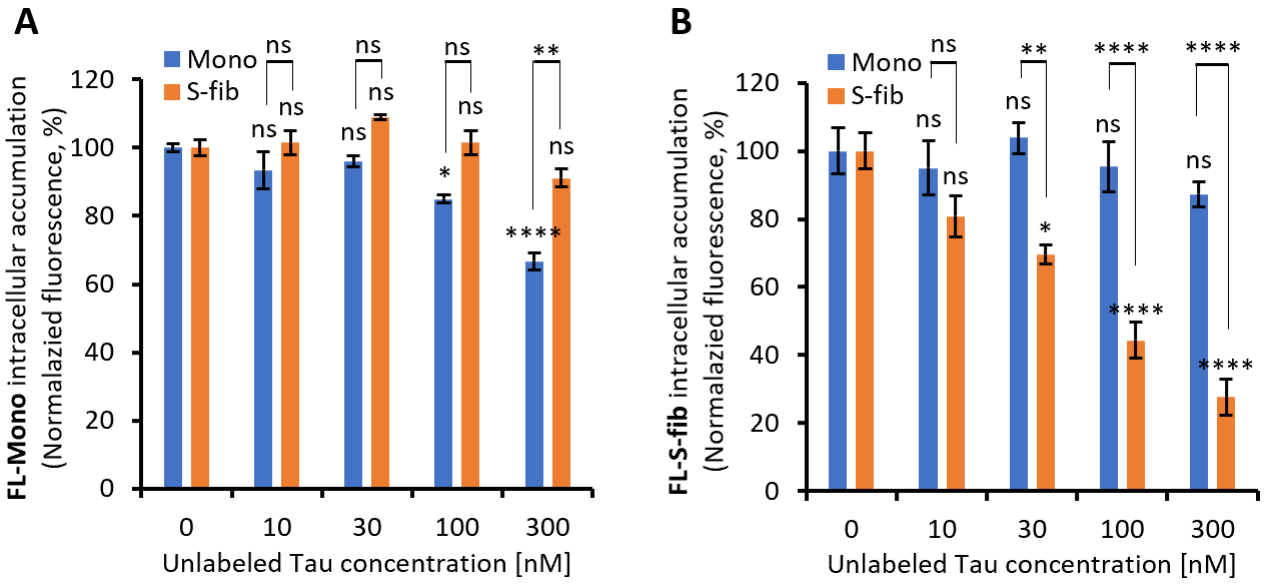

Figure 4.17 Uptake competition between Tau monomers and small fibrils in LUHMES neurons. A Intracellular accumulation of 50 nM fluorescently labeled monomers (FL-Mono) in the presence of an increasing concentration of unlabeled Tau monomers (Mono) and small fibrils (S-fib) after 20 hours in LUHMES neurons. **B** Intracellular accumulation of 50 nM fluorescently labeled S-fib (FL-S-fib) in the presence of an increasing concentration of unlabeled Mono and S-fib after 20 hours in LUHMES neurons. Significance was calculated by comparing Mono and S-fib at each concentration versus "0" and versus each other. Error bars represent SEM; n≥3 independent experiments per experimental condition. Two-way ANOVA followed by Tukey post-hoc test; ns: none significant, *p<0.05, **p<0.01, ***p<0.001, ****p<0.0001.

We also studied the uptake competition in primary mouse neurons to compare with human neurons. Increasing the concentration of both Mono and S-fib reduced the accumulation of FL-Mono significantly; however, the effect of Mono was significantly higher than S-fib. This result was very similar to the data obtained from iPSCNs (**Figure 4.18A**). Conversely, the impact of Mono and S-fib on FL-S-fib accumulation in primary mouse neurons was completely different from human neurons. Because we observed a more vigorous competition between Mono and S-fib at 100 nM compared to S-fib and S-fib at the same concentration, however, both species' impact became similar and insignificant at 300 nM (**Figure 4.18B**). This suggests that there is a cross-species competition in primary mouse cortical neurons, unlike human neurons.

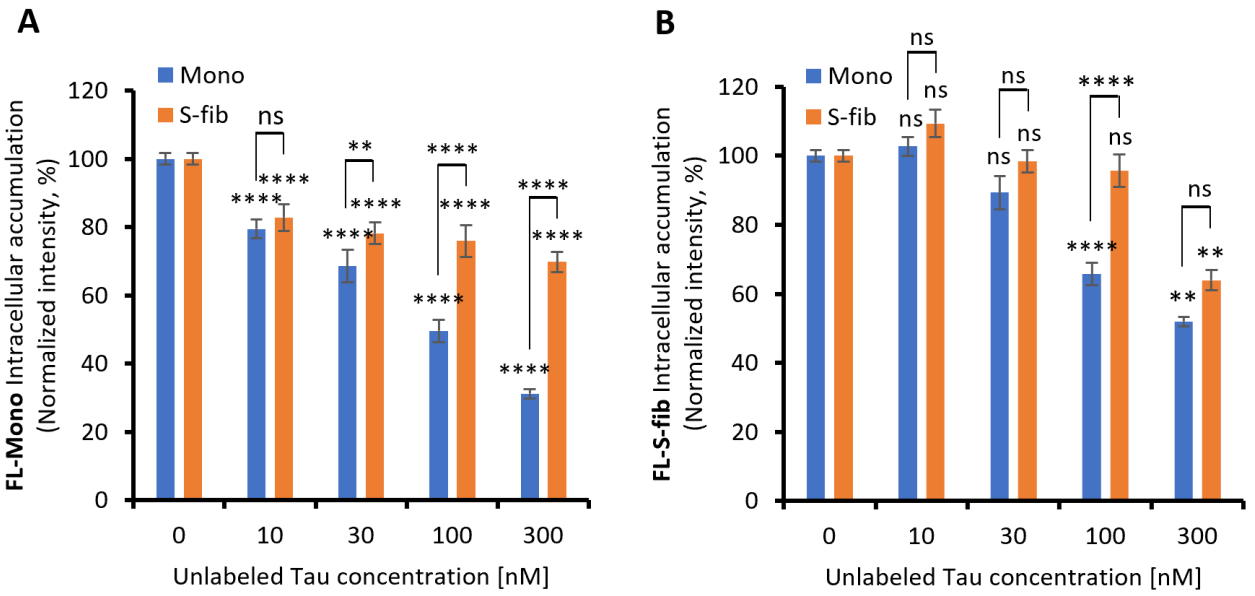

Figure 4.18 Uptake competition between Tau monomers and small fibrils in primary mouse neurons. A Intracellular accumulation of 50 nM fluorescently labeled monomers (FL-Mono) in the presence of an increasing concentration of unlabeled Tau monomers (Mono) and small fibrils (S-fib) after 20 hours in primary mouse cortical neurons. **B** Intracellular accumulation of 50 nM fluorescently labeled S-fib (FL-S-fib) in the presence of an increasing concentration of unlabeled Mono and S-fib after 20 hours in primary mouse cortical neurons. Significance was calculated by comparing Mono and S-fib at each concentration versus "0" and versus each other. Error bars represent SEM; n=2-4 independent experiments per experimental condition. Two-way ANOVA followed by Tukey post-hoc test; ns: none significant, **p<0.01, ***p<0.001, ****p<0.0001.

4.7 Examining the impact of endocytosis and protein degradation inhibitors on the uptake of Tau monomers and aggregates in iPSCNs

We conducted experiments using small molecule inhibitors targeting different endocytic pathways to delve deeper into the cellular mechanisms underlying the specific uptake and accumulation routes of Tau monomers and aggregates. iPSCNs were treated with the inhibitors in **Table 4.2** for 30 minutes, followed by exposure to fluorescently labeled Tau monomers or small fibrils for 3 hours. The results showed that Chlorpromazine (CPZ), Cytochalasin-D (CD), 5-(N-ethyl-N-isopropyl)-amiloride (EIPA),

and Dyngo-4a (DYNGO) significantly reduced the uptake of both Mono and S-fib. However, Genistein (GEN) and Nystatin (NYST) had no effect (**Figure 4.19A and B**).

Table 4.2 The cellular functions of endocytosis inhibitors.

No.	Name	Function
1	Chlorpromazine (CPZ)	An inhibitor of clathrin-mediated endocytosis via binding to adaptor protein -2 (AP-2) subunit (Wang et al., 1993)
2	Cytochalasin-D (CD)	An inhibitor of actin polymerization (Mortensen & Larsson, 2003), which is involved in various endocytic processes (Engqvist-Goldstein & Drubin, 2003)
3	5-(N-ethyl-N-isopropyl)-amiloride (EIPA)	An inhibitor of macropinocytosis, which interferes with Na^+/H^+ exchange (Koivusalo et al., 2010)
4	Dyngo-4a (DYNGO)	An inhibitor of both dynamin I and II (McCluskey et al., 2013)
5	Genistein (GEN)	An inhibitor of tyrosine kinases involved in caveolar-mediated endocytosis (Aoki et al., 1999)
6	Nystatin (NYST)	A Cholesterol-chelating that disrupts lipid rafts and inhibits clathrin-independent, caveolar-mediated endocytosis (Puri et al., 2001)
7	Bafilomycin A1 (Baf)	An inhibitor of vacuolar ATPase that prevents lysosomal acidification, inhibiting the activation of lysosomal proteases (Vinod et al., 2014)
8	Chloroquine (CQ)	An inhibitor of autophagic flux by blocking the fusion of autophagosomes with lysosomes (Mauthe et al., 2018)

Viability assays confirmed that the mentioned treatments did not affect cell viability (**Figure 4.19C**). These findings suggest the involvement of clathrin-mediated endocytosis and micropinocytosis in Tau uptake, with actin polymerization and dynamin function necessary for this process. However, clathrin-independent or caveolin-mediated endocytosis might not be involved in Tau uptake in iPSCNs.

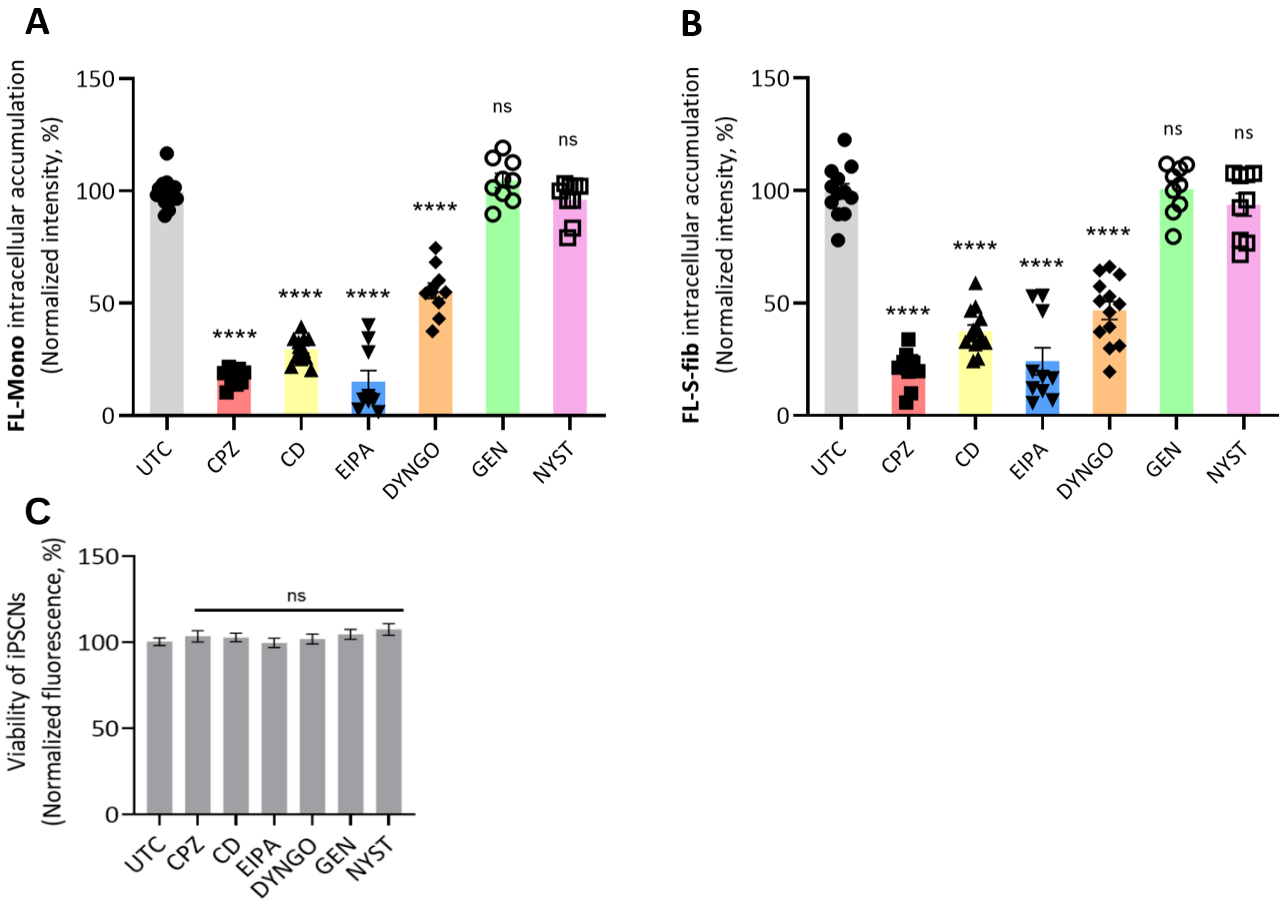

Figure 4.19 The impact of endocytic inhibitors on the uptake of Tau in iPSC-derived neurons. The study investigated the intracellular level of Tau in cells left as untreated control (UTC) or treated with different compounds before incubation with (A) fluorescently labeled Tau monomers (FL-Mono) and (B) fluorescently labeled small fibrils (FL-S-fib). The compounds used were: Chlorpromazine (CPZ) at a concentration of 50 µM, Cytochalasin D (CD) at a concentration of 20 µM, 5-N-ethyl-N-isopropyl amiloride (EIPA) at a concentration of 30 µM, Dyngo-4a (DYNGO) at a concentration of 75 µM, Genistein (GEN) at a concentration of 200 µM, Nystatin (NYST) at a concentration of 10 µM. The cells were treated with these compounds for 30 minutes before incubation with FL-Mono or FL-S-fib at a concentration of 250 nM for 3 hours. In the case of EIPA, it was present during the incubation with Tau. Error bars represent SEM; n=9-14 independent experiments per experimental condition. One-way ANOVA followed by post-hoc test; ns: none significant, ****$p<0.0001$ vs. UTC. C) Viability assessment of cells treated with the small molecule inhibitors. Error bars represent SEM; n=16-26 independent experiments per experimental condition. One-way ANOVA followed by post-hoc test; ns: none significant.

To further explore the differences in cellular accumulation between Tau monomers and small fibrils, we tested small molecule inhibitors of protein degradation pathways and muscarinic receptors, which have been implicated in Tau uptake. iPSCNs were treated with the inhibitors in **Table 4.3** along with Tau monomers or small fibrils, and the intracellular Tau levels were measured after 20 hours of incubation. Among the protein degradation inhibitors, only Chloroquine (CQ) significantly reduced Tau uptake for both monomers and small fibrils, while Bafilomycin and MG132 had no effect (**Figure 4.20A and B**).

Table 4.3 The mechanism of action for inhibitors of protein degradation pathway.

No.	Name	Function
1	Bafilomycin A1 (Baf)	An inhibitor of vacuolar ATPase that prevents lysosomal acidification, inhibiting the activation of lysosomal proteases (Vinod et al., 2014)
2	Chloroquine (CQ)	An inhibitor of autophagic flux by blocking the fusion of autophagosomes with lysosomes (Mauthe et al., 2018)
3	MG132	An inhibitor of proteasome activity by blocking the proteolytic activity of the 26S proteasome complex (Lee & Goldberg, 1996)
4	Atropine (Atr)	A non-selective antagonist of the muscarinic receptor that inhibits Tau uptake (Morozova et al., 2019)
5	Pirenzepine (Pirz)	An antagonist of the M1 muscarinic receptor that inhibits Tau uptake (Morozova et al., 2019)

Viability assays confirmed the lack of toxicity for all treatment conditions, suggesting that protein degradation is not a critical factor in determining Tau levels in cells within a short timeframe of less than 20 hours. The unexpected impact of CQ may be related to its interference with receptor recovery to the cell membrane, as the endo-lysosomal system is involved in receptor recycling (Hu et al., 2015). Among the muscarinic receptor antagonists, only Pirenzepine mildly but significantly reduced the accumulation of Tau monomers in iPSCNs, whereas it had no effect on small fibril accumulation. We find no changes in the viability of cells treated with the aforementioned small molecules (**Figure 4.20C and D**). These results suggest that protein degradation pathways and muscarinic receptors play limited roles in determining Tau accumulation in iPSCNs.

Next, we examined the impact of heparin treatment on Tau uptake and accumulation. Heparin is a known inhibitor of Tau uptake, as it interacts with heparan sulfate proteoglycans (HSPGs) on the cell surface and blocks Tau harboring (Holmes et al., 2013). iPSCNs were treated with Tau monomers or small fibrils

in the presence or absence of heparin and incubated for approximately 20 hours. The results showed that heparin significantly reduced the accumulation of small fibrillar Tau but did not affect monomeric Tau uptake (**Figure 4.20E**).

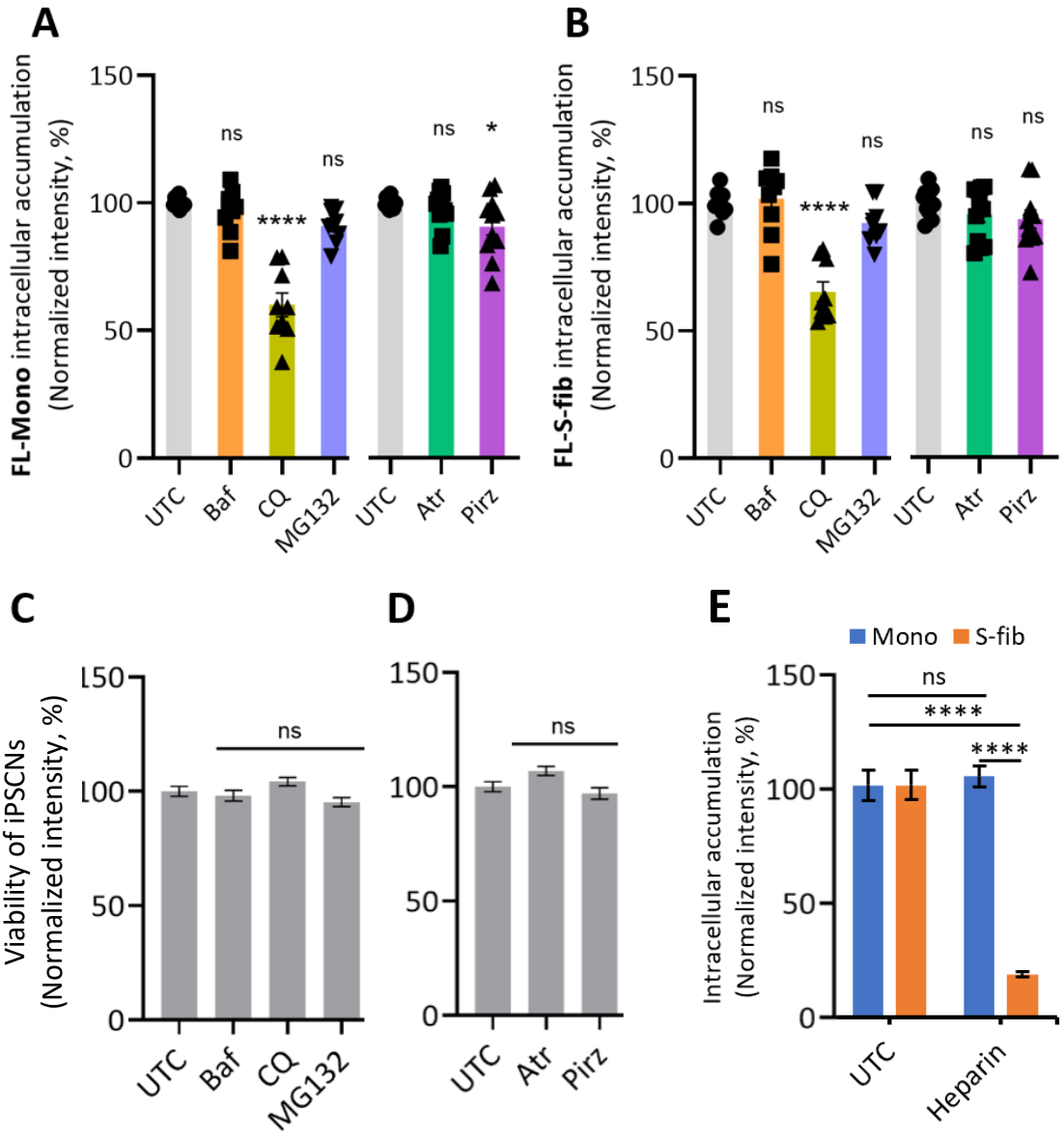

Figure 4.20 The effect of protein degradation machinery, muscarinic receptor antagonist, and heparin on Tau uptake in iPSC-derived neurons. The intracellular accumulation of fluorescently labeled (A) Tau monomers (FL-Mono) and (B) small fibrils (FL-S-fib) was measured in cells left as untreated control (UTC) or treated with different compounds for 20 hours. The compounds used were: Bafilomycin A1 (Baf) at a

concentration of 100 nM, Chloroquine (CQ) at a concentration of 30 μM, MG132 at a concentration of 100 nM, Atropine (Atr) at a concentration of 200 μM, Pirenzepine (Pirz) at a concentration of 20 μM. The cells were treated with these compounds along with FL-Mono or FL-S-fib at a concentration of 25 nM for 20 hours. Error bars represent SEM; n=9-14 independent experiments per experimental condition. One-way ANOVA followed by post-hoc test; ****$p<0.0001$ and *$p<0.05$ vs. UTC. C) and D) The viability of iPSCNs was measured after 20 hours of treatment with compounds in parts A and B at the aforementioned concentration using calcein fluorescence. Error bars represent SEM; n=21-25 independent experiments per experimental condition. One-way ANOVA followed by post-hoc test. E) The intracellular accumulation of fluorescently labeled Tau monomers (Mono) and small fibrils (S-fib) was analyzed in iPSCNs treated with 25 nM Tau in the presence of 2 μM Heparin for 20 hours. Error bars represent SEM; n=3. One-way ANOVA followed by post-hoc test; ****$p<0.0001$ vs. UTC. ns: not significant.

4.8 Examining the impact of endocytosis and protein degradation inhibitors on the uptake of Tau monomers and aggregates in LUHMES neurons

In LUHMES neurons, similar to iPSCNs, the treatment with non-toxic doses of CPZ, CD, and EIPA significantly reduced the uptake of Tau Mono, while GEN had no effect (**Figure 4.21A**). However, only CPZ reduced the uptake of Tau S-fib, and the other inhibitors were ineffective (**Figure 4.21B**). Surprisingly, inhibiting dynamin in LUHMES neurons led to an increase in both Mono and S-fib uptake. Further analysis using LDL-BODIPY as a marker for clathrin-mediated endocytosis and Dextran-FITC as a marker for macropinocytosis revealed that increasing the concentration of DYNGO reduced LDL uptake as expected but also significantly increased the uptake of Dextran (**Figure 4.21C and D**). This suggests that inhibiting dynamin-mediated endocytosis in LUHMES neurons triggers the over-activation of macropinocytosis as a compensatory mechanism for the uptake of essential cargoes. Moreover, this indicates that both Mono and S-fib Tau can be taken up by macropinocytosis as well as clathrin-mediated endocytosis. The absence of this response in iPSCNs may be associated with differences in neural type or maturity.

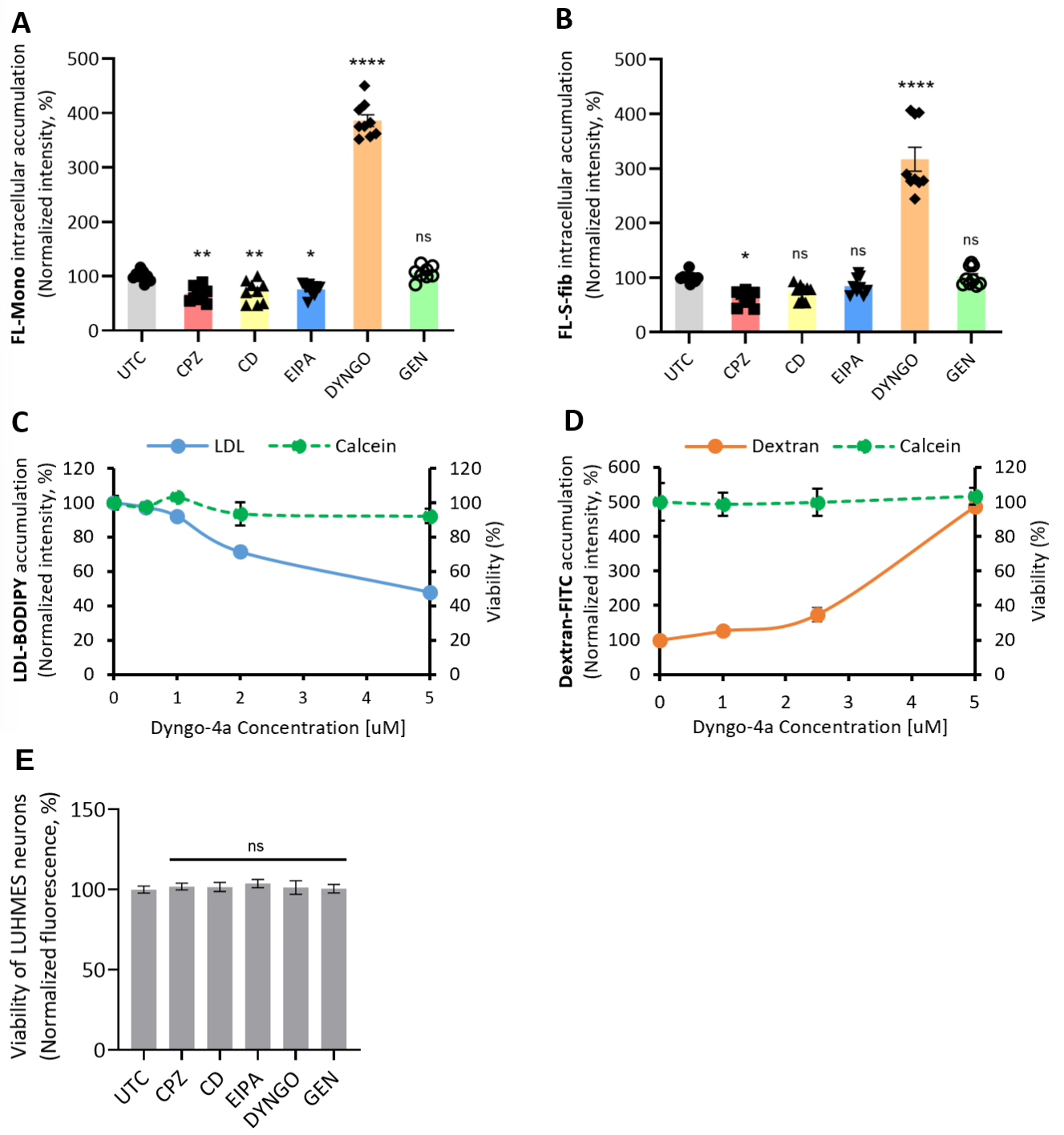

Figure 4.21 The impact of endocytic inhibitors on the uptake of Tau in iPSC-derived neurons. Cells left as untreated control (UTC) or treated with different compounds, including 50 µM Chlorpromazine (CPZ), 20 µM Cytochalasin D (CD), 30 µM 5-N-ethyl-N-isopropyl amiloride (EIPA), 5 µM Dyngo-4a (DYNGO), and 200 µM Genistein (GEN), for 30 minutes before being exposed to A) fluorescently labeled Tau monomers (FL-Mono)

at a concentration of 500 nM, and B) fluorescently labeled small fibrils (FL-S-fib) at a concentration of 250 nM, for 3 hours. Exceptionally, EIPA was present during the entire incubation with Tau. Error bars represent SEM; n=8-9 independent experiments per experimental condition. One-way ANOVA followed by post-hoc test; *p<0.05, **p<0.01, ***p<0.001, or ****p<0.0001 vs. UTC. The uptake and accumulation of C) Dextran-FITC at a concentration of 100 μM, and D) low-density lipoprotein-BODIPY (LDL-BODIPY) at a concentration of 5 μM, were studied in LUHMES neurons following pre-treated with increasing concentrations of Dyngo-4a for 3 hours. E) Cell viability was assessed using calcein treatment in LUHMES neurons treated with small molecules in A and B for 30 min and incubated without small molecules for 3 hours. Error bars represent SEM; n=18-23. One-way ANOVA followed by post-hoc test; ns: not significant.

The small molecule inhibitors of protein degradation and muscarinic receptors were also tested in LUHMES neurons, showing a similar impact on Tau uptake as in iPSCNs (**Figure 4.22A and B**), and no toxicity was observed (**Figure 4.22C and D**). Similar to iPSCNs, heparin treatment inhibited the uptake of Tau fibrils but had no effect on Tau monomers (**Figure 4.22E**). These findings suggest that HSPGs are involved in the differential uptake and accumulation of Tau monomers versus aggregates in human neurons.

To further understand the impact of heparin, we examined the effect of heparin pretreatment on Tau uptake. Cells were incubated with heparin for 2 hours, followed by removal of heparin-containing media and washing with PBS before Tau treatment. The intracellular fluorescence intensity was measured at different time points over 12 hours. For cells treated with FL-Mono, no significant differences were observed between untreated and heparin-pretreated cells in the accumulation of fluorescence signal over time (**Figure 4.23A**). However, heparin pretreatment significantly reduced the intracellular fluorescence signal for cells treated with S-fib compared to untreated cells (**Figure 4.23B**). This suggests that heparin has a lasting inhibitory effect, specifically on the uptake and accumulation of Tau fibrils.

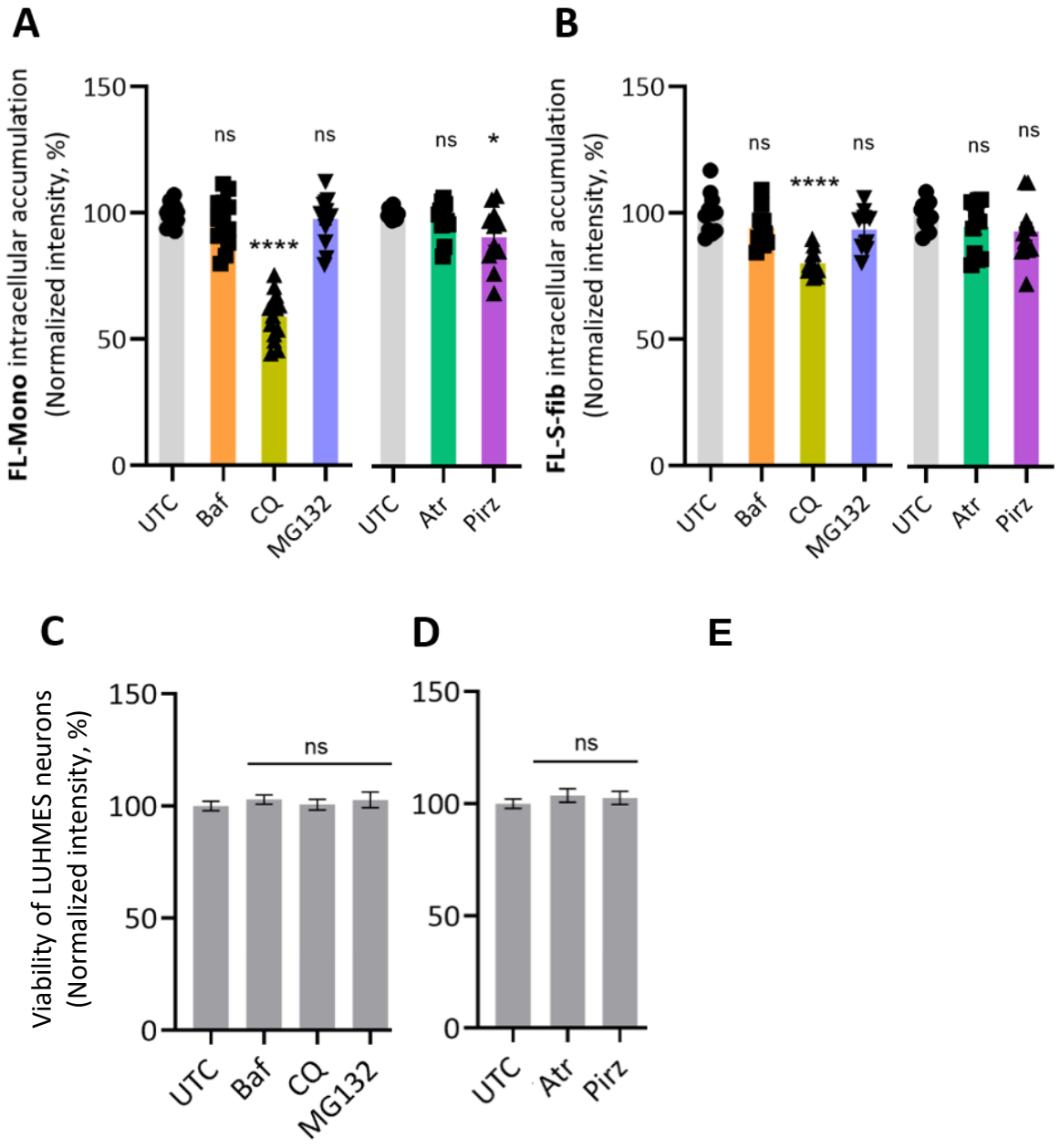

Figure 4.22 The impact of protein degradation machinery, muscarinic receptor antagonist, and heparin on Tau uptake in LUHMES neurons. The fluorescence was measured in cells left as untreated control (UTC) or treated with 25 nM of fluorescently labeled Tau A) monomers (FL-Mono), and B) small fibrils (FL-S-fib) for 20 hours, along with the presence of various compounds, including 100 nM bafilomycin A1 (Baf), 30 µM chloroquine (CQ), 100 nM MG132, 200 µM Atropine (Atr), or 20 µM Pirenzepine (Pirz). Error bars represent SEM; n=8-12 independent experiments per experimental condition. One-way ANOVA followed by post-hoc test; *p<0.05 and ***p<0.001 vs. UTC. C and D)

The viability of LUHMES neurons were measured after 20 hours of treatment with compounds in part A and B at the aforementioned concentration using calcein fluorescence. Error bars represent SEM; n=15-20 independent experiments per experimental condition. One-way ANOVA followed by a post-hoc test. E) The fluorescence analysis was conducted in LUHMES neurons treated with 25 nM fluorescently labeled monomers (Mono) and small fibrils (S-fib) for 20 hours in the presence of 8 μM Heparin. Error bars represent SEM; n=3 independent experiments per experimental condition. One-way ANOVA followed by a post hoc test; ***p<0.001 and ****p<0.0001 vs. UTC. ns: not significant.

Furthermore, we investigated the competition dynamics between the same species of Tau by pretreating LUHMES neurons with unlabeled Tau monomers or Tau fibrils for 2 hours. After removing the media and washing the cells, the same species labeled with fluorescence were added. The intracellular fluorescence was monitored at different time points during a 24-hour incubation. The results showed that pretreatment with Tau monomers did not significantly impact the intracellular accumulation of labeled Tau monomers (**Figure 4.23C**). In contrast, pretreatment with Tau fibrils led to a significantly slower accumulation rate of labeled Tau fibrils in the early hours up to 9 hours after treatment (**Figure 4.23D**). However, after 12 hours of incubation with labeled Tau fibrils, the rate of fluorescence signal increase became similar between pretreated and untreated cells. This suggests the existence of a recovery point where cells can regain their capacity to internalize and accumulate aggregates. These findings further indicate the divergence between the uptake and accumulation pathway of Tau aggregates and monomers.

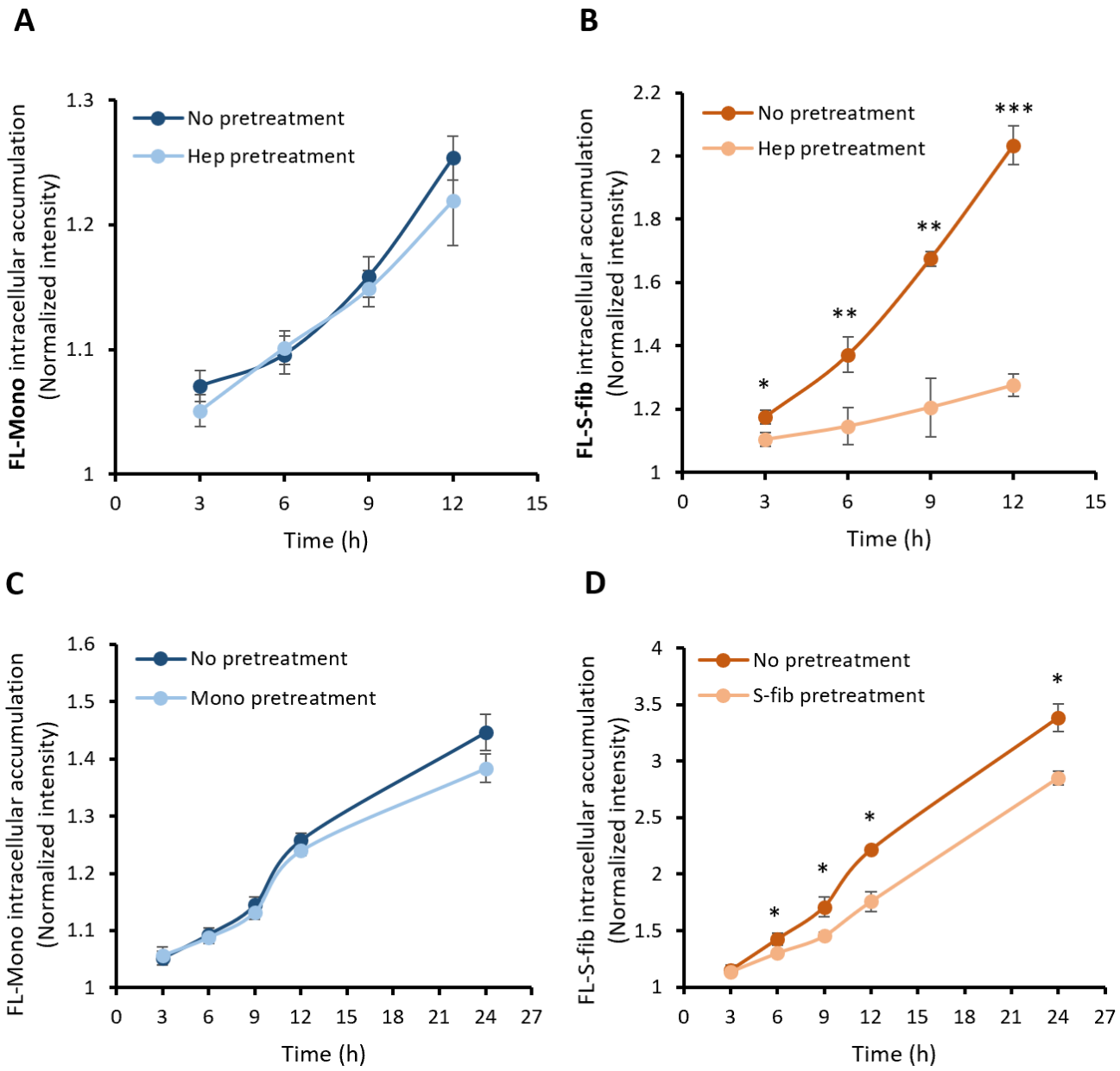

Figure 4.23 The effect of Heparin and Tau pretreatment on intracellular Tau accumulation in LUHMES neurons. Cells were pre-treated with 100 µM Heparin (Hep) for 2 hours before being exposed to A) fluorescently labeled monomers (FL-Mono) at a concentration of 250 nM and B) fluorescently labeled small fibrils (FL-S-fib) at a concentration of 150 nM. The intracellular Tau accumulation was monitored over time. C) Cells were pre-treated with 200 uM unlabeled monomers (Mono) for 2 hours before exposure to 250 nM FL-Mono. The kinetics of Tau accumulation were subsequently measured. D) Cells were pre-treated with 200 uM unlabeled small fibrils (S-fib) for 2 hours before being exposed to 150 nM FL-S-fib. The intracellular Tau accumulation was

monitored over time. The significance was calculated between the "No pretreat" condition (cells without any pre-treatment) and the "Pretreat" condition (cells with the specific pre-treatment) at each time point. Error bars represent SD; n=3 independent experiments per experimental condition. ٣

4.9 Studying the role of molecular mediators of Tau uptake on the neuronal accumulation of Tau monomers and aggregates

We conducted an *in vitro* knockdown experiment targeting specific genes involved in Tau uptake and cell sorting pathways to validate the differential uptake and accumulation of Tau monomers and aggregates. Both iPSCNs and LUHMES neurons were treated with siRNA on day two of differentiation, followed by incubation with Tau Mono or S-fib for 16 to 24 hours between days 6 to 8 of differentiation, as illustrated in **Figure 4.24A**. Three genes, namely low-density lipoprotein receptor-related protein 1 (LRP1), Exostosin Glycosyltransferase 2 (EXT2), and vacuolar protein sorting-associated protein 35 (VPS35), showed differential regulation of Mono and S-fib uptake in both cell types (**Figure 4.24B – G**). Downregulating these genes was ineffective on cell viability (**Figure 4.24H and I**).

Previous research has identified the surface receptor LRP1 as a key regulator of Tau uptake. In a previous study (Jennifer N. Rauch et al., 2020), the knockout of LRP1 in iPSCNs demonstrated nearly complete inhibition of Tau monomer uptake, while only a partial inhibition of fibril uptake was observed. Consistent with these findings, our study revealed that knocking down LRP1 in iPSCNs resulted in a significant reduction in the intracellular accumulation of both Tau monomers and small fibrils. However, the reduction in fibril uptake was notably less pronounced compared to monomer uptake (**Figure 4.24B**). Surprisingly, in LUHMES neurons, LRP1 knockdown significantly impacted monomer uptake and accumulation but did not affect fibril uptake (**Figure 4.24E**). These results suggest that in LUHMES neurons, the uptake of Tau fibrils is independent of LRP1, unlike the uptake of Tau monomers.

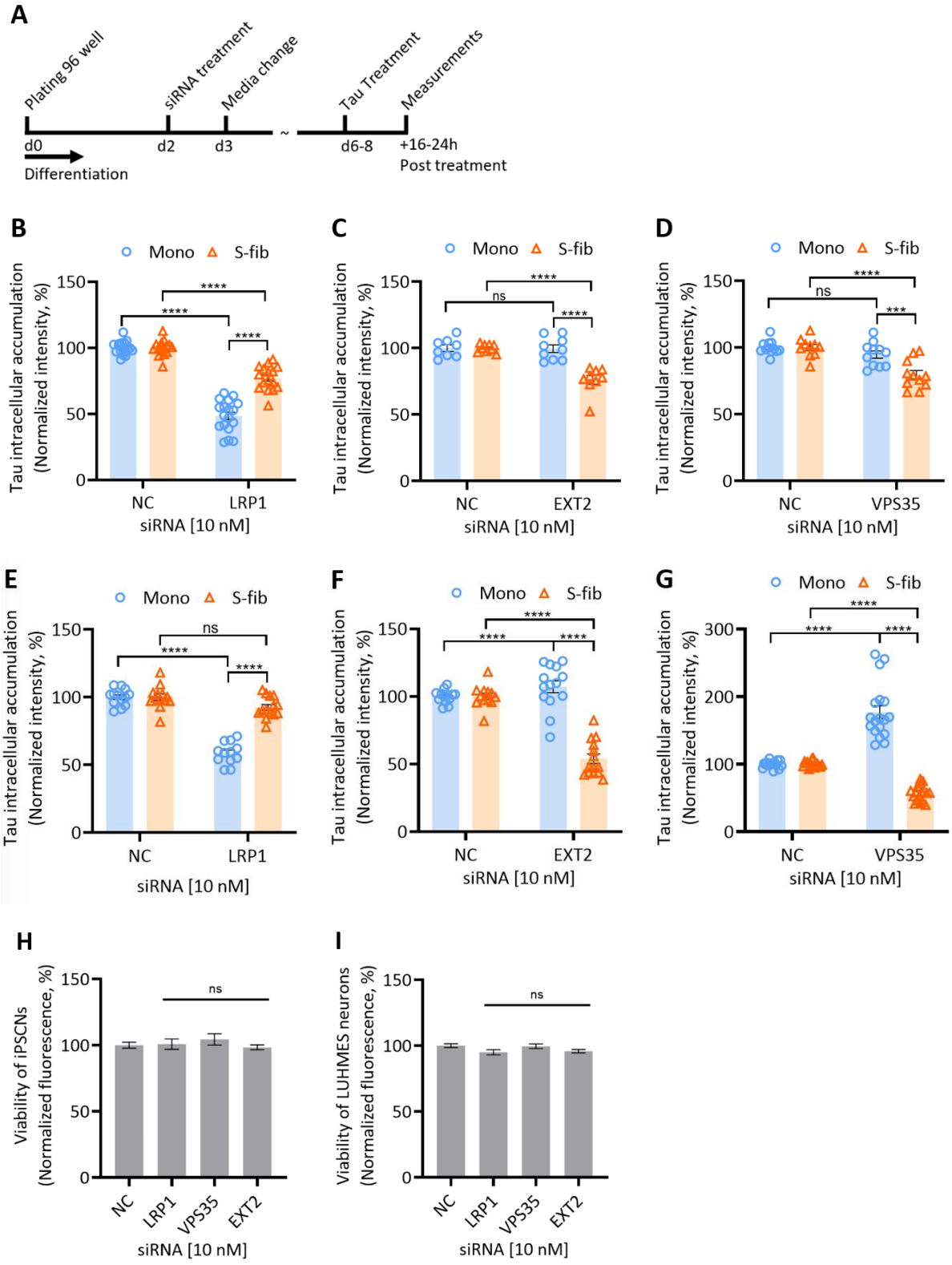
A
Plating 96 well
siRNA treatment
Media change
Tau Treatment
Measurements
d0
d2
d3
d6-8
+16-24h
Post treatment
Differentiation
B
C
D
E
F
G
Mono
S-fib
Tau intracellular accumulation (Normalized intensity, %)
NC
LRP1
EXT2
VPS35
siRNA [10 nM]
ns
****
***
H
I
Viability of iPSCNs (Normalized fluorescence, %)
Viability of LUHMES neurons (Normalized fluorescence, %)

Figure 4.24 The impact of gene knockdown on the uptake and accumulation of Tau monomers and aggregates. A) The experimental scheme provides a timeline of events. iPSC-derived neurons or neuronally differentiated LUHMES cells were cultured in 96 well-plates using a differentiation medium. On day 2 of differentiation, the cells were treated with 10 nM siRNA overnight, followed by a media change. From day 6 to 8, the neurons were exposed to fluorescently labeled Tau, and intracellular fluorescence was measured within a 16 to 24-hour timeframe after treatment. B, C, D) The intracellular accumulation of labeled Tau monomers (Mono) and small fibrils (S-fib) in iPSC-derived neurons treated with siRNAs of none-coding (NC), LRP1, EXT2, and VPS35. E, F, G) The intracellular accumulation of labeled Tau Mono and S-fib in LUHMES neurons treated with LRP1, EXT2, and VPS35 siRNAs. Error bars represent SEM; n=9-18 independent experiments per experimental condition. One-way ANOVA followed by a post-hoc test; ***$p<0.001$ and ****$p<0.0001$. The viability of (H) iPSC-derived neurons and (I) LUHMES neurons treated with 10 nM of the aforementioned siRNAs. Error bars represent SEM; n=9-14 independent experiments per experimental condition. One-way ANOVA followed by a post-hoc test. ns: not significant vs. NC.

EXT2, a member of the Exostosin Glycosyltransferase family involved in HSPG synthesis, also showed differential effects on Mono and S-fib uptake (Rauch et al., 2018; Stopschinski et al., 2018). Knocking down EXT2 reduced the intracellular accumulation of S-fib significantly but did not affect Mono in both iPSCNs and LUHMES neurons (**Figure 4.24C and F**). Interestingly, Mono accumulation in EXT2 knockdown LUHMES neurons showed a slight but significant increase. These findings further support the role of HSPGs in the uptake of Tau aggregates but not monomers in human neurons.

In our hypothesis-based screening, we also investigated the impact of VPS35 downregulation on the uptake and accumulation of Tau monomers and fibrils. In iPSCNs, the knockdown of VPS35 significantly reduced S-fib accumulation while having no effect on Mono (**Figure 4.24D**). Interestingly, in LUHMES neurons, the downregulation of VPS35 resulted in a significant reduction in S-fib accumulation but a marked increase in the accumulation of Mono (**Figure 4.24G**). VPS35 is an essential component of the retromer complex, and our data suggest that this complex may play a critical role in regulating Tau's uptake and intracellular accumulation. Further analysis is needed to determine the exact role of the retromer complex in Tau transfer and its distribution within cells. Our assessment of cell

viability following siRNA treatment showed no evidence of toxicity in both cell types (**Figure 4.24H and I**).

We also investigated the impact of LRP1 and EXT2 downregulation on Tau oligomers (Oligo) uptake in LUHMES neurons. Knockdown of LRP1 did not affect Oligo accumulation, while EXT1 knockdown (another member of the Exostosin Glycosyltransferase family) reduced Oligo uptake by approximately 50% (**Figure 4.25A**). This suggests that the uptake and accumulation of oligomers are similar to small fibrils in LUHMES neurons. Furthermore, we tested the uptake of co-factor-free Tau fibrils under LRP1 and EXT1 siRNA treatment, and the results showed a similar modulation as observed for Oligo uptake (**Figure 4.25A**). No toxicity was observed in these conditions (**Figure 4.25B**).

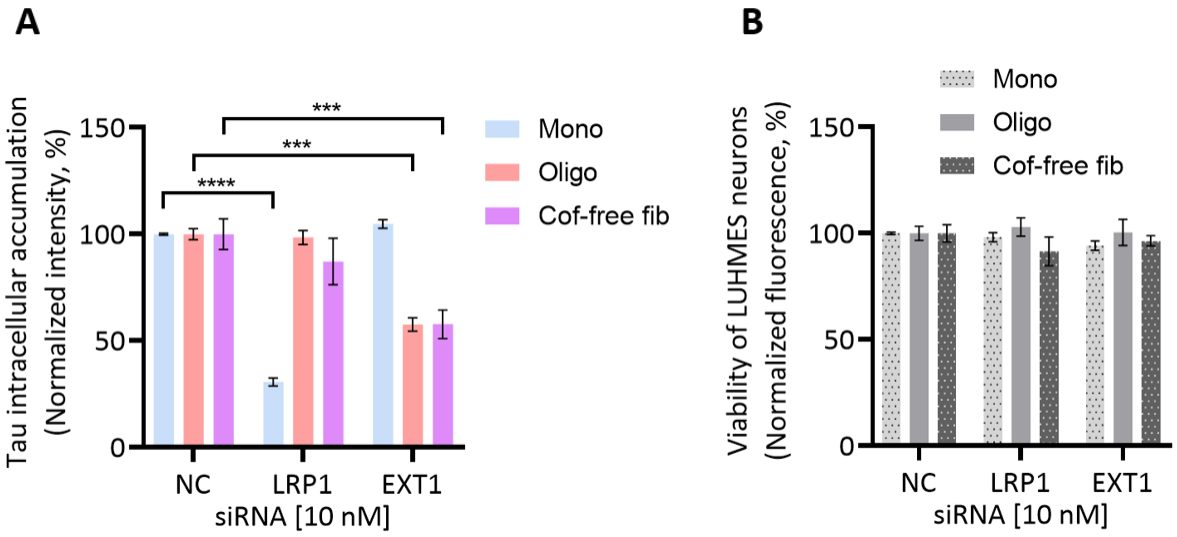

Figure 4.25 The impact of gene downregulation on Tau oligomers and cofactor-free fibrils uptake. A) The effect of gene knockdown on the internalization and accumulation of Tau monomers (Mono), oligomers (Oligo), and co-factor-free fibrils (Cof-free fib) in LUHMES neurons. B) The viability of LUHMES neurons following treatment with siRNAs targeting non-coding (NC), LRP1, and EXT1. Error bars represent SEM; n=3 independent experiments per experimental condition. One-way ANOVA followed by a post-hoc test; ***p<0.001 and ****p<0.0001 vs. NC. Results without significance are denoted as not significant (ns).

4.10 Studying the cellular localization of internalized Tau monomers and aggregates

To visualize the uptake and accumulation of Tau monomers and aggregates, we conducted an experiment in iPSCNs and LUHMES neurons using confocal imaging. In iPSCNs, red-labeled monomeric Tau (Mono) and green-labeled Tau fibrils (S-fib) were applied for 3 hours, and imaging was performed either immediately or after 21 hours of incubation without Tau in the differentiation media. Confocal imaging was performed after cellular staining with calcein-red orange as a marker of viable cells. Imaging immediately after 3 hours of incubation with FL-Tau revealed small red, green, and a few yellow puncta representing vesicles containing only Mono, only S-fib, or both, respectively. Puncta were distributed in both soma and neurites (**Figure 4.26**). However, after 21 hours, larger yellow dots appeared, predominantly localized in the soma, indicating the accumulation of endocytic vesicles over time, which were subsequently transferred to the soma. Similar results were obtained when examining Tau oligomers (**Figure 4.27**).

We repeated the experiment in LUHMES neurons, where smaller and more dispersed green, red, and yellow puncta were observed after 3 hours. After 21 hours, larger dots were primarily localized in the soma (**Figure 4.28**). Notably, even after 21 hours, distinct green and red dots were still present inside the soma of LUHMES neurons, suggesting further segregation in the intracellular processing of exogenous Tau Mono and S-fib in the downstream pathway compared to iPSCNs.

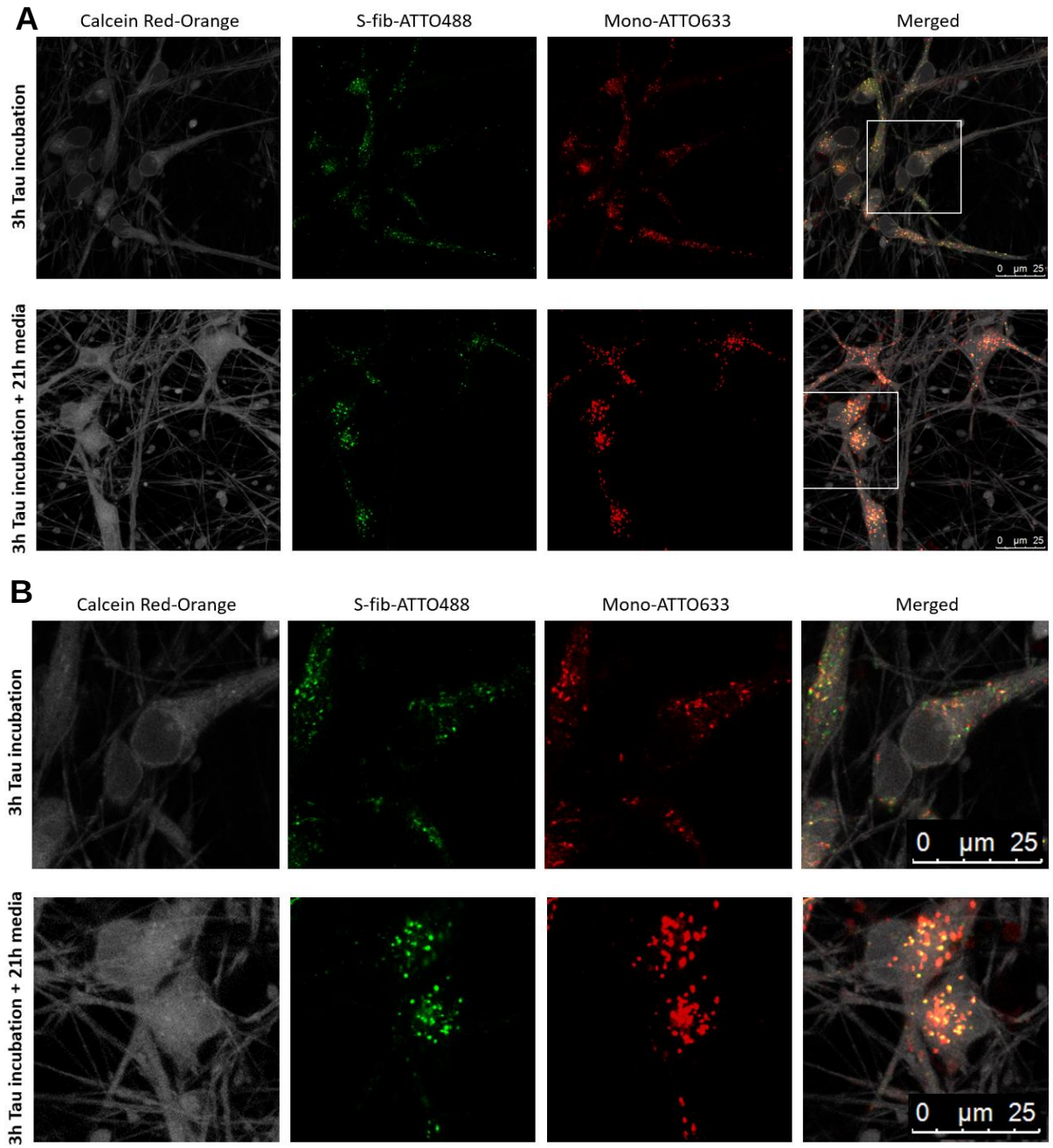

Figure 4.26 Confocal imaging of Tau monomers and small fibrils in iPSC-derived neurons. A) Confocal imaging of iPSC-derived neurons (iPSCNs) treated simultaneously with 100 nM Tau monomers labeled with ATTO633 (Mono-ATTO633) and 100 nM small fibrils labeled with ATTO488 (S-fib-ATTO488). The cells were incubated with Tau for 3 hours, and imaging was carried out immediately or after 21 hours of further incubation in the standard differentiation media without Tau. B) A higher magnification view of the region indicated by the square in part A.

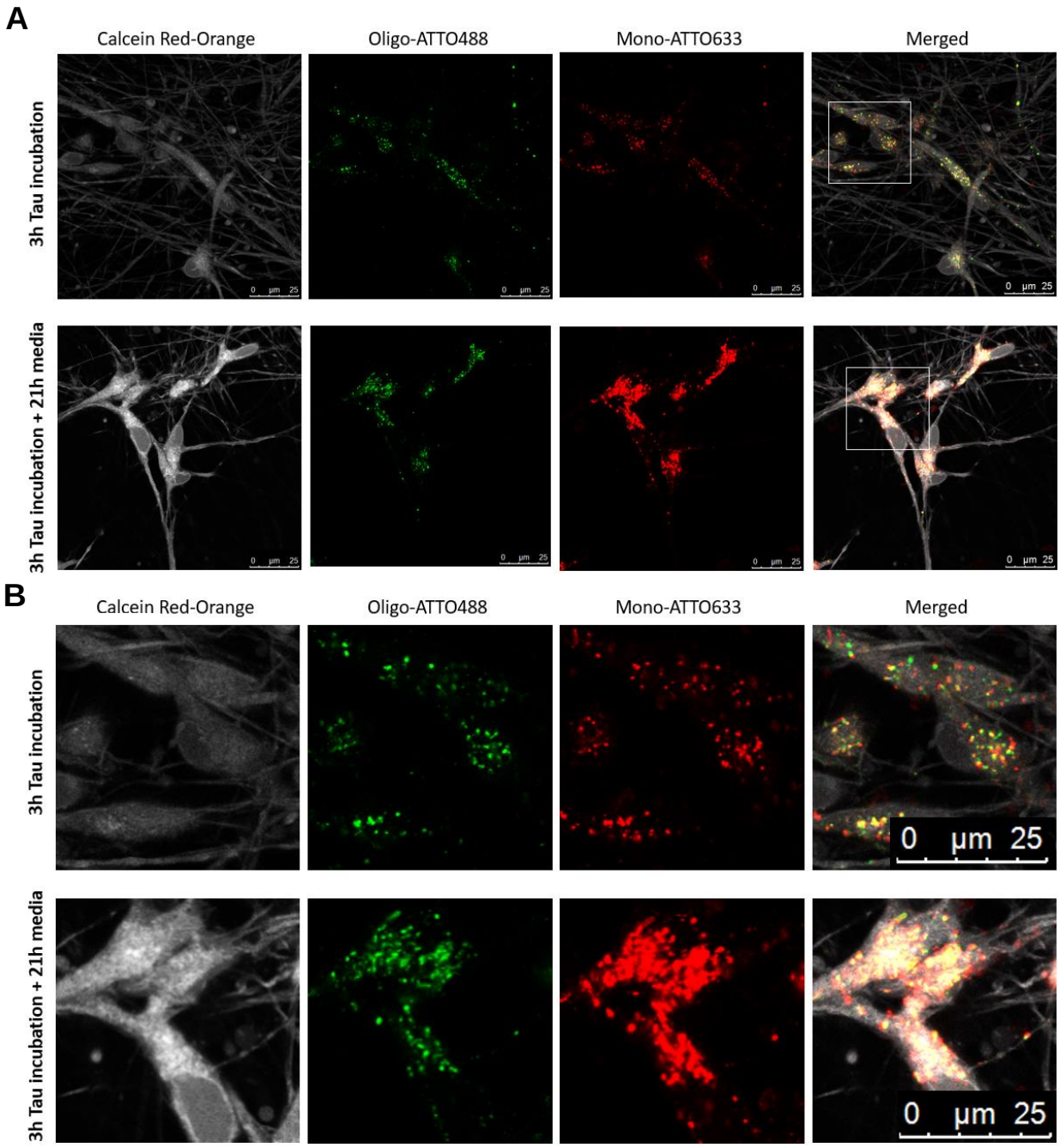

Figure 4.27 Confocal imaging of Tau monomers and oligomers in iPSC-derived neurons. A) Confocal imaging of iPSC-derived neurons (iPSCNs) co-treated with 100 nM Tau monomers labeled with ATTO633 (Mono-ATTO633) and 100 nM oligomers labeled with ATTO488 (Oligo-ATTO488). The cells were incubated with Tau for 3 hours, and imaging was carried out immediately or after 21 hours of further incubation in the standard differentiation media without Tau. Calcein red-orange was utilized as a cell tracker. B) A higher magnification view of the region indicated by the square in part A.

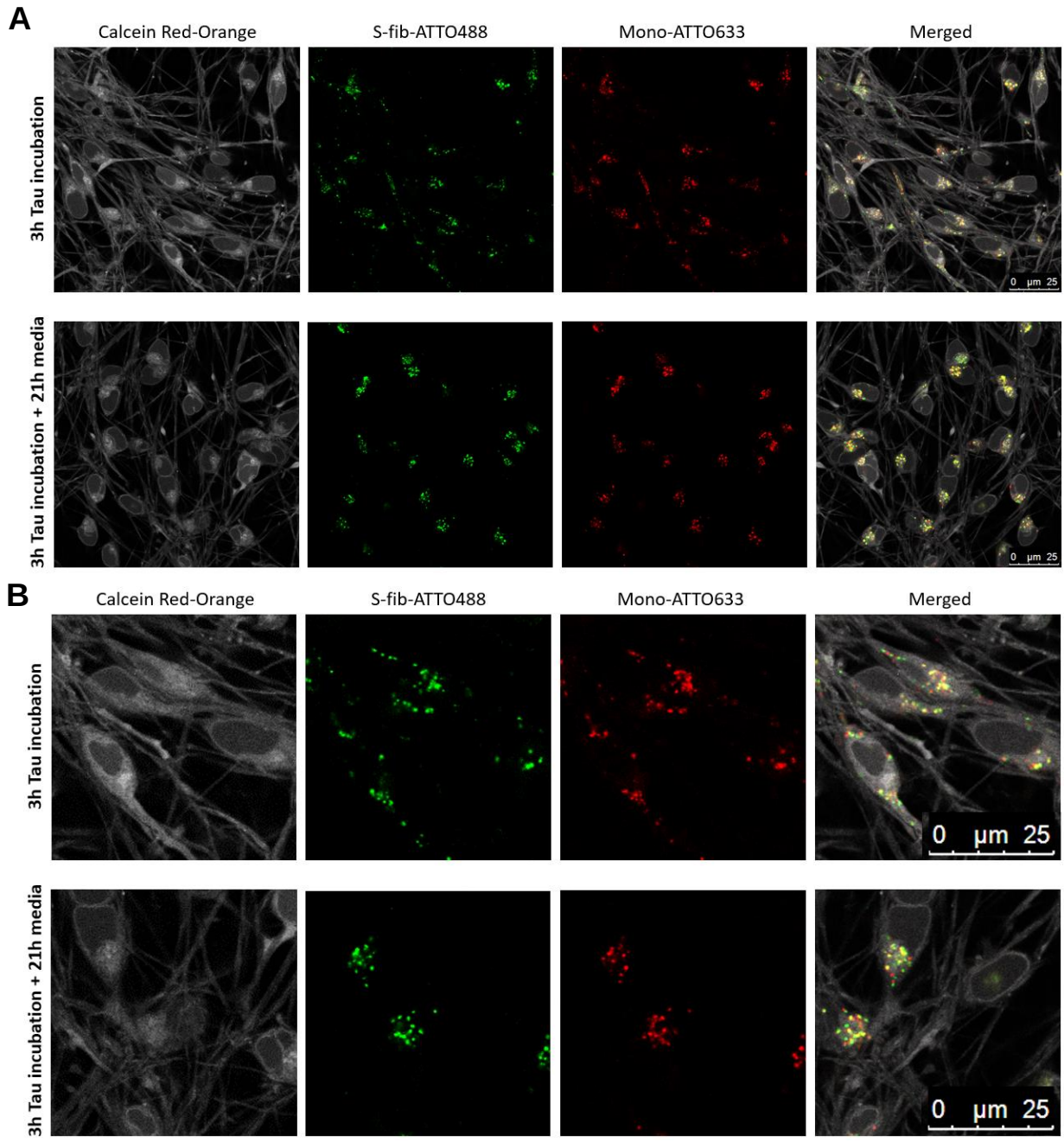

Figure 4.28 Confocal imaging of Tau monomers and small fibrils in LUHMES neurons. A) Confocal imaging of LUHMES neurons co-treated with 500 nM Tau monomers labeled with ATTO633 (Mono-ATTO633) and 100 nM small fibrils labeled with ATTO488 (S-fib-ATTO488) for 3 hours. Imaging was carried out immediately or after 21 hours of incubation in the standard differentiation media without Tau. Calcein red-orange was utilized as a cell tracker. B) A higher magnification view of the region indicated by the square in part A.

5. Discussion

5.1 Which Tau species may play the role of seeds in pathology propagation?

Previous studies have demonstrated the formation of various aggregated species during Tau fibrillation (Limorenko & Lashuel, 2022). In our preparations, we also confirmed the presence of various Tau aggregated species through atomic force microscopy (AFM) imaging. Here we employed a biophysical fractionation technique to obtain a more homogeneous population of aggregated Tau species. A similar approach has been utilized for the isolation of α-synuclein aggregates in previous research (Kumar et al., 2020).

While the distinction and definition of different Tau aggregated species remain unclear, our fractionation analysis using circular dichroism (CD) spectroscopy revealed that the soluble oligomeric fraction exhibited a lower β-sheet content compared to fibrils, indicating an intermediate structure. Furthermore, AFM and electron microscopy (EM) imaging revealed morphological differences between oligomers and small fibrils. Interestingly, the soluble oligomers were found to exert mild toxicity when incubated with cells at high concentrations over an extended period. These findings are consistent with previous studies that have demonstrated the toxicity of extracellular Tau (eTau) oligomers *in vitro* (Kaniyappan et al., 2017; Pampuscenko et al., 2021), while fibrillar eTau did not exhibit detrimental effects on cell viability (Ward et al., 2012).

Comparing the biological characteristics of different fractions, we observed that small insoluble fibrils and soluble oligomers displayed higher uptake and accumulation efficiency in human neurons compared to large fibrils. This finding aligns with previous reports demonstrating the efficient uptake of low molecular weight and short Tau fibrils, but not long fibrils, in primary mouse neurons (Wu et al., 2013) and induced pluripotent stem cell-derived neurons (iPSCNs) (Usenovic et al., 2015). Similarly, a comparison of various Tau species' uptake in H4 neuroglioma cells and iPSCNs for one hour revealed lower uptake efficiency for fibrils compared to monomers, oligomers, and sonicated fibrils (Jennifer N. Rauch et al., 2020). Sonication-induced fragmentation of fibrils has proven highly effective in increasing

the uptake of synuclein aggregates and is now commonly employed in seeding studies (Karpowicz et al., 2017).

The prion-like spreading hypothesis proposes that for the spread of Tau pathology, a seed must be taken up by cells, escape the endosomal system to access the endogenous pool of monomeric Tau in the cytosol, and subsequently induce endogenous aggregation (Vogels et al., 2020). Our study demonstrated that oligomers and small fibrils exhibited the most efficient internalization and accumulation in human neurons. Furthermore, these intermediates were capable of escaping endosomal entrapment and inducing endogenous aggregation. These findings suggest that intermediate Tau species possess characteristics that make them potent candidates for playing the role of pathological seeds in the context of the prion-like spreading hypothesis. Therefore, understanding the mechanisms underlying the uptake and accumulation of intermediate Tau aggregates may pave the way for developing preventive strategies to halt or slow down the process of Tau pathology spreading in the brain.

5.2 Do Tau monomers and aggregates share the same neuronal uptake and accumulation mechanism?

Despite the well-described intracellular functions of Tau (Brandt et al., 2020), it is essential to note that Tau monomers are also present in the extracellular environment and body fluids under physiological conditions (Zetterberg, 2017), and they are actively secreted from neurons (Pooler et al., 2013; Wu et al., 2016; Yamada et al., 2014). Moreover, identifying a specific receptor for eTau monomers (Jennifer N. Rauch et al., 2020) suggests an unknown physiological role for this species. This emphasizes the need to develop strategies that selectively target pathological Tau species while preserving the physiological transport of eTau, to enhance therapeutic efficacy and minimize unintended side effects.

In our study, we observed a higher neuronal accumulation of Tau aggregates compared to monomers in human neurons, indicating a distinct mechanism of cell internalization and storage. This finding is consistent with an earlier report that demonstrated a significantly higher uptake of Tau aggregates compared to monomers in C17.2 mouse neuronal precursor cells after 3 and 9 hours of exposure (Frost et al., 2009). Similarly, in primary mouse neurons, Tau monomers were not detected inside the cells

even after treatment with a five-fold higher dose compared to aggregates (Wu et al., 2013). However, a study investigating Tau uptake in HEK293T cells reported a comparable internalization efficiency for both monomers and aggregates (Falcon et al., 2015). The differential results of the latter study may be attributed to the use of a proliferating cell line with a highly dynamic membrane compared to non-dividing neuronal cells. This highlights the considerable variation in cellular uptake mechanisms among different cell types and emphasizes the importance of selecting physiologically relevant cell models for studying Tau uptake.

A recent study employed a pH-sensitive fluorescence label to track Tau within low-pH endosomes in iPSCNs and reported a comparable rate of internalization for both Tau monomers and aggregates after 3 hours (Evans et al., 2018). The discrepancy between their findings and ours in the same cell type could be attributed to methodological differences, as pH-sensitive labels are only active in low-pH vesicles and not after entry into the cytosol. Our study demonstrated that all Tau species can escape endosomal vesicles and enter the cytosol within a few hours, underscoring the importance of using a stable fluorescent label for comprehensive evaluation of total internalized and accumulated Tau.

Evans and colleagues also reported a similar monomeric and aggregated Tau uptake ratio (Evans et al., 2018). In line with this, our kinetic study indicated that within the first 3 hours of exposure to extracellular Tau, the accumulation of monomers and aggregates in iPSCNs was similar. This suggests that a post-internalization process may be involved in the differential neuronal accumulation of Tau. However, inhibiting various protein degradation processes did not increase the storage of Tau monomers within 24 hours. It is possible to hypothesize that Tau monomers are expelled from neurons following uptake, while aggregates become entrapped and accumulate. In LUHMES neurons, we observed a much lower accumulation of monomers compared to iPSCNs, suggesting the involvement of more stringent regulatory mechanisms. Interestingly, the knockdown of vacuolar protein sorting 35 (VPS35), a component of the cellular sorting machinery, including the retromer complex, in LUHMES neurons resulted in a significant increase in the accumulation of Tau monomers. This suggests the importance of the cellular sorting machinery, particularly the retromer complex, in this process.

Overall, our study provides further insights into the differential mechanisms of uptake and accumulation of Tau monomers and aggregates in human neurons. These findings contribute to our understanding of

the cellular processes involved in Tau pathology and may guide the development of therapeutic strategies aimed at selectively targeting pathological Tau species while preserving the physiological functions of eTau.

5.3 What cellular mechanisms are involved in the neuronal uptake and accumulation of Tau monomers and aggregates?

5.3.1 Clathrin- and dynamin-mediated endocytosis

The molecular mechanism of Tau internalization is still debated, and there is conflicting evidence regarding the specific endocytic machinery involved in this process. Our study indicates that the uptake of Tau monomers and aggregates in iPSCNs and LUHMES neurons depended on clathrin and dynamin but not caveolin. However, in LUHMES neurons, inhibition of dynamin resulted in the induction of macropinocytosis, which masked the impact of dynamin inhibition on Tau uptake. Dynamin is a critical component of clathrin-mediated endocytosis (Prichard et al., 2021), and our data support the involvement of both clathrin and dynamin in the endocytosis of Tau species in human neurons. This is consistent with previous studies demonstrating the role of dynamin in the uptake of Tau aggregates in primary mouse neurons (Calafate et al., 2016; Soares et al., 2021; Wu et al., 2013), SH-SY5Y neuroblastoma cells (Falcon et al., 2018), and iPSCNs (Evans et al., 2018). The clathrin-mediated internalization of both Tau monomers and aggregates was also confirmed in SH-SY5Y cells (Falcon et al., 2018). However, in contrast to our findings, Evans and colleagues reported that the uptake of Tau monomers was a dynamin-independent process in iPSCNs differentiated for 75 days (Evans et al., 2018). Moreover, the uptake of Tau aggregates in primary mouse neurons was described as a clathrin-independent process (Holmes et al., 2013; Soares et al., 2021). These discrepancies may be attributed to differences in cell types, particularly since studies on mouse neurons consistently show clathrin independence while most studies on human neurons indicate clathrin dependency. This suggests a potential interspecies difference in the neuronal uptake of Tau. Methodological variations could also contribute to the contradictory outcomes between experiments, such as using different inhibitors.

5.3.2 Macropinocytosis

Regarding the role of actin polymerization and macropinocytosis, we observed a distinction between iPSCNs and LUHMES neurons. The uptake of Tau monomers and aggregates in iPSCNs and monomers in LUHMES neurons were sensitive to inhibitors of actin polymerization and macropinocytosis. However, the uptake of Tau aggregates in LUHMES neurons was independent of both processes. Previous studies have indicated actin-dependent endocytosis of Tau aggregates in primary mouse neurons (Holmes et al., 2013; Soares et al., 2021) and of both monomers and aggregates in SH-SY5Y cells (Falcon et al., 2018). However, in iPSCNs differentiated for 65 days, the uptake of monomers was actin-dependent, while the uptake of aggregates was actin-independent (Evans et al., 2018). The uptake of monomers and aggregates in LUHMES neurons appears to be similar to the pattern observed in more mature iPSCNs with 65 days of differentiation than in less mature iPSCNs in our study with approximately 15 days of differentiation. The unexpected induction of macropinocytosis upon dynamin inhibition in LUHMES neurons resulted in the accumulation of both monomers and aggregates, indicating that this process can internalize both species. However, under normal conditions, the level of macropinocytosis in LUHMES neurons is relatively low. These findings highlight the need for further studies on the role of neural maturation in the endocytic mechanisms of Tau aggregates.

5.4 What molecular mediators are involved in the distinct neuronal uptake and accumulation of Tau monomers versus aggregates?

5.4.1 Heparan sulfate proteoglycans (HSPGs)

The role of HSPGs in Tau uptake has been a subject of debate. Initially, HSPGs were identified as the first molecular mediators of Tau cellular internalization (Holmes et al., 2013). However, a subsequent study challenged this finding by showing that the uptake of Tau is independent of glycosaminoglycans (Michel et al., 2014). The conflicting results could be attributed to the use of different Tau species in the studies, with the first study using Tau fibrils and the second using Tau monomers. To investigate the role of HSPGs in Tau uptake, we employed heparin as an inhibitor of HSPGs and performed siRNA-mediated knockdown of genes involved in HSPG synthesis, such as EXT1 and EXT2, in iPSCNs and

LUHMES neurons. Our data confirmed that treatment with heparin or knockdown of EXT1 and EXT2 reduced the uptake and accumulation of Tau aggregates but not monomers in human neurons. While there is consensus on the role of HSPGs in the uptake of Tau aggregates (Mah et al., 2021), discrepancies exist regarding the role of HSPGs in the uptake of Tau monomers. Astrocytes have been reported to exhibit HSPGs-independent uptake of Tau monomers (76), whereas EXT2 knockout was shown to significantly reduce the uptake of Tau monomers in H4 neuroglioma cells and to a lesser extent in iPSCNs (Rauch et al., 2018). Additionally, HSPGs-dependent uptake of Tau monomers has been identified in C6 glioma cells (Song et al., 2022). These contradictory results may be explained by differences in cell types (C6 glioma cells vs. astrocytes and neuroglioma cells), methodological differences, or a combination of both. Further studies are required to fully elucidate the role of HSPGs in the uptake of Tau monomers in human neurons.

5.4.2 LDL-receptor-related protein-1 (LRP1)

Recent studies have identified LRP1 as a critical receptor for Tau (Jennifer N. Rauch et al., 2020). It has been shown that the knockout of LRP1 completely blocks the uptake of Tau monomers in neuroglioma cells and iPSCNs. However, a partial reduction in the uptake of sonicated fibrils was observed in neuroglioma cells. Similarly, our study demonstrated that the knockdown of LRP1 in iPSCNs led to a significant decrease in the uptake and accumulation of Tau monomers but only a slight reduction in small fibrils. Interestingly, we found that the knockdown of LRP1 in LUHMES neurons strongly reduced the uptake of monomers but had no impact on the uptake of Tau fibrils. This suggests that the uptake of Tau fibrils in LUHMES neurons is entirely independent of LRP1. Consistent with our findings, a CRISPR screen for Tau uptake in iPSCNs identified LRP1 as one of the top-ranked genes associated with monomer uptake but not with oligomer uptake (Evans et al., 2020). Furthermore, the knockout of LRP1 in CHO cells confirmed that LRP1 is not the sole receptor for Tau (Cooper et al., 2021). Thus, further research is needed to elucidate other potential receptors for Tau, particularly in human neurons.

Moreover, the uptake of Tau oligomers has been reported to be highly dependent on LRP1, similar to monomeric Tau (Jennifer N. Rauch et al., 2020). However, in our study, the knockdown of LRP1 in LUHMES neurons did not reduce the uptake of Tau oligomers, similar to small fibrils. This discrepancy may be attributed to differences in the preparation protocol of Tau oligomers. Rauch et al. induced

oligomerization through a 4-hour incubation without specifying any purification or enrichment steps. This may have led to a mixture of oligomers and monomeric Tau that influenced the observed impact. Here, we enriched the oligomers by removing the monomeric protein using ultrafiltration, resulting in a pure fraction of soluble aggregates or oligomers. Therefore, a thorough characterization of Tau oligomers is crucial before interpreting any results related to these intermediate aggregated species.

Our study revealed that the uptake of Tau aggregates in iPSCNs is partially dependent on LRP1, while in LUHMES neurons, it is entirely independent of LRP1. Additionally, the cellular accumulation of Tau monomers, which is highly reliant on LRP1, was significantly higher in iPSCNs compared to LUHMES neurons. These variations could be attributed to two main differences between the cell models. First, there are differences in neuronal types, with iPSCNs representing cortical neurons (Strauss et al., 2021), while LUHMES neurons are dopaminergic neurons (Zhang et al., 2014). Second, the degree of neuronal maturity varies between these cell models. iPSCs undergo an epigenetic reset to the pluripotent state of human embryonic stem cells (de Boni et al., 2018), while LUHMES neurons are cultured for an additional eight weeks *in vivo* before isolation (Lotharius et al., 2002). Moreover, studies have shown that LUHMES neurons differentiate into mature and functional neurons within one week (Lauter et al., 2020; Loser et al., 2021). In contrast, the maturity degree of neurons derived from iPSCs can vary (Volpato et al., 2018; Xia et al., 2016), especially with short differentiation protocols as in our study (Nicholas et al., 2013). The initial study reporting the role of LRP1 in the uptake of Tau aggregates was also conducted on iPSCNs differentiated for a short period of 14 to 18 days (Jennifer N. Rauch et al., 2020). However, a CRISPR screen for identifying genes involved in Tau uptake was performed on iPSCNs at day 65 of differentiation, where LRP1 did not reach the study's threshold for oligomer uptake (Evans et al., 2020). These pieces of evidence highlight the importance of further studies investigating the role of LRP1 in the uptake of Tau aggregates in various types of human neurons with different degrees of maturity.

5.4.3 Vacuolar protein sorting 35 (VPS35)

VPS35 is a crucial component of the retromer complex (Seaman et al., 1997), which plays a role in recycling endosomal transmembrane proteins and sorting cargoes within cells. Previous studies have implicated VPS35 in several neurodegenerative diseases (Williams et al., 2022). A genetic study

exploring the connection between AD and specific variations in retromer-related genes, alongside an extensive genome-wide association analysis, focused on sporadic AD, have both furnished compelling evidence endorsing the involvement of VPS35 and retromer in the development of AD (Lambert et al., 2013; Rogaeva et al., 2007). Our data indicates the involvement of VPS35 in the cellular accumulation of eTau. We demonstrated that the knockdown of VPS35 leads to a reduction in the accumulation of aggregated Tau in both iPSCNs and LUHMES neurons.

A previous study reported contrasting results, showing that the knockdown of VPS35 in HEK cells increased the cytosol entry of Tau aggregates (Tuck et al., 2022). Despite the different effects observed, this study also supports the involvement of VPS35 in the trafficking of extracellular Tau, while the contrasting results might be due to the differences in cell type and assay.

Notably, we observed a significant increase in the accumulation of Tau monomers upon VPS35 knockdown in LUHMES neurons. This implies that VPS35 may play a role in the exocytosis or clearance of Tau monomers, potentially contributing to their differential sorting compared to Tau aggregates. Further investigations are required to validate the role of VPS35 and the retromer complex in Tau pathology spreading and elucidate the underlying mechanisms involved.

Previous studies with transgenic mice with knock-in of VPS35 mutation D620N revealed an increase in phosphorylated Tau and neuronal loss (Chiu et al., 2020; Niu et al., 2021). Understanding the precise functions of VPS35 and the retromer complex in Tau metabolism and pathology could provide valuable insights into the development and progression of Tau-related neurodegenerative diseases. Further studies are necessary to decipher these mechanisms and explore potential therapeutic strategies targeting VPS35 and retromer-mediated pathways.

5.5 Is the uptake of Tau aggregates a selective process?

HSPGs serve as docking sites on cell surfaces that interact with various molecules and facilitate the delivery of various cargoes (Sarrazin et al., 2011). It has been observed that other protein aggregates, such as amyloid-beta and alpha-synuclein, also utilize HSPGs for cellular internalization (Stopschinski et al., 2018), suggesting a potential role of HSPGs in the unspecific internalization of amyloid

aggregates. However, our study using amyloid aggregates of bovine serum albumin (BSA) demonstrated that the uptake of Tau aggregates is not unspecific. Treatment of iPSCNs with thioflavin T (ThT)-positive amyloid BSA aggregates resulted in cell surface interactions, but no intracellular signals were observed. This indicates the specific involvement of HSPGs in the cellular internalization of Tau aggregates. The specificity of HSPG-mediated internalization may be attributed to the cooperation of HSPGs with specific cell surface receptors or the sulfation pattern of HSPGs (Mah et al., 2021). Recent studies have proposed that the sulfation pattern of HSPGs acts as a coding system that influences the interaction of HSPGs with aggregates of different structures (Ferreira et al., 2022; Rauch et al., 2018; Stopschinski et al., 2018; Zhao et al., 2020).

The sulfation code refers to the specific arrangement and modification of sulfate groups on the heparan sulfate chains of HSPGs. This sulfation pattern can vary among different cell types and tissues, leading to functional diversity in HSPG-mediated interactions. It has been suggested that the sulfation code of HSPGs may dictate the selectivity and specificity of HSPG-mediated interactions with various ligands, including protein aggregates. Protein aggregates ' different structural features and conformations may engage specific sulfate modifications on HSPGs, enabling selective binding and internalization. This sulfation-dependent recognition may contribute to the particular internalization of Tau aggregates mediated by HSPGs.

The emerging understanding of the sulfation code and its influence on HSPG-mediated interactions provides insights into the molecular mechanisms underlying the specific internalization of Tau aggregates. Further research is necessary to unravel the precise sulfation patterns and potential cooperative interactions with cell surface receptors that contribute to the selective internalization of Tau aggregates via HSPGs.

5.6 Are recombinant Tau aggregates reliable tools for studying cellular uptake?

In this study, we utilized heparin-induced recombinant Tau aggregates as a model system to investigate the molecular mechanisms of Tau uptake. These aggregates were chosen because they exhibit similar

structural features, such as β-sheet conformation, to pathological Tau aggregates found in the brains of patients (Goedert et al., 1996). Importantly, heparin-induced Tau aggregates have been shown to seed Tau pathology in transgenic mouse models, indicating their pathological relevance (Iba et al., 2015).

Despite core-structural differences (Zhang et al., 2019), and lower seeding efficiency of recombinant fibrils compared to patient-derived Tau fibrils (Guo et al., 2016), heparin-induced Tau aggregates have been demonstrated to share similar uptake mechanisms with brain-derived aggregates (Falcon et al., 2015). Studies have shown that the cellular uptake of both heparin-induced Tau aggregates and patient-derived Tau fibrils is mediated by receptors such as LRP1 and HSPGs in various cell models (Cooper et al., 2021; Puangmalai et al., 2020).

Here, we primarily confirmed the presence of disease-relevant conformational epitopes in heparin-induced Tau aggregates using conformational antibodies that recognize Tau pathology in the brain. This suggests that our aggregates possess structural similarities to patient-derived pathological Tau, at least in the fibril's surrounding epitopes. We also demonstrated the seeding capacity of our aggregates by inducing endogenous aggregation in HEK-biosensor cells. Moreover, due to the scarcity of patients-derived aggregates, we tested our result from heparin-induced aggregates using novel recombinant Tau fibrils that formed without any cofactor as an inducer and shared core-structural similarity with patients' derived Tau fibrils. The data from Cofactor-free Tau fibrils further confirmed our finding with heparin-induced aggregates, suggesting that recombinant Tau aggregates seem reliable for studying molecular mechanisms of Tau uptake and accumulation in human neurons. Further research would be necessary to decipher whether the neuronal uptake and accumulation of Tau fibrils are sensitive to the fibril's core structure or only associated with the amino acid sequence regardless of the conformational structures.

5.7 Are the transport of vesicle-free extracellular Tau species the only possible form of Tau spreading?

It is well-established that both normal monomeric Tau and abnormal aggregated Tau can be secreted into the extracellular environment through various physiological and pathological processes (Merezhko et al., 2020; Pernegre et al., 2019). The extracellular Tau (eTau) has been detected in different forms,

including association with synaptic vesicles (Pooler et al., 2013), exosomes (Asai et al., 2015; Saman et al., 2012; Wang et al., 2017), and ectosomes (Dujardin et al., 2014).

While the presence of Tau in different vesicular compartments has been observed, recent studies have highlighted the significance of vesicle-free Tau as the predominant extracellular form (Bright et al., 2015; Chai et al., 2012; Karch et al., 2012; Sato et al., 2018; Wegmann et al., 2016). One study, in particular, quantified approximately 90% of eTau as vesicle-free Tau, confirming previous findings that free Tau is the main form of Tau found in the extracellular space.

In this study, we primarily focused on the uptake of vesicle-free eTau. However, it is essential to note that additional investigations into the uptake and accumulation of eTau-containing vesicles would be necessary to obtain a comprehensive understanding of Tau spreading and its implications in neurodegenerative diseases. Further studies will contribute to the development of a complete picture of Tau propagation mechanisms and their potential therapeutic targets.

6. Conclusion

In this study, we aimed to generate and characterize different forms of recombinant Tau aggregated species and investigate their biological functions. Our results indicate that small fibrils and oligomers are potent species to play the role of Tau seed for pathology spreading due to high neuronal uptake ratio, escaping from the endosomal system, and seeding endogenous aggregation. Large fibrils showed lower efficiency for neuronal internalization, and monomers were unable to induce endogenous aggregation.

We also found that Tau aggregates were taken up and accumulated in human neurons more than monomeric Tau, which was mainly associated with a higher accumulation ratio of oligomers and small fibrils. Importantly, we observed minimal competition between Tau monomers and intermediate aggregates during neuronal uptake and intracellular accumulation, suggesting distinct processes of internalization and entrapment with minimal overlap. Our analysis revealed that this differential mechanism is likely mediated by specific molecular mediators rather than the different endocytic processes since both used clathrin-mediated endocytosis and macropinocytosis in iPSCNs. However, in LUHMES neurons, we found a distinction in endocytosis mechanisms since monomers used clathrin-mediated endocytosis and macropinocytosis while aggregates only used clathrin-mediated pathway for neuronal internalization. In general, the accumulation of Tau monomers was much lower in LUHMES neurons compared to iPSCNs, suggesting further separation between the uptake and accumulation mechanism of Tau monomers and aggregates in this cell line compared to iPSCNs. As iPSCNs and LUHMES neurons vary regarding neuronal type and maturity degree, further investigation is necessary to decipher the endocytic mechanisms of Tau species in various types of neurons.

At the molecular level, we found more consistent results among the neuronal types. As illustrated in **Figure 6.1**, the uptake of Tau monomers chiefly depends on the LRP1 and is independent of HSPGs. In contrast, the uptake of aggregates largely relies on HSPGs and is partially dependent or independent of LRP1. These findings provide insights into the possibility of specifically targeting pathological extracellular Tau without affecting the transport of physiological extracellular Tau, which could be a promising strategy for future therapeutic approaches.

Additionally, our data indicates that the vacuolar protein sorting 35 (VPS35), a component of the vesicle sorting machinery, differentially modulates the cellular accumulation of Tau monomers and aggregates. Knockdown of VPS35 reduced the accumulation of Tau aggregates in both iPSCNs and LUHMES neurons, while it was ineffective on the uptake of monomers in iPSCNs and even increased the monomers accumulation in LUHMES neurons. Our results also revealed the cell-type variation in Tau uptake, even between human neurons, highlighting the importance of cell-specific studies.

Importantly, our study represents the first report to differentiate the uptake of Tau monomers and aggregates at both cellular and molecular levels in human neurons. These findings offer valuable insights into the potential to target pathological Tau spreading while preserving the physiological transport of native monomeric Tau, thus providing a safe and promising approach for future therapeutic strategies.

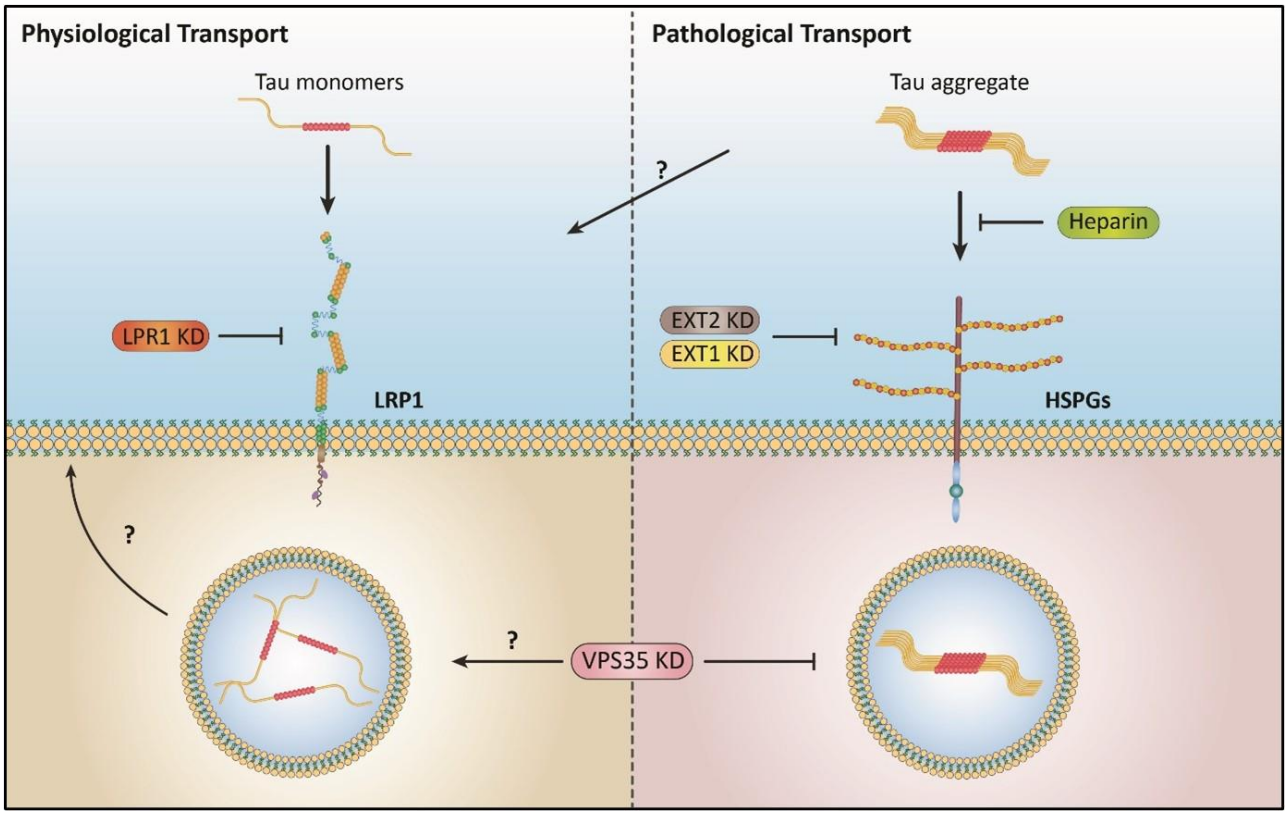

Figure 6.1 Model of differential uptake and accumulation of Tau monomers and aggregates in human neurons. In the model proposed, the uptake and accumulation of Tau monomers and aggregates in human neurons are governed by distinct mechanisms depending on the physiological or pathological conditions. Under physiological conditions,

Tau monomers enter neurons through low-density lipoprotein receptor-related protein 1 (LRP1)-mediated endocytosis since its knockdown inhibits Tau monomers internalization. However, the role of LRP1 in the uptake of Tau aggregates in mature human neurons needs further investigation. Under pathological conditions, neurons take up Tau aggregates through endocytosis mediated by heparan sulfate proteoglycans (HSPGs) since the treatment with heparin or knockdown of HSPGs synthesizing enzymes such as exostosin-1 (EXT1) and exostosin-2 (EXT2) inhibit the uptake of Tau aggregates. Beyond the internalization processes, the neuronal accumulation of Tau monomers and aggregates is separated at the intracellular sorting machinery, where we found vacuolar protein sorting 35 (VPS35), a critical component of the retromer complex, plays a significant role in the sorting of Tau within cells. Downregulation of VPS35 reduced the neuronal accumulation of Tau aggregates in both neuronal cells in our study while increasing the accumulation of Tau monomers in only one of the neuronal types in our study. Thus the impact of VPS35 on the neuronal accumulation of monomeric Tau requires further exploration. Our data also suggest that monomeric Tau might be released from the neuron after internalization, which might be associated with the VPS35 sorting function and needs further investigation.

List of Publications

Journals:

1. Rosler T.W.*, **Tayaranian Marvian A.***, Brendel M., Nykanen N.P., Hollerhage M., Schwarz S.C., Hopfner F., Köglsperger T., Respondek G., Schweyer K., Levin J., Villemagne V. L., Bartherl H., Sabri O., Müller U., Meissner W. G., Kovacs G. G., Höglinger G. (2019) Four-repeat Tauopathies. Prog Neurobiol.180:101644. (*co-first authors)

2. Strauss T, **Tayaranian Marvian A**, Sadikoglou E., Dhingra A., Wegner F., Trumbach D., Wurst W., Heutink P., Schwarz S., Höglinger G. (2021) iPS Cell-Based Model for MAPT Haplotype as a Risk Factor for Human Tauopathies Identifies No Major Differences in TAU Expression. Front Cell Dev Biol.;9:726866.

3. Parts of this thesis will be submitted for publication: **Tayaranian Marvian A.**, Strauss T., Tang Q., Tuck B., Keeling S., Rüdiger D., Mirzazadeh-Dizaji N., Mohammad-Beigi H., Nuscher B., Sutherland S.S., McEwan W., Köglsperger T., Zahler S., Zweckstetter M., Lichtenthaler S., Wurst W., Schwarz S., Höglinger G. (2023) The uptake and intracellular accumulation of Tau monomers and aggregates are differentially regulated in human neurons. [in preparation]

Conferences:

1. **Tayaranian Marvian A.**, Strauss T., Tang Q., Rüdiger D., Feng X., Nuscher B., Köglsperger T., McEwan W., Schwarz S., Zahler S., Lichtenthaler S., Wurst W., Höglinger G. (2022) Monomers and aggregates of Tau use different mediators for intracellular uptake and accumulation. ADPD 2022, Barcelona, Spain.

2. **Tayaranian Marvian A.**, Strauss T., Rudiger D., Mohammad-Beigi H., Nuscher B., McEwan W., Schwarz S., Zahler S., Wurst W., Höglinger G. (2021) The differential biological functions of various species of heparin-induced Tau aggregates. EuroTau 2021, Lille, France.

Declaration of Contributions

The purification of recombinant Tau using fast protein liquid chromatography and circular dichroism analysis was conducted through the valuable cooperation of Brigitte Nuscher at the German Center for Neurodegenerative Disease (DZNE), Munich, Germany.

Dr. Daniel Rodrigues performed AFM imaging of Tau aggregates under the supervision of Prof. Stefan Zahler at the Department of Pharmacy, Ludwig-Maximilians-University (LMU), Munich, Germany.

Dr. Hossein Mohammad-Beigi carried out TEM imaging under the supervision of Prof. Duncan Sutherland at the Interdisciplinary Nanoscience Centre (iNANO), Aarhus University, Aarhus, Denmark.

Negar Mirzazadeh-Dizaji performed DLS measurements at the Faculty for Chemistry and Pharmacy, Ludwig-Maximilians-University (LMU), Munich, Germany.

The production of cofactor-free Tau fibrils were carried out by Pijush Chakraborty under supervision of Prof. Markus Zweckstetter at the Department for NMR-based Structural Biology, Max Planck Institute for Multidisciplinary Sciences, Göttingen, Germany.

Dr. Xiao Feng performed the primary mouse cortical culture at the Department of Neuroproteomics, German Center for Neurodegenerative Disease (DZNE), Munich, Germany.

Dr. Will McEwan generously provided tau plasmid and HEK biosensor cells at the Department of Clinical Neurosciences, UK Dementia Research Institute at the University of Cambridge, Cambridge, United Kingdom. The cell entry assay was also conducted as a collaborative project with the McEwan lab, which performed by Benjamin Tuck and Sophie Keeling.

We would like to express our sincere appreciation to all individuals and organizations mentioned above for their valuable contributions, expertise, and support, which significantly enhanced the progress and outcomes of this study.

Funding

Amir Tayaranian Marvian was awarded a doctoral research grant for this project from the German Academic Exchange Service (DAAD) from 2017 - 2022.

The project was supported by German Federal Ministry of Education and Research (BMBF, 01EK1605A HitTau).

References

Ahmed, Z., Cooper, J., Murray, T. K., Garn, K., McNaughton, E., Clarke, H., Parhizkar, S., Ward, M. A., Cavallini, A., Jackson, S., Bose, S., Clavaguera, F., Tolnay, M., Lavenir, I., Goedert, M., Hutton, M. L., & O'Neill, M. J. (2014). A novel in vivo model of tau propagation with rapid and progressive neurofibrillary tangle pathology: the pattern of spread is determined by connectivity, not proximity. *Acta Neuropathol*, *127*(5), 667-683. https://doi.org/10.1007/s00401-014-1254-6

Alonso, A. C., Grundke-Iqbal, I., & Iqbal, K. (1996). Alzheimer's disease hyperphosphorylated tau sequesters normal tau into tangles of filaments and disassembles microtubules. *Nat Med*, *2*(7), 783-787. https://www.ncbi.nlm.nih.gov/pubmed/8673924

Andreadis, A., Brown, W. M., & Kosik, K. S. (1992). Structure and novel exons of the human tau gene. *Biochemistry*, *31*(43), 10626-10633. http://www.ncbi.nlm.nih.gov/pubmed/1420178

Aoki, T., Nomura, R., & Fujimoto, T. (1999). Tyrosine phosphorylation of caveolin-1 in the endothelium. *Exp Cell Res*, *253*(2), 629-636. https://doi.org/10.1006/excr.1999.4652

Arima, K., Nakamura, M., Sunohara, N., Nishio, T., Ogawa, M., Hirai, S., Kawai, M., & Ikeda, K. (1999). Immunohistochemical and ultrastructural characterization of neuritic clusters around ghost tangles in the hippocampal formation in progressive supranuclear palsy brains. *Acta Neuropathol*, *97*(6), 565-576. https://www.ncbi.nlm.nih.gov/pubmed/10378375

Asai, H., Ikezu, S., Tsunoda, S., Medalla, M., Luebke, J., Haydar, T., Wolozin, B., Butovsky, O., Kugler, S., & Ikezu, T. (2015). Depletion of microglia and inhibition of exosome synthesis halt tau propagation. *Nat Neurosci*, *18*(11), 1584-1593. https://doi.org/10.1038/nn.4132

Barten, D. M., Cadelina, G. W., Hoque, N., DeCarr, L. B., Guss, V. L., Yang, L., Sankaranarayanan, S., Wes, P. D., Flynn, M. E., Meredith, J. E., Ahlijanian, M. K., & Albright, C. F. (2011). Tau transgenic mice as models for cerebrospinal fluid tau biomarkers. *J Alzheimers Dis*, *24 Suppl 2*, 127-141. https://doi.org/10.3233/JAD-2011-110161

Barthelemy, N. R., Gabelle, A., Hirtz, C., Fenaille, F., Sergeant, N., Schraen-Maschke, S., Vialaret, J., Buee, L., Junot, C., Becher, F., & Lehmann, S. (2016). Differential Mass Spectrometry Profiles of Tau Protein in the Cerebrospinal Fluid of Patients with Alzheimer's Disease, Progressive Supranuclear Palsy, and Dementia with Lewy Bodies. *J Alzheimers Dis*, *51*(4), 1033-1043. https://doi.org/10.3233/JAD-150962

Berry, R. W., Abraha, A., Lagalwar, S., LaPointe, N., Gamblin, T. C., Cryns, V. L., & Binder, L. I. (2003). Inhibition of tau polymerization by its carboxy-terminal caspase cleavage fragment. *Biochemistry*, *42*(27), 8325-8331. https://doi.org/10.1021/bi027348m

Biernat, J., Wu, Y. Z., Timm, T., Zheng-Fischhofer, Q., Mandelkow, E., Meijer, L., & Mandelkow, E. M. (2002). Protein kinase MARK/PAR-1 is required for neurite outgrowth and establishment of neuronal polarity. *Mol Biol Cell*, *13*(11), 4013-4028. https://doi.org/10.1091/mbc.02-03-0046

Binder, L. I., Frankfurter, A., & Rebhun, L. I. (1985). The distribution of tau in the mammalian central nervous system. *J Cell Biol*, *101*(4), 1371-1378. http://www.ncbi.nlm.nih.gov/pubmed/3930508

Binder, L. I., Guillozet-Bongaarts, A. L., Garcia-Sierra, F., & Berry, R. W. (2005). Tau, tangles, and Alzheimer's disease. *Biochim Biophys Acta*, *1739*(2-3), 216-223. https://doi.org/10.1016/j.bbadis.2004.08.014

Braak, H., & Braak, E. (1991). Neuropathological stageing of Alzheimer-related changes. *Acta Neuropathol*, *82*(4), 239-259. https://doi.org/10.1007/BF00308809

Braak, H., Thal, D. R., Ghebremedhin, E., & Del Tredici, K. (2011). Stages of the pathologic process in Alzheimer disease: age categories from 1 to 100 years. *J Neuropathol Exp Neurol*, *70*(11), 960-969. https://doi.org/10.1097/NEN.0b013e318232a379

Brandt, R., Trushina, N. I., & Bakota, L. (2020). Much More Than a Cytoskeletal Protein: Physiological and Pathological Functions of the Non-microtubule Binding Region of Tau. *Front Neurol*, *11*, 590059. https://doi.org/10.3389/fneur.2020.590059

Bright, J., Hussain, S., Dang, V., Wright, S., Cooper, B., Byun, T., Ramos, C., Singh, A., Parry, G., Stagliano, N., & Griswold-Prenner, I. (2015). Human secreted tau increases amyloid-beta production. *Neurobiol Aging*, *36*(2), 693-709. https://doi.org/10.1016/j.neurobiolaging.2014.09.007

Bugiani, O., Murrell, J. R., Giaccone, G., Hasegawa, M., Ghigo, G., Tabaton, M., Morbin, M., Primavera, A., Carella, F., Solaro, C., Grisoli, M., Savoiardo, M., Spillantini, M. G., Tagliavini, F., Goedert, M., & Ghetti, B. (1999). Frontotemporal dementia and corticobasal degeneration in a family with a P301S mutation in tau. *J Neuropathol Exp Neurol*, *58*(6), 667-677. https://doi.org/10.1097/00005072-199906000-00011

Butner, K. A., & Kirschner, M. W. (1991). Tau protein binds to microtubules through a flexible array of distributed weak sites. *J Cell Biol*, *115*(3), 717-730. http://www.ncbi.nlm.nih.gov/pubmed/1918161

Caceres, A., & Kosik, K. S. (1990). Inhibition of neurite polarity by tau antisense oligonucleotides in primary cerebellar neurons. *Nature*, *343*(6257), 461-463. https://doi.org/10.1038/343461a0

Calafate, S., Flavin, W., Verstreken, P., & Moechars, D. (2016). Loss of Bin1 Promotes the Propagation of Tau Pathology. *Cell Rep*, *17*(4), 931-940. https://doi.org/10.1016/j.celrep.2016.09.063

Castillo-Carranza, D. L., Sengupta, U., Guerrero-Munoz, M. J., Lasagna-Reeves, C. A., Gerson, J. E., Singh, G., Estes, D. M., Barrett, A. D., Dineley, K. T., Jackson, G. R., & Kayed, R. (2014). Passive immunization with Tau oligomer monoclonal antibody reverses tauopathy phenotypes without affecting hyperphosphorylated neurofibrillary tangles. *J Neurosci*, *34*(12), 4260-4272. https://doi.org/10.1523/JNEUROSCI.3192-13.2014

Chai, X., Dage, J. L., & Citron, M. (2012). Constitutive secretion of tau protein by an unconventional mechanism. *Neurobiol Dis*, *48*(3), 356-366. https://doi.org/10.1016/j.nbd.2012.05.021

Chakraborty, P., Riviere, G., Liu, S., de Opakua, A. I., Dervisoglu, R., Hebestreit, A., Andreas, L. B., Vorberg, I. M., & Zweckstetter, M. (2021). Co-factor-free aggregation of tau into seeding-competent RNA-sequestering amyloid fibrils. *Nat Commun*, *12*(1), 4231. https://doi.org/10.1038/s41467-021-24362-8

Chen, J., Kanai, Y., Cowan, N. J., & Hirokawa, N. (1992). Projection domains of MAP2 and tau determine spacings between microtubules in dendrites and axons. *Nature*, *360*(6405), 674-677. https://doi.org/10.1038/360674a0

Chirita, C. N., Congdon, E. E., Yin, H., & Kuret, J. (2005). Triggers of full-length tau aggregation: a role for partially folded intermediates. *Biochemistry*, *44*(15), 5862-5872. https://doi.org/10.1021/bi0500123

Chirita, C. N., Necula, M., & Kuret, J. (2003). Anionic micelles and vesicles induce tau fibrillization in vitro. *J Biol Chem*, *278*(28), 25644-25650. https://doi.org/10.1074/jbc.M301663200

Chiu, C. C., Weng, Y. H., Huang, Y. Z., Chen, R. S., Liu, Y. C., Yeh, T. H., Lu, C. S., Lin, Y. W., Chen, Y. J., Hsu, C. C., Chiu, C. H., Wang, Y. T., Chen, W. S., Liu, S. Y., & Wang, H. L. (2020). (D620N) VPS35 causes the impairment of Wnt/beta-catenin signaling cascade and mitochondrial

dysfunction in a PARK17 knockin mouse model. *Cell Death Dis*, *11*(11), 1018. https://doi.org/10.1038/s41419-020-03228-9

Clavaguera, F., Bolmont, T., Crowther, R. A., Abramowski, D., Frank, S., Probst, A., Fraser, G., Stalder, A. K., Beibel, M., Staufenbiel, M., Jucker, M., Goedert, M., & Tolnay, M. (2009). Transmission and spreading of tauopathy in transgenic mouse brain. *Nat Cell Biol*, *11*(7), 909-913. https://doi.org/10.1038/ncb1901

Clavaguera, F., Duyckaerts, C., & Haik, S. (2020). Prion-like properties of Tau assemblies. *Curr Opin Neurobiol*, *61*, 49-57. https://doi.org/10.1016/j.conb.2019.11.022

Clavaguera, F., Hench, J., Goedert, M., & Tolnay, M. (2015). Invited review: Prion-like transmission and spreading of tau pathology. *Neuropathol Appl Neurobiol*, *41*(1), 47-58. https://doi.org/10.1111/nan.12197

Cleveland, D. W., Hwo, S. Y., & Kirschner, M. W. (1977). Physical and chemical properties of purified tau factor and the role of tau in microtubule assembly. *J Mol Biol*, *116*(2), 227-247. http://www.ncbi.nlm.nih.gov/pubmed/146092

Collaborators, G. B. D. D. (2019). Global, regional, and national burden of Alzheimer's disease and other dementias, 1990-2016: a systematic analysis for the Global Burden of Disease Study 2016. *Lancet Neurol*, *18*(1), 88-106. https://doi.org/10.1016/S1474-4422(18)30403-4

Collaborators, G. B. D. D. F. (2022). Estimation of the global prevalence of dementia in 2019 and forecasted prevalence in 2050: an analysis for the Global Burden of Disease Study 2019. *Lancet Public Health*, *7*(2), e105-e125. https://doi.org/10.1016/S2468-2667(21)00249-8

Cooper, J. M., Lathuiliere, A., Migliorini, M., Arai, A. L., Wani, M. M., Dujardin, S., Muratoglu, S. C., Hyman, B. T., & Strickland, D. K. (2021). Regulation of tau internalization, degradation, and seeding by LRP1 reveals multiple pathways for tau catabolism. *J Biol Chem*, *296*, 100715. https://doi.org/10.1016/j.jbc.2021.100715

de Boni, L., Gasparoni, G., Haubenreich, C., Tierling, S., Schmitt, I., Peitz, M., Koch, P., Walter, J., Wullner, U., & Brustle, O. (2018). DNA methylation alterations in iPSC- and hESC-derived neurons: potential implications for neurological disease modeling. *Clin Epigenetics*, *10*, 13. https://doi.org/10.1186/s13148-018-0440-0

De La-Rocque, S., Moretto, E., Butnaru, I., & Schiavo, G. (2021). Knockin' on heaven's door: Molecular mechanisms of neuronal tau uptake. *J Neurochem*, *156*(5), 563-588. https://doi.org/10.1111/jnc.15144

DeLeo, A. M., & Ikezu, T. (2018). Extracellular Vesicle Biology in Alzheimer's Disease and Related Tauopathy. *J Neuroimmune Pharmacol*, *13*(3), 292-308. https://doi.org/10.1007/s11481-017-9768-z

Despres, C., Byrne, C., Qi, H., Cantrelle, F. X., Huvent, I., Chambraud, B., Baulieu, E. E., Jacquot, Y., Landrieu, I., Lippens, G., & Smet-Nocca, C. (2017). Identification of the Tau phosphorylation pattern that drives its aggregation. *Proc Natl Acad Sci U S A*, *114*(34), 9080-9085. https://doi.org/10.1073/pnas.1708448114

Dhingra, A., Tager, J., Bressan, E., Rodriguez-Nieto, S., Bedi, M. S., Broer, S., Sadikoglou, E., Fernandes, N., Castillo-Lizardo, M., Rizzu, P., & Heutink, P. (2020). Automated Production of Human Induced Pluripotent Stem Cell-Derived Cortical and Dopaminergic Neurons with Integrated Live-Cell Monitoring. *J Vis Exp*(162). https://doi.org/10.3791/61525

Dixit, R., Ross, J. L., Goldman, Y. E., & Holzbaur, E. L. (2008). Differential regulation of dynein and kinesin motor proteins by tau. *Science*, *319*(5866), 1086-1089. https://doi.org/10.1126/science.1152993

Dixon, A. S., Schwinn, M. K., Hall, M. P., Zimmerman, K., Otto, P., Lubben, T. H., Butler, B. L., Binkowski, B. F., Machleidt, T., Kirkland, T. A., Wood, M. G., Eggers, C. T., Encell, L. P., & Wood, K. V. (2016). NanoLuc Complementation Reporter Optimized for Accurate Measurement of Protein Interactions in Cells. *ACS Chem Biol*, *11*(2), 400-408. https://doi.org/10.1021/acschembio.5b00753

Dujardin, S., Begard, S., Caillierez, R., Lachaud, C., Delattre, L., Carrier, S., Loyens, A., Galas, M. C., Bousset, L., Melki, R., Auregan, G., Hantraye, P., Brouillet, E., Buee, L., & Colin, M. (2014). Ectosomes: a new mechanism for non-exosomal secretion of tau protein. *PLoS One*, *9*(6), e100760. https://doi.org/10.1371/journal.pone.0100760

Dujardin, S., & Hyman, B. T. (2019). Tau Prion-Like Propagation: State of the Art and Current Challenges. *Adv Exp Med Biol*, *1184*, 305-325. https://doi.org/10.1007/978-981-32-9358-8_23

Engqvist-Goldstein, A. E., & Drubin, D. G. (2003). Actin assembly and endocytosis: from yeast to mammals. *Annu Rev Cell Dev Biol*, *19*, 287-332. https://doi.org/10.1146/annurev.cellbio.19.111401.093127

Evans, L. D., Strano, A., Campbell, A., Karakoç, E., Iorio, F., Bassett, A. R., & Livesey, F. J. (2020). Whole genome CRISPR screens identify LRRK2-regulated endocytosis as a major mechanism for extracellular tau uptake by human neurons. *bioRxiv*.

Evans, L. D., Wassmer, T., Fraser, G., Smith, J., Perkinton, M., Billinton, A., & Livesey, F. J. (2018). Extracellular Monomeric and Aggregated Tau Efficiently Enter Human Neurons through Overlapping but Distinct Pathways. *Cell Rep*, *22*(13), 3612-3624. https://doi.org/10.1016/j.celrep.2018.03.021

Fa, M., Puzzo, D., Piacentini, R., Staniszewski, A., Zhang, H., Baltrons, M. A., Li Puma, D. D., Chatterjee, I., Li, J., Saeed, F., Berman, H. L., Ripoli, C., Gulisano, W., Gonzalez, J., Tian, H., Costa, J. A., Lopez, P., Davidowitz, E., Yu, W. H., . . . Arancio, O. (2016). Extracellular Tau Oligomers Produce An Immediate Impairment of LTP and Memory. *Sci Rep*, *6*, 19393. https://doi.org/10.1038/srep19393

Falcon, B., Cavallini, A., Angers, R., Glover, S., Murray, T. K., Barnham, L., Jackson, S., O'Neill, M. J., Isaacs, A. M., Hutton, M. L., Szekeres, P. G., Goedert, M., & Bose, S. (2015). Conformation determines the seeding potencies of native and recombinant Tau aggregates. *J Biol Chem*, *290*(2), 1049-1065. https://doi.org/10.1074/jbc.M114.589309

Falcon, B., Noad, J., McMahon, H., Randow, F., & Goedert, M. (2018). Galectin-8-mediated selective autophagy protects against seeded tau aggregation. *J Biol Chem*, *293*(7), 2438-2451. https://doi.org/10.1074/jbc.M117.809293

Ferreira, A., Royaux, I., Liu, J., Wang, Z., Su, G., Moechars, D., Callewaert, N., & De Muynck, L. (2022). The 3-O sulfation of heparan sulfate proteoglycans contributes to the cellular internalization of tau aggregates. *BMC Mol Cell Biol*, *23*(1), 61. https://doi.org/10.1186/s12860-022-00462-1

Fitzpatrick, A. W. P., Falcon, B., He, S., Murzin, A. G., Murshudov, G., Garringer, H. J., Crowther, R. A., Ghetti, B., Goedert, M., & Scheres, S. H. W. (2017). Cryo-EM structures of tau filaments from Alzheimer's disease. *Nature*, *547*(7662), 185-190. https://doi.org/10.1038/nature23002

Florenzano, F., Veronica, C., Ciasca, G., Ciotti, M. T., Pittaluga, A., Olivero, G., Feligioni, M., Iannuzzi, F., Latina, V., Maria Sciacca, M. F., Sinopoli, A., Milardi, D., Pappalardo, G., Marco, S., Papi, M., Atlante, A., Bobba, A., Borreca, A., Calissano, P., & Amadoro, G. (2017). Extracellular truncated tau causes early presynaptic dysfunction associated with Alzheimer's disease and other tauopathies. *Oncotarget*, *8*(39), 64745-64778. https://doi.org/10.18632/oncotarget.17371

Fontaine, S. N., Zheng, D., Sabbagh, J. J., Martin, M. D., Chaput, D., Darling, A., Trotter, J. H., Stothert, A. R., Nordhues, B. A., Lussier, A., Baker, J., Shelton, L., Kahn, M., Blair, L. J., Stevens, S. M., Jr., & Dickey, C. A. (2016). DnaJ/Hsc70 chaperone complexes control the extracellular release of neurodegenerative-associated proteins. *EMBO J*, *35*(14), 1537-1549. https://doi.org/10.15252/embj.201593489

Frost, B., Jacks, R. L., & Diamond, M. I. (2009). Propagation of tau misfolding from the outside to the inside of a cell. *J Biol Chem*, *284*(19), 12845-12852. https://doi.org/10.1074/jbc.M808759200

Ganguly, P., Do, T. D., Larini, L., LaPointe, N. E., Sercel, A. J., Shade, M. F., Feinstein, S. C., Bowers, M. T., & Shea, J. E. (2015). Tau assembly: the dominant role of PHF6 (VQIVYK) in microtubule binding region repeat R3. *J Phys Chem B*, *119*(13), 4582-4593. https://doi.org/10.1021/acs.jpcb.5b00175

Gerson, J. E., Sengupta, U., Lasagna-Reeves, C. A., Guerrero-Munoz, M. J., Troncoso, J., & Kayed, R. (2014). Characterization of tau oligomeric seeds in progressive supranuclear palsy. *Acta Neuropathol Commun*, *2*, 73. https://doi.org/10.1186/2051-5960-2-73

Goedert, M. (2015). NEURODEGENERATION. Alzheimer's and Parkinson's diseases: The prion concept in relation to assembled Abeta, tau, and alpha-synuclein. *Science*, *349*(6248), 1255555. https://doi.org/10.1126/science.1255555

Goedert, M., & Jakes, R. (1990). Expression of separate isoforms of human tau protein: correlation with the tau pattern in brain and effects on tubulin polymerization. *EMBO J*, *9*(13), 4225-4230. https://www.ncbi.nlm.nih.gov/pubmed/2124967

Goedert, M., Jakes, R., Spillantini, M. G., Hasegawa, M., Smith, M. J., & Crowther, R. A. (1996). Assembly of microtubule-associated protein tau into Alzheimer-like filaments induced by sulphated glycosaminoglycans. *Nature*, *383*(6600), 550-553. https://doi.org/10.1038/383550a0

Goedert, M., & Spillantini, M. G. (2017). Propagation of Tau aggregates. *Mol Brain*, *10*(1), 18. https://doi.org/10.1186/s13041-017-0298-7

Goedert, M., Spillantini, M. G., Potier, M. C., Ulrich, J., & Crowther, R. A. (1989). Cloning and sequencing of the cDNA encoding an isoform of microtubule-associated protein tau containing four tandem repeats: differential expression of tau protein mRNAs in human brain. *EMBO J*, *8*(2), 393-399. http://www.ncbi.nlm.nih.gov/pubmed/2498079

Gomez-Ramos, A., Diaz-Hernandez, M., Cuadros, R., Hernandez, F., & Avila, J. (2006). Extracellular tau is toxic to neuronal cells. *FEBS Lett*, *580*(20), 4842-4850. https://doi.org/10.1016/j.febslet.2006.07.078

Gomez-Ramos, A., Diaz-Hernandez, M., Rubio, A., Diaz-Hernandez, J. I., Miras-Portugal, M. T., & Avila, J. (2009). Characteristics and consequences of muscarinic receptor activation by tau protein. *Eur Neuropsychopharmacol*, *19*(10), 708-717. https://doi.org/10.1016/j.euroneuro.2009.04.006

Gomez-Ramos, A., Diaz-Hernandez, M., Rubio, A., Miras-Portugal, M. T., & Avila, J. (2008). Extracellular tau promotes intracellular calcium increase through M1 and M3 muscarinic receptors in neuronal cells. *Mol Cell Neurosci*, *37*(4), 673-681. https://doi.org/10.1016/j.mcn.2007.12.010

Guix, F. X., Corbett, G. T., Cha, D. J., Mustapic, M., Liu, W., Mengel, D., Chen, Z., Aikawa, E., Young-Pearse, T., Kapogiannis, D., Selkoe, D. J., & Walsh, D. M. (2018). Detection of Aggregation-Competent Tau in Neuron-Derived Extracellular Vesicles. *Int J Mol Sci*, *19*(3). https://doi.org/10.3390/ijms19030663

Guo, J. L., & Lee, V. M. (2011). Seeding of normal Tau by pathological Tau conformers drives pathogenesis of Alzheimer-like tangles. *J Biol Chem*, *286*(17), 15317-15331. https://doi.org/10.1074/jbc.M110.209296

Guo, J. L., Narasimhan, S., Changolkar, L., He, Z., Stieber, A., Zhang, B., Gathagan, R. J., Iba, M., McBride, J. D., Trojanowski, J. Q., & Lee, V. M. (2016). Unique pathological tau conformers from Alzheimer's brains transmit tau pathology in nontransgenic mice. *J Exp Med*, *213*(12), 2635-2654. https://doi.org/10.1084/jem.20160833

Hanger, D. P., Anderton, B. H., & Noble, W. (2009). Tau phosphorylation: the therapeutic challenge for neurodegenerative disease. *Trends Mol Med*, *15*(3), 112-119. https://doi.org/10.1016/j.molmed.2009.01.003

Holmes, B. B., DeVos, S. L., Kfoury, N., Li, M., Jacks, R., Yanamandra, K., Ouidja, M. O., Brodsky, F. M., Marasa, J., Bagchi, D. P., Kotzbauer, P. T., Miller, T. M., Papy-Garcia, D., & Diamond, M. I. (2013). Heparan sulfate proteoglycans mediate internalization and propagation of specific proteopathic seeds. *Proc Natl Acad Sci U S A*, *110*(33), E3138-3147. https://doi.org/10.1073/pnas.1301440110

Holmes, B. B., & Diamond, M. I. (2014). Prion-like properties of Tau protein: the importance of extracellular Tau as a therapeutic target. *J Biol Chem*, *289*(29), 19855-19861. https://doi.org/10.1074/jbc.R114.549295

Horowitz, P. M., LaPointe, N., Guillozet-Bongaarts, A. L., Berry, R. W., & Binder, L. I. (2006). N-terminal fragments of tau inhibit full-length tau polymerization in vitro. *Biochemistry*, *45*(42), 12859-12866. https://doi.org/10.1021/bi061325g

Hu, N. W., Corbett, G. T., Moore, S., Klyubin, I., O'Malley, T. T., Walsh, D. M., Livesey, F. J., & Rowan, M. J. (2018). Extracellular Forms of Abeta and Tau from iPSC Models of Alzheimer's Disease Disrupt Synaptic Plasticity. *Cell Rep*, *23*(7), 1932-1938. https://doi.org/10.1016/j.celrep.2018.04.040

Hu, Y. B., Dammer, E. B., Ren, R. J., & Wang, G. (2015). The endosomal-lysosomal system: from acidification and cargo sorting to neurodegeneration. *Transl Neurodegener*, *4*, 18. https://doi.org/10.1186/s40035-015-0041-1

Hudak, A., Kusz, E., Domonkos, I., Josvay, K., Kodamullil, A. T., Szilak, L., Hofmann-Apitius, M., & Letoha, T. (2019). Contribution of syndecans to cellular uptake and fibrillation of alpha-synuclein and tau. *Sci Rep*, *9*(1), 16543. https://doi.org/10.1038/s41598-019-53038-z

Iba, M., McBride, J. D., Guo, J. L., Zhang, B., Trojanowski, J. Q., & Lee, V. M. (2015). Tau pathology spread in PS19 tau transgenic mice following locus coeruleus (LC) injections of synthetic tau fibrils is determined by the LC's afferent and efferent connections. *Acta Neuropathol*, *130*(3), 349-362. https://doi.org/10.1007/s00401-015-1458-4

Iqbal, K., Liu, F., & Gong, C. X. (2016). Tau and neurodegenerative disease: the story so far. *Nat Rev Neurol*, *12*(1), 15-27. https://doi.org/10.1038/nrneurol.2015.225

Jackson, N. A., Guerrero-Munoz, M. J., & Castillo-Carranza, D. L. (2022). The prion-like transmission of tau oligomers via exosomes. *Front Aging Neurosci*, *14*, 974414. https://doi.org/10.3389/fnagi.2022.974414

Jackson, S. J., Kerridge, C., Cooper, J., Cavallini, A., Falcon, B., Cella, C. V., Landi, A., Szekeres, P. G., Murray, T. K., Ahmed, Z., Goedert, M., Hutton, M., O'Neill, M. J., & Bose, S. (2016). Short Fibrils Constitute the Major Species of Seed-Competent Tau in the Brains of Mice Transgenic for Human P301S Tau. *J Neurosci*, *36*(3), 762-772. https://doi.org/10.1523/JNEUROSCI.3542-15.2016

Jicha, G. A., Bowser, R., Kazam, I. G., & Davies, P. (1997). Alz-50 and MC-1, a new monoclonal antibody raised to paired helical filaments, recognize conformational epitopes on recombinant tau. *J Neurosci Res*, *48*(2), 128-132. https://doi.org/10.1002/(sici)1097-4547(19970415)48:2<128::aid-jnr5>3.0.co;2-e

Josephs, K. A. (2017). Current Understanding of Neurodegenerative Diseases Associated With the Protein Tau. *Mayo Clin Proc*, *92*(8), 1291-1303. https://doi.org/10.1016/j.mayocp.2017.04.016

Kampers, T., Friedhoff, P., Biernat, J., Mandelkow, E. M., & Mandelkow, E. (1996). RNA stimulates aggregation of microtubule-associated protein tau into Alzheimer-like paired helical filaments. *FEBS Lett*, *399*(3), 344-349. https://www.ncbi.nlm.nih.gov/pubmed/8985176

Kanaan, N. M., Morfini, G. A., LaPointe, N. E., Pigino, G. F., Patterson, K. R., Song, Y., Andreadis, A., Fu, Y., Brady, S. T., & Binder, L. I. (2011). Pathogenic forms of tau inhibit kinesin-dependent axonal transport through a mechanism involving activation of axonal phosphotransferases. *J Neurosci*, *31*(27), 9858-9868. https://doi.org/10.1523/JNEUROSCI.0560-11.2011

Kaniyappan, S., Chandupatla, R. R., Mandelkow, E. M., & Mandelkow, E. (2017). Extracellular low-n oligomers of tau cause selective synaptotoxicity without affecting cell viability. *Alzheimers Dement*, *13*(11), 1270-1291. https://doi.org/10.1016/j.jalz.2017.04.002

Kanmert, D., Cantlon, A., Muratore, C. R., Jin, M., O'Malley, T. T., Lee, G., Young-Pearse, T. L., Selkoe, D. J., & Walsh, D. M. (2015). C-Terminally Truncated Forms of Tau, But Not Full-Length Tau or Its C-Terminal Fragments, Are Released from Neurons Independently of Cell Death. *J Neurosci*, *35*(30), 10851-10865. https://doi.org/10.1523/JNEUROSCI.0387-15.2015

Karch, C. M., Jeng, A. T., & Goate, A. M. (2012). Extracellular Tau levels are influenced by variability in Tau that is associated with tauopathies. *J Biol Chem*, *287*(51), 42751-42762. https://doi.org/10.1074/jbc.M112.380642

Karpowicz, R. J., Jr., Haney, C. M., Mihaila, T. S., Sandler, R. M., Petersson, E. J., & Lee, V. M. (2017). Selective imaging of internalized proteopathic alpha-synuclein seeds in primary neurons reveals mechanistic insight into transmission of synucleinopathies. *J Biol Chem*, *292*(32), 13482-13497. https://doi.org/10.1074/jbc.M117.780296

Katsinelos, T., Zeitler, M., Dimou, E., Karakatsani, A., Muller, H. M., Nachman, E., Steringer, J. P., Ruiz de Almodovar, C., Nickel, W., & Jahn, T. R. (2018). Unconventional Secretion Mediates the Trans-cellular Spreading of Tau. *Cell Rep*, *23*(7), 2039-2055. https://doi.org/10.1016/j.celrep.2018.04.056

Koivusalo, M., Welch, C., Hayashi, H., Scott, C. C., Kim, M., Alexander, T., Touret, N., Hahn, K. M., & Grinstein, S. (2010). Amiloride inhibits macropinocytosis by lowering submembranous pH and preventing Rac1 and Cdc42 signaling. *J Cell Biol*, *188*(4), 547-563. https://doi.org/10.1083/jcb.200908086

Kolarova, M., Garcia-Sierra, F., Bartos, A., Ricny, J., & Ripova, D. (2012). Structure and pathology of tau protein in Alzheimer disease. *Int J Alzheimers Dis*, *2012*, 731526. https://doi.org/10.1155/2012/731526

Kovacs, G. G., Lukic, M. J., Irwin, D. J., Arzberger, T., Respondek, G., Lee, E. B., Coughlin, D., Giese, A., Grossman, M., Kurz, C., McMillan, C. T., Gelpi, E., Compta, Y., van Swieten, J. C., Laat, L. D., Troakes, C., Al-Sarraj, S., Robinson, J. L., Roeber, S., . . . Hoglinger, G. U. (2020). Distribution patterns of tau pathology in progressive supranuclear palsy. *Acta Neuropathol*, *140*(2), 99-119. https://doi.org/10.1007/s00401-020-02158-2

Kumar, S. T., Donzelli, S., Chiki, A., Syed, M. M. K., & Lashuel, H. A. (2020). A simple, versatile and robust centrifugation-based filtration protocol for the isolation and quantification of alpha-

synuclein monomers, oligomers and fibrils: Towards improving experimental reproducibility in alpha-synuclein research. *J Neurochem*, *153*(1), 103-119. https://doi.org/10.1111/jnc.14955

Kundel, F., Hong, L., Falcon, B., McEwan, W. A., Michaels, T. C. T., Meisl, G., Esteras, N., Abramov, A. Y., Knowles, T. J. P., Goedert, M., & Klenerman, D. (2018). Measurement of Tau Filament Fragmentation Provides Insights into Prion-like Spreading. *ACS Chem Neurosci*, *9*(6), 1276-1282. https://doi.org/10.1021/acschemneuro.8b00094

Kuret, J., Chirita, C. N., Congdon, E. E., Kannanayakal, T., Li, G., Necula, M., Yin, H., & Zhong, Q. (2005). Pathways of tau fibrillization. *Biochim Biophys Acta*, *1739*(2-3), 167-178. https://doi.org/10.1016/j.bbadis.2004.06.016

Lambert, J. C., Ibrahim-Verbaas, C. A., Harold, D., Naj, A. C., Sims, R., Bellenguez, C., DeStafano, A. L., Bis, J. C., Beecham, G. W., Grenier-Boley, B., Russo, G., Thorton-Wells, T. A., Jones, N., Smith, A. V., Chouraki, V., Thomas, C., Ikram, M. A., Zelenika, D., Vardarajan, B. N., . . . Amouyel, P. (2013). Meta-analysis of 74,046 individuals identifies 11 new susceptibility loci for Alzheimer's disease. *Nat Genet*, *45*(12), 1452-1458. https://doi.org/10.1038/ng.2802

Lasagna-Reeves, C. A., Castillo-Carranza, D. L., Sengupta, U., Clos, A. L., Jackson, G. R., & Kayed, R. (2011). Tau oligomers impair memory and induce synaptic and mitochondrial dysfunction in wild-type mice. *Mol Neurodegener*, *6*, 39. https://doi.org/10.1186/1750-1326-6-39

Lasagna-Reeves, C. A., Castillo-Carranza, D. L., Sengupta, U., Guerrero-Munoz, M. J., Kiritoshi, T., Neugebauer, V., Jackson, G. R., & Kayed, R. (2012). Alzheimer brain-derived tau oligomers propagate pathology from endogenous tau. *Sci Rep*, *2*, 700. https://doi.org/10.1038/srep00700

Lasagna-Reeves, C. A., Castillo-Carranza, D. L., Sengupta, U., Sarmiento, J., Troncoso, J., Jackson, G. R., & Kayed, R. (2012). Identification of oligomers at early stages of tau aggregation in Alzheimer's disease. *FASEB J*, *26*(5), 1946-1959. https://doi.org/10.1096/fj.11-199851

Lauter, G., Coschiera, A., Yoshihara, M., Sugiaman-Trapman, D., Ezer, S., Sethurathinam, S., Katayama, S., Kere, J., & Swoboda, P. (2020). Differentiation of ciliated human midbrain-derived LUHMES neurons. *J Cell Sci*, *133*(21). https://doi.org/10.1242/jcs.249789

Lee, C. C., Nayak, A., Sethuraman, A., Belfort, G., & McRae, G. J. (2007). A three-stage kinetic model of amyloid fibrillation. *Biophys J*, *92*(10), 3448-3458. https://doi.org/10.1529/biophysj.106.098608

Lee, D. H., & Goldberg, A. L. (1996). Selective inhibitors of the proteasome-dependent and vacuolar pathways of protein degradation in Saccharomyces cerevisiae. *J Biol Chem*, *271*(44), 27280-27284. https://doi.org/10.1074/jbc.271.44.27280

Leonard, C., Phillips, C., & McCarty, J. (2021). Insight Into Seeded Tau Fibril Growth From Molecular Dynamics Simulation of the Alzheimer's Disease Protofibril Core. *Front Mol Biosci*, *8*, 624302. https://doi.org/10.3389/fmolb.2021.624302

Li, W., & Lee, V. M. (2006). Characterization of two VQIXXK motifs for tau fibrillization in vitro. *Biochemistry*, *45*(51), 15692-15701. https://doi.org/10.1021/bi061422+

Li, X., Feng, X., Sun, X., Hou, N., Han, F., & Liu, Y. (2022). Global, regional, and national burden of Alzheimer's disease and other dementias, 1990-2019. *Front Aging Neurosci*, *14*, 937486. https://doi.org/10.3389/fnagi.2022.937486

Limorenko, G., & Lashuel, H. A. (2022). Revisiting the grammar of Tau aggregation and pathology formation: how new insights from brain pathology are shaping how we study and target Tauopathies. *Chem Soc Rev*, *51*(2), 513-565. https://doi.org/10.1039/d1cs00127b

LoPresti, P., Szuchet, S., Papasozomenos, S. C., Zinkowski, R. P., & Binder, L. I. (1995). Functional implications for the microtubule-associated protein tau: localization in oligodendrocytes. *Proc Natl Acad Sci U S A*, *92*(22), 10369-10373. http://www.ncbi.nlm.nih.gov/pubmed/7479786

Loser, D., Schaefer, J., Danker, T., Moller, C., Brull, M., Suciu, I., Uckert, A. K., Klima, S., Leist, M., & Kraushaar, U. (2021). Human neuronal signaling and communication assays to assess functional neurotoxicity. *Arch Toxicol*, *95*(1), 229-252. https://doi.org/10.1007/s00204-020-02956-3

Lotharius, J., Barg, S., Wiekop, P., Lundberg, C., Raymon, H. K., & Brundin, P. (2002). Effect of mutant alpha-synuclein on dopamine homeostasis in a new human mesencephalic cell line. *J Biol Chem*, *277*(41), 38884-38894. https://doi.org/10.1074/jbc.M205518200

Lotharius, J., Falsig, J., van Beek, J., Payne, S., Dringen, R., Brundin, P., & Leist, M. (2005). Progressive degeneration of human mesencephalic neuron-derived cells triggered by dopamine-dependent oxidative stress is dependent on the mixed-lineage kinase pathway. *J Neurosci*, *25*(27), 6329-6342. https://doi.org/10.1523/JNEUROSCI.1746-05.2005

Lu, P. J., Wulf, G., Zhou, X. Z., Davies, P., & Lu, K. P. (1999). The prolyl isomerase Pin1 restores the function of Alzheimer-associated phosphorylated tau protein. *Nature*, *399*(6738), 784-788. https://doi.org/10.1038/21650

Maeda, S., Sahara, N., Saito, Y., Murayama, M., Yoshiike, Y., Kim, H., Miyasaka, T., Murayama, S., Ikai, A., & Takashima, A. (2007). Granular tau oligomers as intermediates of tau filaments. *Biochemistry*, *46*(12), 3856-3861. https://doi.org/10.1021/bi061359o

Magnoni, S., Esparza, T. J., Conte, V., Carbonara, M., Carrabba, G., Holtzman, D. M., Zipfel, G. J., Stocchetti, N., & Brody, D. L. (2012). Tau elevations in the brain extracellular space correlate with reduced amyloid-beta levels and predict adverse clinical outcomes after severe traumatic brain injury. *Brain*, *135*(Pt 4), 1268-1280. https://doi.org/10.1093/brain/awr286

Mah, D., Zhao, J., Liu, X., Zhang, F., Liu, J., Wang, L., Linhardt, R., & Wang, C. (2021). The Sulfation Code of Tauopathies: Heparan Sulfate Proteoglycans in the Prion Like Spread of Tau Pathology. *Front Mol Biosci*, *8*, 671458. https://doi.org/10.3389/fmolb.2021.671458

Mandelkow, E., von Bergen, M., Biernat, J., & Mandelkow, E. M. (2007). Structural principles of tau and the paired helical filaments of Alzheimer's disease. *Brain Pathol*, *17*(1), 83-90. https://doi.org/10.1111/j.1750-3639.2007.00053.x

Mandelkow, E. M., & Mandelkow, E. (2012). Biochemistry and cell biology of tau protein in neurofibrillary degeneration. *Cold Spring Harb Perspect Med*, *2*(7), a006247. https://doi.org/10.1101/cshperspect.a006247

Margittai, M., & Langen, R. (2004). Template-assisted filament growth by parallel stacking of tau. *Proc Natl Acad Sci U S A*, *101*(28), 10278-10283. https://doi.org/10.1073/pnas.0401911101

Mauthe, M., Orhon, I., Rocchi, C., Zhou, X., Luhr, M., Hijlkema, K. J., Coppes, R. P., Engedal, N., Mari, M., & Reggiori, F. (2018). Chloroquine inhibits autophagic flux by decreasing autophagosome-lysosome fusion. *Autophagy*, *14*(8), 1435-1455. https://doi.org/10.1080/15548627.2018.1474314

McCluskey, A., Daniel, J. A., Hadzic, G., Chau, N., Clayton, E. L., Mariana, A., Whiting, A., Gorgani, N. N., Lloyd, J., Quan, A., Moshkanbaryans, L., Krishnan, S., Perera, S., Chircop, M., von Kleist, L., McGeachie, A. B., Howes, M. T., Parton, R. G., Campbell, M., . . . Robinson, P. J. (2013). Building a better dynasore: the dyngo compounds potently inhibit dynamin and endocytosis. *Traffic*, *14*(12), 1272-1289. https://doi.org/10.1111/tra.12119

McEwan, W. A., Falcon, B., Vaysburd, M., Clift, D., Oblak, A. L., Ghetti, B., Goedert, M., & James, L. C. (2017). Cytosolic Fc receptor TRIM21 inhibits seeded tau aggregation. *Proc Natl Acad Sci U S A*, *114*(3), 574-579. https://doi.org/10.1073/pnas.1607215114

Merezhko, M., Brunello, C. A., Yan, X., Vihinen, H., Jokitalo, E., Uronen, R. L., & Huttunen, H. J. (2018). Secretion of Tau via an Unconventional Non-vesicular Mechanism. *Cell Rep*, *25*(8), 2027-2035 e2024. https://doi.org/10.1016/j.celrep.2018.10.078

Merezhko, M., Uronen, R. L., & Huttunen, H. J. (2020). The Cell Biology of Tau Secretion. *Front Mol Neurosci*, *13*, 569818. https://doi.org/10.3389/fnmol.2020.569818

Michel, C. H., Kumar, S., Pinotsi, D., Tunnacliffe, A., St George-Hyslop, P., Mandelkow, E., Mandelkow, E. M., Kaminski, C. F., & Kaminski Schierle, G. S. (2014). Extracellular monomeric tau protein is sufficient to initiate the spread of tau protein pathology. *J Biol Chem*, *289*(2), 956-967. https://doi.org/10.1074/jbc.M113.515445

Mirbaha, H., Chen, D., Morazova, O. A., Ruff, K. M., Sharma, A. M., Liu, X., Goodarzi, M., Pappu, R. V., Colby, D. W., Mirzaei, H., Joachimiak, L. A., & Diamond, M. I. (2018). Inert and seed-competent tau monomers suggest structural origins of aggregation. *Elife*, *7*. https://doi.org/10.7554/eLife.36584

Mirbaha, H., Holmes, B. B., Sanders, D. W., Bieschke, J., & Diamond, M. I. (2015). Tau Trimers Are the Minimal Propagation Unit Spontaneously Internalized to Seed Intracellular Aggregation. *J Biol Chem*, *290*(24), 14893-14903. https://doi.org/10.1074/jbc.M115.652693

Mohammad-Beigi, H., Hayashi, Y., Zeuthen, C. M., Eskandari, H., Scavenius, C., Juul-Madsen, K., Vorup-Jensen, T., Enghild, J. J., & Sutherland, D. S. (2020). Mapping and identification of soft corona proteins at nanoparticles and their impact on cellular association. *Nat Commun*, *11*(1), 4535. https://doi.org/10.1038/s41467-020-18237-7

Moloney, C. M., Lowe, V. J., & Murray, M. E. (2021). Visualization of neurofibrillary tangle maturity in Alzheimer's disease: A clinicopathologic perspective for biomarker research. *Alzheimers Dement*, *17*(9), 1554-1574. https://doi.org/10.1002/alz.12321

Morozova, V., Cohen, L. S., Makki, A. E., Shur, A., Pilar, G., El Idrissi, A., & Alonso, A. D. (2019). Normal and Pathological Tau Uptake Mediated by M1/M3 Muscarinic Receptors Promotes Opposite Neuronal Changes. *Front Cell Neurosci*, *13*, 403. https://doi.org/10.3389/fncel.2019.00403

Morris, A. M., Watzky, M. A., Agar, J. N., & Finke, R. G. (2008). Fitting neurological protein aggregation kinetic data via a 2-step, minimal/"Ockham's razor" model: the Finke-Watzky mechanism of nucleation followed by autocatalytic surface growth. *Biochemistry*, *47*(8), 2413-2427. https://doi.org/10.1021/bi701899y

Mortensen, K., & Larsson, L. I. (2003). Effects of cytochalasin D on the actin cytoskeleton: association of neoformed actin aggregates with proteins involved in signaling and endocytosis. *Cell Mol Life Sci*, *60*(5), 1007-1012. https://doi.org/10.1007/s00018-003-3022-x

Mudher, A., Colin, M., Dujardin, S., Medina, M., Dewachter, I., Alavi Naini, S. M., Mandelkow, E. M., Mandelkow, E., Buee, L., Goedert, M., & Brion, J. P. (2017). What is the evidence that tau pathology spreads through prion-like propagation? *Acta Neuropathol Commun*, *5*(1), 99. https://doi.org/10.1186/s40478-017-0488-7

Mukrasch, M. D., Bibow, S., Korukottu, J., Jeganathan, S., Biernat, J., Griesinger, C., Mandelkow, E., & Zweckstetter, M. (2009). Structural polymorphism of 441-residue tau at single residue resolution. *PLoS Biol*, *7*(2), e34. https://doi.org/10.1371/journal.pbio.1000034

Narasimhan, S., Guo, J. L., Changolkar, L., Stieber, A., McBride, J. D., Silva, L. V., He, Z., Zhang, B., Gathagan, R. J., Trojanowski, J. Q., & Lee, V. M. Y. (2017). Pathological Tau Strains from Human Brains Recapitulate the Diversity of Tauopathies in Nontransgenic Mouse Brain. *J Neurosci*, *37*(47), 11406-11423. https://doi.org/10.1523/JNEUROSCI.1230-17.2017

Nicholas, C. R., Chen, J., Tang, Y., Southwell, D. G., Chalmers, N., Vogt, D., Arnold, C. M., Chen, Y. J., Stanley, E. G., Elefanty, A. G., Sasai, Y., Alvarez-Buylla, A., Rubenstein, J. L., & Kriegstein, A. R. (2013). Functional maturation of hPSC-derived forebrain interneurons requires an extended timeline and mimics human neural development. *Cell Stem Cell*, *12*(5), 573-586. https://doi.org/10.1016/j.stem.2013.04.005

Niu, M., Zhao, F., Bondelid, K., Siedlak, S. L., Torres, S., Fujioka, H., Wang, W., Liu, J., & Zhu, X. (2021). VPS35 D620N knockin mice recapitulate cardinal features of Parkinson's disease. *Aging Cell*, *20*(5), e13347. https://doi.org/10.1111/acel.13347

Nizynski, B., Dzwolak, W., & Nieznanski, K. (2017). Amyloidogenesis of Tau protein. *Protein Sci*, *26*(11), 2126-2150. https://doi.org/10.1002/pro.3275

Noguchi, M., Yoshita, M., Matsumoto, Y., Ono, K., Iwasa, K., & Yamada, M. (2005). Decreased beta-amyloid peptide42 in cerebrospinal fluid of patients with progressive supranuclear palsy and corticobasal degeneration. *J Neurol Sci*, *237*(1-2), 61-65. https://doi.org/10.1016/j.jns.2005.05.015

Pampuscenko, K., Morkuniene, R., Krasauskas, L., Smirnovas, V., Tomita, T., & Borutaite, V. (2021). Distinct Neurotoxic Effects of Extracellular Tau Species in Primary Neuronal-Glial Cultures. *Mol Neurobiol*, *58*(2), 658-667. https://doi.org/10.1007/s12035-020-02150-7

Patterson, K. R., Remmers, C., Fu, Y., Brooker, S., Kanaan, N. M., Vana, L., Ward, S., Reyes, J. F., Philibert, K., Glucksman, M. J., & Binder, L. I. (2011). Characterization of prefibrillar Tau oligomers in vitro and in Alzheimer disease. *J Biol Chem*, *286*(26), 23063-23076. https://doi.org/10.1074/jbc.M111.237974

Pernegre, C., Duquette, A., & Leclerc, N. (2019). Tau Secretion: Good and Bad for Neurons. *Front Neurosci*, *13*, 649. https://doi.org/10.3389/fnins.2019.00649

Plouffe, V., Mohamed, N. V., Rivest-McGraw, J., Bertrand, J., Lauzon, M., & Leclerc, N. (2012). Hyperphosphorylation and cleavage at D421 enhance tau secretion. *PLoS One*, *7*(5), e36873. https://doi.org/10.1371/journal.pone.0036873

Polanco, J. C., Scicluna, B. J., Hill, A. F., & Gotz, J. (2016). Extracellular Vesicles Isolated from the Brains of rTg4510 Mice Seed Tau Protein Aggregation in a Threshold-dependent Manner. *J Biol Chem*, *291*(24), 12445-12466. https://doi.org/10.1074/jbc.M115.709485

Pooler, A. M., Phillips, E. C., Lau, D. H., Noble, W., & Hanger, D. P. (2013). Physiological release of endogenous tau is stimulated by neuronal activity. *EMBO Rep*, *14*(4), 389-394. https://doi.org/10.1038/embor.2013.15

Prichard, K. L., O'Brien, N. S., Murcia, S. R., Baker, J. R., & McCluskey, A. (2021). Role of Clathrin and Dynamin in Clathrin Mediated Endocytosis/Synaptic Vesicle Recycling and Implications in Neurological Diseases. *Front Cell Neurosci*, *15*, 754110. https://doi.org/10.3389/fncel.2021.754110

Przedborski, S., Vila, M., & Jackson-Lewis, V. (2003). Neurodegeneration: what is it and where are we? *J Clin Invest*, *111*(1), 3-10. https://doi.org/10.1172/JCI17522

Puangmalai, N., Bhatt, N., Montalbano, M., Sengupta, U., Gaikwad, S., Ventura, F., McAllen, S., Ellsworth, A., Garcia, S., & Kayed, R. (2020). Internalization mechanisms of brain-derived tau

oligomers from patients with Alzheimer's disease, progressive supranuclear palsy and dementia with Lewy bodies. *Cell Death Dis*, *11*(5), 314. https://doi.org/10.1038/s41419-020-2503-3

Puri, V., Watanabe, R., Singh, R. D., Dominguez, M., Brown, J. C., Wheatley, C. L., Marks, D. L., & Pagano, R. E. (2001). Clathrin-dependent and -independent internalization of plasma membrane sphingolipids initiates two Golgi targeting pathways. *J Cell Biol*, *154*(3), 535-547. https://doi.org/10.1083/jcb.200102084

Rauch, J. N., Chen, J. J., Sorum, A. W., Miller, G. M., Sharf, T., See, S. K., Hsieh-Wilson, L. C., Kampmann, M., & Kosik, K. S. (2018). Tau Internalization is Regulated by 6-O Sulfation on Heparan Sulfate Proteoglycans (HSPGs). *Sci Rep*, *8*(1), 6382. https://doi.org/10.1038/s41598-018-24904-z

Rauch, J. N., Luna, G., Guzman, E., Audouard, M., Challis, C., Sibih, Y. E., Leshuk, C., Hernandez, I., Wegmann, S., Hyman, B. T., Gradinaru, V., Kampmann, M., & Kosik, K. S. (2020). LRP1 is a master regulator of tau uptake and spread. *Nature*, *580*(7803), 381-385. https://doi.org/10.1038/s41586-020-2156-5

Rauch, J. N., Luna, G., Guzman, E., Audouard, M., Challis, C., Sibih, Y. E., Leshuk, C., Hernandez, I., Wegmann, S., Hyman, B. T., Gradinaru, V., Kampmann, M., & Kosik, K. S. (2020). LRP1 is a master regulator of tau uptake and spread. *Nature*. https://doi.org/10.1038/s41586-020-2156-5

Ren, Y., & Sahara, N. (2013). Characteristics of tau oligomers. *Front Neurol*, *4*, 102. https://doi.org/10.3389/fneur.2013.00102

Rogaeva, E., Meng, Y., Lee, J. H., Gu, Y., Kawarai, T., Zou, F., Katayama, T., Baldwin, C. T., Cheng, R., Hasegawa, H., Chen, F., Shibata, N., Lunetta, K. L., Pardossi-Piquard, R., Bohm, C., Wakutani, Y., Cupples, L. A., Cuenco, K. T., Green, R. C., . . . St George-Hyslop, P. (2007). The neuronal sortilin-related receptor SORL1 is genetically associated with Alzheimer disease. *Nat Genet*, *39*(2), 168-177. https://doi.org/10.1038/ng1943

Rojas, J. C., Bang, J., Lobach, I. V., Tsai, R. M., Rabinovici, G. D., Miller, B. L., Boxer, A. L., & Investigators, A. L. (2018). CSF neurofilament light chain and phosphorylated tau 181 predict disease progression in PSP. *Neurology*, *90*(4), e273-e281. https://doi.org/10.1212/WNL.0000000000004859

Rosler, T. W., Tayaranian Marvian, A., Brendel, M., Nykanen, N. P., Hollerhage, M., Schwarz, S. C., Hopfner, F., Koeglsperger, T., Respondek, G., Schweyer, K., Levin, J., Villemagne, V. L., Barthel, H., Sabri, O., Muller, U., Meissner, W. G., Kovacs, G. G., & Hoglinger, G. U. (2019). Four-repeat tauopathies. *Prog Neurobiol*, 101644. https://doi.org/10.1016/j.pneurobio.2019.101644

Saman, S., Kim, W., Raya, M., Visnick, Y., Miro, S., Saman, S., Jackson, B., McKee, A. C., Alvarez, V. E., Lee, N. C., & Hall, G. F. (2012). Exosome-associated tau is secreted in tauopathy models and is selectively phosphorylated in cerebrospinal fluid in early Alzheimer disease. *J Biol Chem*, *287*(6), 3842-3849. https://doi.org/10.1074/jbc.M111.277061

Samudra, N., Lane-Donovan, C., VandeVrede, L., & Boxer, A. L. (2023). Tau pathology in neurodegenerative disease: disease mechanisms and therapeutic avenues. *J Clin Invest*, *133*(12). https://doi.org/10.1172/JCI168553

Sang, H., Lu, Z., Li, Y., Ru, B., Wang, W., & Chen, J. (2001). Phosphorylation of tau by glycogen synthase kinase 3beta in intact mammalian cells influences the stability of microtubules. *Neurosci Lett*, *312*(3), 141-144. https://doi.org/10.1016/s0304-3940(01)02206-6

Sarrazin, S., Lamanna, W. C., & Esko, J. D. (2011). Heparan sulfate proteoglycans. *Cold Spring Harb Perspect Biol*, *3*(7). https://doi.org/10.1101/cshperspect.a004952

Sato, C., Barthelemy, N. R., Mawuenyega, K. G., Patterson, B. W., Gordon, B. A., Jockel-Balsarotti, J., Sullivan, M., Crisp, M. J., Kasten, T., Kirmess, K. M., Kanaan, N. M., Yarasheski, K. E., Baker-Nigh, A., Benzinger, T. L. S., Miller, T. M., Karch, C. M., & Bateman, R. J. (2018). Tau Kinetics in Neurons and the Human Central Nervous System. *Neuron*, *98*(4), 861-864. https://doi.org/10.1016/j.neuron.2018.04.035

Savelieff, M. G., Lee, S., Liu, Y., & Lim, M. H. (2013). Untangling amyloid-beta, tau, and metals in Alzheimer's disease. *ACS Chem Biol*, *8*(5), 856-865. https://doi.org/10.1021/cb400080f

Seaman, M. N., Marcusson, E. G., Cereghino, J. L., & Emr, S. D. (1997). Endosome to Golgi retrieval of the vacuolar protein sorting receptor, Vps10p, requires the function of the VPS29, VPS30, and VPS35 gene products. *J Cell Biol*, *137*(1), 79-92. https://doi.org/10.1083/jcb.137.1.79

Sengupta, U., Portelius, E., Hansson, O., Farmer, K., Castillo-Carranza, D., Woltjer, R., Zetterberg, H., Galasko, D., Blennow, K., & Kayed, R. (2017). Tau oligomers in cerebrospinal fluid in Alzheimer's disease. *Ann Clin Transl Neurol*, *4*(4), 226-235. https://doi.org/10.1002/acn3.382

Sibille, N., Sillen, A., Leroy, A., Wieruszeski, J. M., Mulloy, B., Landrieu, I., & Lippens, G. (2006). Structural impact of heparin binding to full-length Tau as studied by NMR spectroscopy. *Biochemistry*, *45*(41), 12560-12572. https://doi.org/10.1021/bi060964o

Soares, A. C., Ferreira, A., Marien, J., Delay, C., Lee, E., Trojanowski, J. Q., Moechars, D., Annaert, W., & De Muynck, L. (2021). PIKfyve activity is required for lysosomal trafficking of tau aggregates and tau seeding. *J Biol Chem*, *296*, 100636. https://doi.org/10.1016/j.jbc.2021.100636

Song, L., Oseid, D. E., Wells, E. A., Coaston, T., & Robinson, A. S. (2022). Heparan Sulfate Proteoglycans (HSPGs) Serve as the Mediator Between Monomeric Tau and Its Subsequent Intracellular ERK1/2 Pathway Activation. *J Mol Neurosci*, *72*(4), 772-791. https://doi.org/10.1007/s12031-021-01943-2

Sperfeld, A. D., Collatz, M. B., Baier, H., Palmbach, M., Storch, A., Schwarz, J., Tatsch, K., Reske, S., Joosse, M., Heutink, P., & Ludolph, A. C. (1999). FTDP-17: an early-onset phenotype with parkinsonism and epileptic seizures caused by a novel mutation. *Ann Neurol*, *46*(5), 708-715. https://doi.org/10.1002/1531-8249(199911)46:5<708::aid-ana5>3.0.co;2-k

Stamelou, M., Respondek, G., Giagkou, N., Whitwell, J. L., Kovacs, G. G., & Hoglinger, G. U. (2021). Evolving concepts in progressive supranuclear palsy and other 4-repeat tauopathies. *Nat Rev Neurol*, *17*(10), 601-620. https://doi.org/10.1038/s41582-021-00541-5

Stern, R. A., Tripodis, Y., Baugh, C. M., Fritts, N. G., Martin, B. M., Chaisson, C., Cantu, R. C., Joyce, J. A., Shah, S., Ikezu, T., Zhang, J., Gercel-Taylor, C., & Taylor, D. D. (2016). Preliminary Study of Plasma Exosomal Tau as a Potential Biomarker for Chronic Traumatic Encephalopathy. *J Alzheimers Dis*, *51*(4), 1099-1109. https://doi.org/10.3233/JAD-151028

Stopschinski, B. E., Holmes, B. B., Miller, G. M., Manon, V. A., Vaquer-Alicea, J., Prueitt, W. L., Hsieh-Wilson, L. C., & Diamond, M. I. (2018). Specific glycosaminoglycan chain length and sulfation patterns are required for cell uptake of tau versus alpha-synuclein and beta-amyloid aggregates. *J Biol Chem*, *293*(27), 10826-10840. https://doi.org/10.1074/jbc.RA117.000378

Strang, K. H., Croft, C. L., Sorrentino, Z. A., Chakrabarty, P., Golde, T. E., & Giasson, B. I. (2018). Distinct differences in prion-like seeding and aggregation between Tau protein variants provide mechanistic insights into tauopathies. *J Biol Chem*, *293*(7), 2408-2421. https://doi.org/10.1074/jbc.M117.815357

Strang, K. H., Golde, T. E., & Giasson, B. I. (2019). MAPT mutations, tauopathy, and mechanisms of neurodegeneration. *Lab Invest*, *99*(7), 912-928. https://doi.org/10.1038/s41374-019-0197-x

Strauss, T., Marvian-Tayaranian, A., Sadikoglou, E., Dhingra, A., Wegner, F., Trumbach, D., Wurst, W., Heutink, P., Schwarz, S. C., & Hoglinger, G. U. (2021). iPS Cell-Based Model for MAPT Haplotype as a Risk Factor for Human Tauopathies Identifies No Major Differences in TAU Expression. *Front Cell Dev Biol*, *9*, 726866. https://doi.org/10.3389/fcell.2021.726866

Swanson, E., Breckenridge, L., McMahon, L., Som, S., McConnell, I., & Bloom, G. S. (2017). Extracellular Tau Oligomers Induce Invasion of Endogenous Tau into the Somatodendritic Compartment and Axonal Transport Dysfunction. *J Alzheimers Dis*, *58*(3), 803-820. https://doi.org/10.3233/JAD-170168

Takahashi, M., Miyata, H., Kametani, F., Nonaka, T., Akiyama, H., Hisanaga, S., & Hasegawa, M. (2015). Extracellular association of APP and tau fibrils induces intracellular aggregate formation of tau. *Acta Neuropathol*, *129*(6), 895-907. https://doi.org/10.1007/s00401-015-1415-2

Takeda, S., Commins, C., DeVos, S. L., Nobuhara, C. K., Wegmann, S., Roe, A. D., Costantino, I., Fan, Z., Nicholls, S. B., Sherman, A. E., Trisini Lipsanopoulos, A. T., Scherzer, C. R., Carlson, G. A., Pitstick, R., Peskind, E. R., Raskind, M. A., Li, G., Montine, T. J., Frosch, M. P., & Hyman, B. T. (2016). Seed-competent high-molecular-weight tau species accumulates in the cerebrospinal fluid of Alzheimer's disease mouse model and human patients. *Ann Neurol*, *80*(3), 355-367. https://doi.org/10.1002/ana.24716

Takeda, S., Wegmann, S., Cho, H., DeVos, S. L., Commins, C., Roe, A. D., Nicholls, S. B., Carlson, G. A., Pitstick, R., Nobuhara, C. K., Costantino, I., Frosch, M. P., Muller, D. J., Irimia, D., & Hyman, B. T. (2015). Neuronal uptake and propagation of a rare phosphorylated high-molecular-weight tau derived from Alzheimer's disease brain. *Nat Commun*, *6*, 8490. https://doi.org/10.1038/ncomms9490

Takei, Y., Teng, J., Harada, A., & Hirokawa, N. (2000). Defects in axonal elongation and neuronal migration in mice with disrupted tau and map1b genes. *J Cell Biol*, *150*(5), 989-1000. https://doi.org/10.1083/jcb.150.5.989

Tanner, C. M. (1992). Epidemiology of Parkinson's disease. *Neurol Clin*, *10*(2), 317-329. http://www.ncbi.nlm.nih.gov/pubmed/1584176

Tardivel, M., Begard, S., Bousset, L., Dujardin, S., Coens, A., Melki, R., Buee, L., & Colin, M. (2016). Tunneling nanotube (TNT)-mediated neuron-to neuron transfer of pathological Tau protein assemblies. *Acta Neuropathol Commun*, *4*(1), 117. https://doi.org/10.1186/s40478-016-0386-4

Tuck, B. J., Miller, L. V. C., Katsinelos, T., Smith, A. E., Wilson, E. L., Keeling, S., Cheng, S., Vaysburd, M. J., Knox, C., Tredgett, L., Metzakopian, E., James, L. C., & McEwan, W. A. (2022). Cholesterol determines the cytosolic entry and seeded aggregation of tau. *Cell Rep*, *39*(5), 110776. https://doi.org/10.1016/j.celrep.2022.110776

Usenovic, M., Niroomand, S., Drolet, R. E., Yao, L., Gaspar, R. C., Hatcher, N. G., Schachter, J., Renger, J. J., & Parmentier-Batteur, S. (2015). Internalized Tau Oligomers Cause Neurodegeneration by Inducing Accumulation of Pathogenic Tau in Human Neurons Derived from Induced Pluripotent Stem Cells. *J Neurosci*, *35*(42), 14234-14250. https://doi.org/10.1523/JNEUROSCI.1523-15.2015

Utton, M. A., Noble, W. J., Hill, J. E., Anderton, B. H., & Hanger, D. P. (2005). Molecular motors implicated in the axonal transport of tau and alpha-synuclein. *J Cell Sci*, *118*(Pt 20), 4645-4654. https://doi.org/10.1242/jcs.02558

Vershinin, M., Carter, B. C., Razafsky, D. S., King, S. J., & Gross, S. P. (2007). Multiple-motor based transport and its regulation by Tau. *Proc Natl Acad Sci U S A*, *104*(1), 87-92. https://doi.org/10.1073/pnas.0607919104

Vinod, V., Padmakrishnan, C. J., Vijayan, B., & Gopala, S. (2014). 'How can I halt thee?' The puzzles involved in autophagic inhibition. *Pharmacol Res*, *82*, 1-8. https://doi.org/10.1016/j.phrs.2014.03.005

Vogels, T., Leuzy, A., Cicognola, C., Ashton, N. J., Smolek, T., Novak, M., Blennow, K., Zetterberg, H., Hromadka, T., Zilka, N., & Scholl, M. (2020). Propagation of Tau Pathology: Integrating Insights From Postmortem and In Vivo Studies. *Biol Psychiatry*, *87*(9), 808-818. https://doi.org/10.1016/j.biopsych.2019.09.019

Volpato, V., Smith, J., Sandor, C., Ried, J. S., Baud, A., Handel, A., Newey, S. E., Wessely, F., Attar, M., Whiteley, E., Chintawar, S., Verheyen, A., Barta, T., Lako, M., Armstrong, L., Muschet, C., Artati, A., Cusulin, C., Christensen, K., . . . Lakics, V. (2018). Reproducibility of Molecular Phenotypes after Long-Term Differentiation to Human iPSC-Derived Neurons: A Multi-Site Omics Study. *Stem Cell Reports*, *11*(4), 897-911. https://doi.org/10.1016/j.stemcr.2018.08.013

von Bergen, M., Barghorn, S., Li, L., Marx, A., Biernat, J., Mandelkow, E. M., & Mandelkow, E. (2001). Mutations of tau protein in frontotemporal dementia promote aggregation of paired helical filaments by enhancing local beta-structure. *J Biol Chem*, *276*(51), 48165-48174. https://doi.org/10.1074/jbc.M105196200

von Bergen, M., Barghorn, S., Muller, S. A., Pickhardt, M., Biernat, J., Mandelkow, E. M., Davies, P., Aebi, U., & Mandelkow, E. (2006). The core of tau-paired helical filaments studied by scanning transmission electron microscopy and limited proteolysis. *Biochemistry*, *45*(20), 6446-6457. https://doi.org/10.1021/bi052530j

von Bergen, M., Friedhoff, P., Biernat, J., Heberle, J., Mandelkow, E. M., & Mandelkow, E. (2000). Assembly of tau protein into Alzheimer paired helical filaments depends on a local sequence motif ((306)VQIVYK(311)) forming beta structure. *Proc Natl Acad Sci U S A*, *97*(10), 5129-5134. https://www.ncbi.nlm.nih.gov/pubmed/10805776

Wang, B., & Han, S. (2018). Exosome-associated tau exacerbates brain functional impairments induced by traumatic brain injury in mice. *Mol Cell Neurosci*, *88*, 158-166. https://doi.org/10.1016/j.mcn.2018.02.002

Wang, L. H., Rothberg, K. G., & Anderson, R. G. (1993). Mis-assembly of clathrin lattices on endosomes reveals a regulatory switch for coated pit formation. *J Cell Biol*, *123*(5), 1107-1117. https://doi.org/10.1083/jcb.123.5.1107

Wang, Y., Balaji, V., Kaniyappan, S., Kruger, L., Irsen, S., Tepper, K., Chandupatla, R., Maetzler, W., Schneider, A., Mandelkow, E., & Mandelkow, E. M. (2017). The release and trans-synaptic transmission of Tau via exosomes. *Mol Neurodegener*, *12*(1), 5. https://doi.org/10.1186/s13024-016-0143-y

Wang, Y., & Mandelkow, E. (2016). Tau in physiology and pathology. *Nat Rev Neurosci*, *17*(1), 5-21. https://doi.org/10.1038/nrn.2015.1

Ward, S. M., Himmelstein, D. S., Lancia, J. K., & Binder, L. I. (2012). Tau oligomers and tau toxicity in neurodegenerative disease. *Biochem Soc Trans*, *40*(4), 667-671. https://doi.org/10.1042/BST20120134

Ward, S. M., Himmelstein, D. S., Lancia, J. K., Fu, Y., Patterson, K. R., & Binder, L. I. (2013). TOC1: characterization of a selective oligomeric tau antibody. *J Alzheimers Dis*, *37*(3), 593-602. https://doi.org/10.3233/JAD-131235

Wegmann, S., Medalsy, I. D., Mandelkow, E., & Muller, D. J. (2013). The fuzzy coat of pathological human Tau fibrils is a two-layered polyelectrolyte brush. *Proc Natl Acad Sci U S A*, *110*(4), E313-321. https://doi.org/10.1073/pnas.1212100110

Wegmann, S., Nicholls, S., Takeda, S., Fan, Z., & Hyman, B. T. (2016). Formation, release, and internalization of stable tau oligomers in cells. *J Neurochem*, *139*(6), 1163-1174. https://doi.org/10.1111/jnc.13866

Williams, E. T., Chen, X., Otero, P. A., & Moore, D. J. (2022). Understanding the contributions of VPS35 and the retromer in neurodegenerative disease. *Neurobiol Dis*, *170*, 105768. https://doi.org/10.1016/j.nbd.2022.105768

Wilson, D. M., & Binder, L. I. (1997). Free fatty acids stimulate the polymerization of tau and amyloid beta peptides. In vitro evidence for a common effector of pathogenesis in Alzheimer's disease. *Am J Pathol*, *150*(6), 2181-2195. https://www.ncbi.nlm.nih.gov/pubmed/9176408

Wolfe, M. S. (2009). Tau mutations in neurodegenerative diseases. *J Biol Chem*, *284*(10), 6021-6025. https://doi.org/10.1074/jbc.R800013200

Wu, J. W., Herman, M., Liu, L., Simoes, S., Acker, C. M., Figueroa, H., Steinberg, J. I., Margittai, M., Kayed, R., Zurzolo, C., Di Paolo, G., & Duff, K. E. (2013). Small misfolded Tau species are internalized via bulk endocytosis and anterogradely and retrogradely transported in neurons. *J Biol Chem*, *288*(3), 1856-1870. https://doi.org/10.1074/jbc.M112.394528

Wu, J. W., Hussaini, S. A., Bastille, I. M., Rodriguez, G. A., Mrejeru, A., Rilett, K., Sanders, D. W., Cook, C., Fu, H., Boonen, R. A., Herman, M., Nahmani, E., Emrani, S., Figueroa, Y. H., Diamond, M. I., Clelland, C. L., Wray, S., & Duff, K. E. (2016). Neuronal activity enhances tau propagation and tau pathology in vivo. *Nat Neurosci*, *19*(8), 1085-1092. https://doi.org/10.1038/nn.4328

Xia, N., Zhang, P., Fang, F., Wang, Z., Rothstein, M., Angulo, B., Chiang, R., Taylor, J., & Reijo Pera, R. A. (2016). Transcriptional comparison of human induced and primary midbrain dopaminergic neurons. *Sci Rep*, *6*, 20270. https://doi.org/10.1038/srep20270

Yamada, K., Cirrito, J. R., Stewart, F. R., Jiang, H., Finn, M. B., Holmes, B. B., Binder, L. I., Mandelkow, E. M., Diamond, M. I., Lee, V. M., & Holtzman, D. M. (2011). In vivo microdialysis reveals age-dependent decrease of brain interstitial fluid tau levels in P301S human tau transgenic mice. *J Neurosci*, *31*(37), 13110-13117. https://doi.org/10.1523/JNEUROSCI.2569-11.2011

Yamada, K., Holth, J. K., Liao, F., Stewart, F. R., Mahan, T. E., Jiang, H., Cirrito, J. R., Patel, T. K., Hochgrafe, K., Mandelkow, E. M., & Holtzman, D. M. (2014). Neuronal activity regulates extracellular tau in vivo. *J Exp Med*, *211*(3), 387-393. https://doi.org/10.1084/jem.20131685

Yan, X., Nykanen, N. P., Brunello, C. A., Haapasalo, A., Hiltunen, M., Uronen, R. L., & Huttunen, H. J. (2016). FRMD4A-cytohesin signaling modulates the cellular release of tau. *J Cell Sci*, *129*(10), 2003-2015. https://doi.org/10.1242/jcs.180745

Zetterberg, H. (2017). Review: Tau in biofluids - relation to pathology, imaging and clinical features. *Neuropathol Appl Neurobiol*, *43*(3), 194-199. https://doi.org/10.1111/nan.12378

Zhang, W., Falcon, B., Murzin, A. G., Fan, J., Crowther, R. A., Goedert, M., & Scheres, S. H. (2019). Heparin-induced tau filaments are polymorphic and differ from those in Alzheimer's and Pick's diseases. *Elife*, *8*. https://doi.org/10.7554/eLife.43584

Zhang, X. M., Yin, M., & Zhang, M. H. (2014). Cell-based assays for Parkinson's disease using differentiated human LUHMES cells. *Acta Pharmacol Sin*, *35*(7), 945-956. https://doi.org/10.1038/aps.2014.36

Zhang, Y., Wu, K. M., Yang, L., Dong, Q., & Yu, J. T. (2022). Tauopathies: new perspectives and challenges. *Mol Neurodegener*, *17*(1), 28. https://doi.org/10.1186/s13024-022-00533-z

Zhao, J., Huvent, I., Lippens, G., Eliezer, D., Zhang, A., Li, Q., Tessier, P., Linhardt, R. J., Zhang, F., & Wang, C. (2017). Glycan Determinants of Heparin-Tau Interaction. *Biophys J*, *112*(5), 921-932. https://doi.org/10.1016/j.bpj.2017.01.024

Zhao, J., Zhu, Y., Song, X., Xiao, Y., Su, G., Liu, X., Wang, Z., Xu, Y., Liu, J., Eliezer, D., Ramlall, T. F., Lippens, G., Gibson, J., Zhang, F., Linhardt, R. J., Wang, L., & Wang, C. (2020). 3-O-Sulfation of Heparan Sulfate Enhances Tau Interaction and Cellular Uptake. *Angew Chem Int Ed Engl*, *59*(5), 1818-1827. https://doi.org/10.1002/anie.201913029

Zhong, Q., Congdon, E. E., Nagaraja, H. N., & Kuret, J. (2012). Tau isoform composition influences rate and extent of filament formation. *J Biol Chem*, *287*(24), 20711-20719. https://doi.org/10.1074/jbc.M112.364067

Zwang, T. J., Woost, B., Bailey, J., Hoglund, Z., Richardson, D. S., Bennett, R. E., & Hyman, B. T. (2023). Spatial characterization of tangle-bearing neurons and ghost tangles in the human inferior temporal gyrus with three-dimensional imaging. *Brain Commun*, *5*(3), fcad130. https://doi.org/10.1093/braincomms/fcad130